

**CHARACTERISATION AND FLUIDISED BED GASIFICATION
OF SELECTED HIGH-ASH SOUTH AFRICAN COALS**

by

André Daniël Engelbrecht
BSc. (Chem. Eng.)

Dissertation submitted in fulfilment of the requirements for the degree of Master of Engineering in Chemical Engineering in the School of Chemical and Minerals Engineering at the North-West University, Potchefstroom Campus, South Africa.

Supervisor: Professor R.C. Everson (North-West University)

Co - supervisor: Professor H.W.J.P. Neomagus (North-West University)

September 2008

Potchefstroom

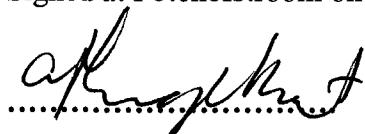
DECLARATION

This dissertation is submitted in fulfilment of the requirements for the degree of Master of Engineering in the School of Chemical and Minerals Engineering of the North-West University.

I, André Daniël Engelbrecht, hereby declare that:

- 1) The dissertation with the title: CHARACTERISATION AND FLUIDISED BED GASIFICATION OF SELECTED HIGH-ASH SOUTH AFRICAN COALS is my own work and has not been submitted at any other university either in whole or in part.
- 2) Commissioning and operation of the fluidised bed gasifier pilot plant at the CSIR was my own work.

Signed at Potchefstroom on this^{1st}..... day of September 2008



A. D. Engelbrecht

ACKNOWLEDGEMENTS

The author wishes to sincerely thank the following people and organisations for their support during this project.

- Professor R.C. Everson and Professor H.W.J.P. Neomagus at the School of Chemical and Minerals Engineering for their guidance and advice throughout the duration of this project.
- Dr. Rufaro Kaitano for assistance with the operation of the thermogravimetric analyser at North-West University and interpretation of the results.
- Mr. Ashton Swartbooi and Mr. Alphius Bokaba for assistance with the operation of the fluidised bed gasifier at the Council for Scientific and Industrial Research (CSIR).
- Colleagues at the CSIR for the useful discussions we had on the subject of coal and fluidised beds.
- The CSIR and the South African National Energy Research Institute for providing financial support.
- New Vaal, Matla, Grootegeluk and Duvha collieries for collection and preparation of coal samples.
- Family and friends for their encouragement.

ABSTRACT

South Africa has abundant coal reserves and produces approximately 75 % of its primary energy from coal. Based on scientific analysis, however, it is generally accepted that a link exists between climate change and the use of fossil fuels such as coal. The development of clean coal technologies (CCT) has therefore received increased attention worldwide. Integrated gasification combined cycle (IGCC) technology, utilising fluidised bed gasification, has been identified as a potential CCT that can be applied in South Africa. A suite of four South African coals was identified as being possible fuels for IGCC power stations which would operate for three to four decades, towards the middle of this century. The selected coals are from New Vaal, Matla, Grootegeluk and Duvha collieries. These coals were subjected to detailed characterisation, thermogravimetric analysis and fluidised bed gasification tests to assess their suitability for use in IGCC power stations.

The characterisation performed consisted of standard coal analytical methods, petrographic techniques and physical analysis. The results of the analysis showed that the coals are low in grade and rich in inertinite. The vitrinite random reflectance (R_r), which is regarded as a reliable rank parameter, showed that the coals selected are representative of the rank variation within South African bituminous coals, with the coals of lower rank having larger surface areas and porosities.

Gasification reactivity experiments were carried out in a thermogravimetric analyser (TGA) at 87.5 kPa, between temperatures of 875 °C and 950 °C, with 100 vol. % CO₂ as the reacting gas. The results of the tests show that the reactivity of coal char increases with a decrease in the rank of the coal. The reactivity of the New Vaal coal, which has the lowest rank, is comparable to the reported reactivity of some overseas lignite coals. The results also show that the grain model can be used to describe char conversion and that the Arrhenius equation describes the effect of temperature on the reaction rate constant.

Pilot-scale fluidised bed gasification tests were carried out on the four selected coals at 925 °C and 950 °C. The results show that the fixed carbon conversion achieved in the gasifier correlates well with the rank parameter (R_r) of the coal. Although the order of ranking of reactivities of the different coals in the fluidised bed gasifier and

the TGA are the same, the variation in the reactivity index in the fluidised bed gasifier is significantly lower than in the TGA. This was attributed to the large amount of fixed carbon that is converted in the FBG by means of the partial combustion reaction which is less sensitive to the reactivity of the char.

The low volatile matter content and the high ash content of the coals tested, together with high gasifier heat losses and nitrogen dilution, contributed to the low calorific value of the gas produced. No agglomeration and clinkering of the coal was observed during the gasification tests and it was concluded that this can be attributed to the low Free Swelling Index (FSI) and Roga Index (RI) of the coals tested.

It was concluded that fluidised bed gasifiers are able to utilise high-ash South African coals and are therefore a candidate technology for IGCC power stations. Due to the relatively low reactivity of most South African bituminous coals, a secondary combustion stage may be required after the fluidised bed gasifier in order to achieve acceptable overall carbon conversions.

OPSOMMING

Suid-Afrika besit volop steenkoolreserwes en produseer ongeveer 75% van sy primêre energie uit steenkool. Op die basis van wetenskaplike analiese, word dit egter algemeen aanvaar dat daar 'n verband tussen die gebruik van fossielbrandstowwe soos steenkool en klimaatverandering bestaan. Die ontwikkeling van skoon steenkooltegnologië geniet dus wêreldwyd groot aandag. Geïntegreerde vergassingsstelsels, wat sweefbedvergassing gebruik, is as 'n potensiële skoon steenkooltegnologie vir toepassing in Suid-Afrika geïdentifiseer. 'n Reeks van vier steenkole is as moontlike brandstowwe vir kragstasies vir die volgende drie tot vier dekades tot die middel van die eeu uitgeken. Die uitgesoekte steenkole is uitkomstig uit die New Vaal-, Matla-, Grootegeluk- en Duvha-steenkoolmyne. Gedetailleerde karakteriseringstoetse, termogravimetriese analise en sweefbedvergassingstoetse is op hierdie steenkole uitgevoer om te bepaal of hulle vir geïntegreerde vergassingskragstasies geskik is.

Die karakteriseringstoetse wat uitgevoer is, het uit standaard steenkoolanalitiese metodes, petrografiese tegnieke en fisiese analiese bestaan. Die resultate toon dat die steenkole laag is in graad en ryk is aan inertiniet. Die vitriniet-refleksiewaardes (R_r), wat as 'n betroubare rangaanwyser beskou word, toon dat die steenkole wat vir die studie gekies is verteenwoordigend van die rangvariasie onder Suid-Afrikaanse bitumineuse steenkole is. Die resultate toon ook dat die laer rang steenkole groter oppervlakte en porositeit het.

Vergassingsreaktiwiteitstoetse is in 'n termogravimetriese analiseerder (TGA) teen 87.5 kPa, tussen temperature van 875 °C en 950 °C uitgevoer, met 100% CO₂ as die reagerende gas. Die toetsresultate toon dat die reaktiwiteit van steenkool met 'n afname in rang toeneem. Die reaktiwiteit van die New Vaal-steenkool, wat die laagste rang het, is met die reaktiwiteit van sekere oorsese lignietsteenkole vergelykbaar. Die resultate toon ook dat die korrelmodel toegepas kan word om die omsetting van vaste koolstof te beskryf en dat die Arrhenius-vergelyking gebruik kan word om die uitwerking van temperatuur op die reaksiesnelheidskonstant te beskryf.

'n Sweefbedproefaanleg is gebruik om vergassingstoetse op die vier steenkole teen 925 °C en 950 °C uit te voer. Die resultate toon dat die vaste koolstofomsetting goed

met die rangaanwyser (R_r) van die steenkool korreleer. Die rangskikking van die steenkoolreaktiwiteite in die sweefbedvergasser is dieselfe as in die TGA, alhoewel die reaktiwiteitsindeks in die sweefbedvergasser 'n betekenisvol laer variasie toon. Die laer variasie kan aan die omsetting van 'n groot hoeveelheid vaste koolstof d.m.v. die gedeeltelike verbrandingsreaksie toegeskryf word, wat minder sensitief is t.o.v. die reaktiwiteit van die verkooltsel.

Die lae vlugstofinhoud en hoë asinhoud van die steenkool, saam met hoë hitteverliese in die vergasser en stikstofverdunning, het tot die lae kaloriewaarde van die gas bygedra. Geen agglomerasie en klinkerformasie van die steenkool is tydens die vergassingstoetse waargeneem nie en die gevolgtrekking is gemaak dat dit aan die lae FSI (Free Swelling Index) en RI (Roga Index) indekse van die steenkool wat getoets is, toegeskryf kan word.

Die gevolgtreking is gemaak dat sweefbedvergassers wel hoë-as Suid-Afrikaanse steenkool kan benut en dus 'n kandidaattegnologie vir geïntegreerde vergassingsstelsels is. As gevolg van die relatief lae reaktiwiteit van meeste Suid-Afrikaanse bitumineuse steenkool, is dit moontlik dat 'n sekondêre verbrandingsstadium na die vergasser nodig sal wees om aanvaarbare totale koolstofomsettings te behaal.

CONTENTS

DECLARATION	i
ACKNOWLEDGEMENTS.....	ii
ABSTRACT.....	iii
OPSOMMING	v
LIST OF FIGURES	xi
LIST OF TABLES.....	xiii
NOMENCLATURE	xiv
LIST OF PUBLICATIONS	xx
CHAPTER 1 GENERAL INTRODUCTION.....	1
1.1 Background and motivation.....	1
1.1.1 The importance of coal in South Africa.....	1
1.1.2 The effect of coal utilisation on the environment.....	2
1.1.3 Clean coal technologies	3
1.1.4 Coal gasification	6
1.2 Objectives of the investigation.....	8
1.3 Scope of the investigation.....	9
1.3.1 Motivation for the research project.....	9
1.3.2 Literature review.....	9
1.3.3 Coal selection and characterisation.....	10
1.3.4 Laboratory thermogravimetric analysis	10
1.3.5 Fluidised bed gasifier pilot scale tests	10
1.3.6 Conclusion and recommendations	11
CHAPTER 2 LITERATURE REVIEW	12
2.1 Introduction.....	12
2.2 Coal characterisation.....	12
2.2.1 Coal properties	12
2.3 Coal gasification kinetics.....	16
2.3.1 Factors affecting gasification rate.....	16
2.3.2 Relative reactivity.....	17

2.3.3	Char conversion models.....	18
2.4	Fluidised bed coal gasification.....	21
2.4.1	Background.....	21
2.4.2	Chemical reactions.....	22
2.4.3	Pilot plant investigations.....	23
2.4.4	Future developments.....	25
2.5	Modelling of fluidised bed gasifiers	26
2.5.1	Introduction.....	26
2.5.2	Models.....	27
CHAPTER 3 COAL CHARACTERISATION		30
3.1	Introduction.....	30
3.2.1	Selection criteria	30
3.2.2	Background information on selected coals	30
3.3	Coal characterisation.....	31
3.3.1	Coal characterisation parameters	31
3.4	Summary of coal characterisation tests.....	35
CHAPTER 4 THERMOGRAVIMETRIC ANALYSIS		37
4.1	Introduction.....	37
4.2	Experimental apparatus.....	37
4.3	Experimental procedure	38
4.4	Experimental programme.....	39
4.5	Results and discussion	40
4.5.1	Normalisation of experimental data.....	40
4.5.2	Gasification reactivity.....	44
4.5.3	Evaluation of experimental data against the grain model.....	46
4.5.4	Arrhenius activation energy.....	49
4.6	Summary of TGA tests	51
CHAPTER 5 PILOT-SCALE FLUIDISED BED GASIFICATION.....		52
5.1	Introduction.....	52
5.2	Pilot-scale fluidised bed coal gasifier	52
5.2.1	Plant and process description.....	52
5.2.2	FBG start-up and control	58

5.2.3	Measurements and analyses.....	59
5.3	Experimental programme.....	61
5.4	Fluidised bed gasification test results	62
5.4.1	Fixed carbon conversion.....	65
5.4.2	Calorific value.....	67
5.4.3	Char fines generation and elutriation.....	68
5.4.4	Bed agglomeration and clinkering.....	70
5.5	Summary of fluidised bed gasification tests	71
CHAPTER 6: GENERAL CONCLUSIONS AND RECOMMENDATIONS.....		73
6.1	General conclusions.....	73
6.2	Contributions to the knowledge base of coal science and technology.....	74
6.3	Recommendations for future investigations	74
REFERENCES		76
APPENDIX A: THERMOGRAVIMETRIC ANALYSIS		82
Appendix A.1:	Char preparation apparatus for Grootegeluk coal	82
Appendix A.2:	The relative char gasification reactivities at 925, 900 and 875 °C..	82
Appendix A.3:	Evaluation of grain model for Matla, Grootegeluk and Duvha chars	84
Appendix A.4:	Conversion rate of chars.....	85
APPENDIX B: PILOT-SCALE FLUIDISED BED GASIFICATION		86
Appendix B.1:	Calculated values of U_{mf} as a function of char particle size.....	86
Appendix B.2:	Distributor pressure drop.....	87
Appendix B.3:	Coal feeder calibration curves	87
Appendix B.4:	Airflow calculation.....	88
Appendix B.5:	Steam flow calibration curve.....	88
Appendix B.6:	Calculation of fluidising velocity, gas calorific value, residence time, fixed carbon conversion and elutriated char percentage.....	89
Appendix B.6.1:	Calculation of fluidising velocity (U)	89
Appendix B.6.2:	Calculation of gas calorific value (CV).....	90
Appendix B.6.3:	Residence time calculation of bed char.....	91
Appendix B.6.4:	Calculation of fixed carbon conversion and percentage char elutriated	93

Appendix B.7: Calculation of reactivity index (R_s) in the fluidised bed gasifier.....	95
Appendix B.8: Particle size distributions of coal, bed char and cyclone char	97
Appendix B.9: Coal, bed char and cyclone char	99
Appendix B.10: Char particles removed from the gasifier	100
Appendix B.11: Distributor of the fluidised bed gasifier (FBG)	101

LIST OF FIGURES

Figure 1.1: Conventional and IGCC power-generation cycles (Henderson, 2003).....	5
Figure 1.2: Fluidised bed and entrained-flow gasifiers (Parekh, 1982).....	7
Figure 3.1: Rank classification system using vitrinite random reflectance	33
Figure 4.1: Schematic representation of the apparatus	38
Figure 4.2: Photograph of the thermogravimetric analyser (Kaitano, 2007).....	39
Figure 4.3: Isothermal gasification of Matla coal at 925 °C in 100 % CO ₂ at 87.5 kPa	41
Figure 4.4: Initial isothermal gasification of Matla coal at 925 °C in 100 % CO ₂ at 87.5 kPa.....	41
Figure 4.5: Isothermal gasification of Matla char at 925 °C in 100 % CO ₂ at 87.5 kPa	42
Figure 4.6: Conversion of Matla char at 925 °C in 100 % CO ₂ at 87.5 kPa.....	43
Figure 4.7: Relative char gasification reactivity at 950 °C in 100 % CO ₂ at 87.5 kPa	44
Figure 4.8: Grain model for New Vaal char at 87.5 kPa in 100 % CO ₂	47
Figure 4.9: Conversion rate of Matla char in 100 % CO ₂ at 925 °C.....	49
Figure 4.10: Arrhenius plots for New Vaal, Matla, Grootegeluk and Duvha chars	50
Figure 5.1: Flow diagram of the FBG pilot plant	53
Figure 5.2: Photograph of the FBG pilot plant	53
Figure 5.3: FBG distributor layout.....	55
Figure 5.4: Details of distributor nozzle	56
Figure 5.5: Dimensions of the FBG furnace.....	57
Figure 5.6: Gasifier temperature profiles for Matla coal at 925 °C	63
Figure 5.7: Gas concentration profiles for Matla coal at 925 °C.....	63
Figure 5.8: Fluidised bed gasifier fixed carbon conversion.....	65
Figure 5.9: Gas calorific value as a function of vitrinite random reflectance (R _r)	67
Figure 5.10: Char fines generated as a function of HGI.....	68
Figure 5.11: Comparison of fixed carbon conversion in the FBG and TGA.....	69
Figure A.1: Char preparation apparatus for Grootegeluk coal	82
Figure A.2a: Relative char gasification reactivity at 875 °C in 100 % CO ₂ at 87.5 kPa	82

Figure A.2b: Relative char gasification reactivity at 900 °C in 100 % CO ₂ at 87.5 kPa	83
Figure A.2c: Relative char gasification reactivity at 925 °C in 100 % CO ₂ at 87.5 kPa	83
Figure A.3a: Grain model for Matla char at 87.5 kPa in 100 % CO ₂	84
Figure A.3b: Grain model for Grootegeluk char at 87.5 kPa in 100 % CO ₂	84
Figure A.3c: Grain model for Duvha char at 87.5 kPa in 100 % CO ₂	85
Figure A.4a: Conversion rate of chars at 1 000° C and 87.5 kPa	85
Figure B.1: U _{mf} as a function of char particle size for various char densities	86
Figure B.2: Distributor pressure drop as a function of airflow	87
Figure B.3: Coal feeder calibration and calculation formulae	87
Figure B.4: Airflow orifice calibration curve	88
Figure B.5: Steam flow orifice calibration curve.....	88
Figure B.8a: Particle size distribution of coal.....	97
Figure B.8b: Particle size distribution of bed char	97
Figure B.8c: Particle size distribution of cyclone char	98
Figure B.9: Appearance and relative amounts of coal and char	99
Figure B.10a: New Vaal bed char particle (2 mm).....	100
Figure B.10b: Duvha bed char particle (2 mm)	100

LIST OF TABLES

Table 1.1: South African and world primary energy sources (Winkler, 2006)	2
Table 1.2: Comparison of fluidised bed and entrained-flow fine coal gasifiers	6
Table 2.1: Relative chemical composition of macerals (Du Cann, 2006)	13
Table 3.1: Information on the selected South African coals	31
Table 3.2: Proximate analysis, ultimate analysis and calorific value	32
Table 3.3: Petrographic analysis	33
Table 3.4: Structural and physical properties	34
Table 3.5: Free swelling index and Roga index of selected coals	35
Table 3.6: Ash melting temperatures and analysis of the ash	36
Table 4.1: Reaction conditions used for gasification experiments	39
Table 4.2: Reactivity indices (h^{-1}) of chars at 875, 900, 925 and 950 °C in 100 % CO ₂ at 87.5 kPa	45
Table 4.3: Grain model parameters k and β for selected chars	47
Table 4.4: Arrhenius activation energy (E) and pre-exponential factor (k_0)	50
Table 5.1: Specifications of the FBG pilot plant	54
Table 5.2: Specification of gas analysers	60
Table 5.3: Operating conditions for fluidised bed gasification tests	61
Table 5.4: Summary of fluidised bed gasification tests at 90 kPa absolute pressure ..	64
Table 5.5: Reactivity index (R_s) of coals in the FBG and TGA (h^{-1})	66
Table B.6.4.1: Calculation of fixed carbon conversion and elutriated char	94
Table B.7.1: Pilot plant data and calculated values of k' , $\tau_{0.5}$ and R_s	95

NOMENCLATURE

A_B	gasifier bed area	m^2
A_E	char elutriated to cyclone	%
C	carbon in coal	%
C_{ash}	ash in coal	%
C_c	total carbon conversion	%
C_{BC}	carbon in bed char	%
C_{EC}	carbon in elutriated char	%
C_d	nozzle discharge coefficient	—
C_{daf}	dry and ash free carbon in coal	%
C_{fixed}	fixed carbon in coal	%
$C_{FIXEDCON}$	fixed carbon conversion	%
CV_{coal}	calorific value of coal	$MJ.kg^{-1}$
CV	calorific value of gas	$MJ.(Nm)^{-3}$
daf	dry ash-free	%
d_p	char particle diameter/coal particle size	m or mm
d_{pore}	average pore diameter by BET analysis	nm
d_{50}	mean particle diameter	m or mm
D_p	pipe diameter	m
DT	deformation temperature	$^{\circ}C$
E	activation energy	$kJ.mol^{-1}$
f_o	relative reactivity factor	—
F(X)	structural factor (char conversion model)	—
FT	fluid temperature	$^{\circ}C$
g	gravitational constant	$9.81 m.s^{-2}$
G_{BC}	bed char flowrate	$kg.h^{-1}$

G_{EC}	elutriated char flowrate	kg.h^{-1}
G_{char}	char feedrate to gasifier	kg.h^{-1}
G_{coal}	coal flowrate	kg.h^{-1}
G_{steam}	steam flowrate	kg.h^{-1}
H	distance from distributor to pressure probe	m
HGI	Hardgrove Grindability Index	-
HT	hemispherical temperature	$^{\circ}\text{C}$
k_{CO_2}	reaction rate constant (CO ₂ gasification)	min^{-1}
k	reaction rate constant ($k_{CO_2} (P_{CO_2})^{\alpha}$)	min^{-1}
k'	apparent reaction rate constant	min^{-1}
k_0	pre-exponential factor	min^{-1}
K_{CO}	adsorption constant for CO	Pa^{-1}
K_{CO_2}	adsorption constant for CO ₂	Pa^{-1}
K_{H_2}	adsorption constant for H ₂	Pa^{-1}
K_{H_2O}	adsorption constant for H ₂ O	Pa^{-1}
L_0	total pore length per unit volume	m.m^{-3}
M_1	bed mass above pressure probe	kg
M_2	bed mass below pressure probe	kg
M_t	total bed mass	kg
m_{ash}	mass of ash/residue	g
m_o	initial mass of char following pyrolysis	g
m_t	mass of coal/char at time t	g
N	nitrogen in coal	%
O	oxygen in coal	%
P_1	gasifier bottom pressure	Pa
P_2	gasifier top pressure	Pa

P_B	gasifier pressure	kPa
P_{CO_2}	partial pressure of CO_2	Pa
P_{H_2}	partial pressure of H_2	Pa
P_{H_2O}	partial pressure of H_2O	Pa
Q_{air}	air flowrate	$(Nm)^3.h^{-1}$
NQ_{total}	total gas flow to the fluidised bed	$(Nm)^3.h^{-1}$
Q_{total}	total gas flow to the fluidised bed	$m^3.h^{-1}$
r	rate of reaction	s^{-1}
R	universal gas constant	$8.314 J.mol^{-1}.K^{-1}$
R_r	vitritine random reflectance	(%)
R_s	reactivity index of char	h^{-1}
S	sulphur in coal	%
S_0	initial surface area of char per unit volume	$m^2.m^{-3}$
S_{BET}	surface area of coal by BET analysis	$m^2.g^{-1}$
ST	softening temperature	$^{\circ}C$
T	temperature	$^{\circ}C$
t	residence time	min
T_1	bottom bed temperature	$^{\circ}C$
T_3	mid-bed temperature	$^{\circ}C$
T_7	gasifier exit temperature	$^{\circ}C$
T_{air}	air temperature	$^{\circ}C$
T_B	fluidised bed temperature	$^{\circ}C$
U	superficial gas velocity in the bed	$m.s^{-1}$
U_{mf}	minimum fluidising velocity	$m.s^{-1}$
U_t	terminal falling velocity	$m.s^{-1}$
v	gas velocity through holes in nozzle	$m.s^{-1}$

V_{CH_4}	CH_4 concentration of the gas	vol. %
V_{CO}	CO concentration of the gas	vol. %
V_{H_2}	H_2 concentration of the gas	vol. %
X	fractional conversion of fixed carbon in coal	—
X_t	fractional conversion of total carbon in coal	—
Y_{CO_2}	Mol fraction CO_2	—
Y_{CO}	Mol fraction CO	—

Greek Letters

α	reaction order with respect to gas concentration	—
β	grain model structural parameter	—
ϵ_o	initial porosity of char	—
ϵ	bed voidage at bed velocity	—
ϵ_{coal}	porosity of coal	(%)
ψ	random pore model structural parameter	—
$\tau_{0.5}$	time for 50 % fixed carbon conversion	h
ΔH	enthalpy change of reaction at 298 K	$kJ.mol^{-1}$
ΔP_B	bed pressure drop	Pa
ΔP_D	distributor pressure drop	Pa
θ	angle of repose	°
μ	gas viscosity	$kg.m^{-1}s^{-1}$
ρ_{char}	char density	$kg.m^{-3}$
ρ_g	gas density	$kg.m^{-3}$
ρ_{coal}	coal density	$kg.m^{-3}$
ϕ	combustion product distribution coefficient	-

Acronyms/Abbreviations

AECI	African Explosives and Chemical Industries
ASTM	American Society for Testing and Materials
BET	Brunauer, Emmett and Teller
BS	British Standard
C ₂ ⁺	Ethane and higher hydrocarbons
CCT	Clean coal technologies
Cycl.	Cyclone
Diff.	Difference
DME	Department of Minerals and Energy (South Africa)
DMT	Deutsche Montan Technologie
Eskom	Electricity Supply Commission (South Africa)
FBAAG	Fluidised Bed Agglomerating Ash Gasifier
FBC	Fluidised bed combustion
FBG	Fluidised bed gasifier
FD	Forced draught
FSI	Free Swelling Index
GDP	Gross Domestic Product
GWe	Gigawatt electrical
HG	Hydro-gasification reaction
HGI	Hardgrove Grindability Index
HTW	High-Temperature Winkler
ID	Induced draught
IGCC	Integrated Gasification Combined Cycle
ISO	International Standards Organization

KBR	Kellogg Brown and Roots
KRW	Kellogg Rust Westinghouse
LPG	Liquefied Petroleum Gas
MEA	Mono-ethanol amine
Mt	Million tons
MW	Megawatt
NO _x	Nitrous oxides
NR	No reading
PSD	Particle size distribution
RI	Roga Index
SABS	South African Bureau of Standards
Sasol	Suid-Afrikaanse Steenkool en Olie
SO _x	Sulphurous oxides
TGA	Thermogravimetric analyser/analysis
USA	United States of America
WGS	Water-gas shift reaction

LIST OF PUBLICATIONS

The following papers were presented at conferences during the course of the research project:

North, B.C., Engelbrecht, A.D. and Hadley, T.D. (2006). Fluidised bed gasification of low-grade South African coal. Presented at the South African Chemical Engineering Congress 2006, International Convention Centre, Durban, South Africa, September 2006.

Engelbrecht, A.D., North, B.C. and Hadley, T.D. (2007). Investigation into the gasification characteristics of South African power station coals. Presented at the Twenty-fourth Annual International Pittsburgh Coal Conference, Sandton Convention Centre, Johannesburg, South Africa, September, 2007.

CHAPTER 1 GENERAL INTRODUCTION

This introductory chapter consists of three sections. Section 1.1 gives background information and the motivation for carrying out this research project. The objectives of the investigation are described in Section 1.2 and finally the scope and outlay of the dissertation are given in Section 1.3. The background information given briefly describes the importance of coal in the South African economy, concerns about the effect of coal utilisation on the environment, clean coal technologies and coal gasifiers. The need for carrying out research on the fluidised bed gasification of high-ash South African coal is motivated.

1.1 Background and motivation

1.1.1 The importance of coal in South Africa

Abundant and relatively cheap coal has contributed to establishing South Africa as the leading economy in Africa and as a major world coal exporter. South Africa has coal reserves amounting to 34 billion tons, of which 240 million tons are mined annually. Domestic consumption of coal amounts to 171 million tons, and 69 million tons are exported (Prévost *et al.*, 2004). Domestically, coal is consumed mainly for the generation of electricity by Eskom (65 %) and the production of synthetic fuels and chemicals by Sasol (25 %).

Table 1 shows that coal is the most important energy source in South Africa, supplying 74.1 % of its primary energy. Due to the high cost and decreasing reserves of oil and gas, their contribution to the energy mix is expected to decrease. Since South Africa is a water-scarce country, the contribution of renewable energy, such as hydro and biomass, is not expected to increase significantly. The use of solar and wind energy is also currently limited by the high cost of these energy sources. Safety and cost are issues that inhibit the increased use of nuclear energy. Coal will therefore remain our most important energy resource for the foreseeable future.

Table 1.1: South African and world primary energy sources (Winkler, 2006)

Energy source		South Africa (%)	World (%)
Coal		74.1	24.0
Oil		12.0	39.0
Nuclear		4.2	8.0
Gas		2.3	23.0
Renewables	Biomass	2.92	2.82
	Hydro	4.44	2.64
	Geothermal	0.00	0.36
	Wind	0.03	0.12
	Solar	0.01	0.06
Total		100	100

1.1.2 The effect of coal utilisation on the environment

The use of coal results in greater volumes of greenhouse gases being emitted per unit of energy generated compared with other energy sources. South Africa currently has a CO₂ emitted per capita ratio (metric tons/annum CO₂ emitted per person) of 7.8, which is almost double the world average (Hietkamp *et al.*, 2004). Based on scientific analysis, it is generally accepted that there is a link between global warming and the emission of greenhouse gases such as carbon dioxide (CO₂). It is estimated that CO₂ emissions are responsible for 61 % of the enhanced greenhouse effect and that the use of coal contributes 30 % to the increase in the CO₂ concentration of the atmosphere (Reck *et al.*, 1996). In the first 150 years after the start of the Industrial Revolution, the CO₂ concentration in the atmosphere increased from 280 ppm to 330 ppm, but in the last 30 years alone it has increased from 330 ppm to 380 ppm (Goede, 2004). To ensure that the CO₂ concentration of the atmosphere rises no higher than 550 ppm, which is considered to be the maximum ceiling allowable, substantial reductions in the amount of CO₂ that is released into the atmosphere are required. Avenues that are being investigated to achieve this include renewable energy, increasing the efficiency of fossil-fuel-fired power stations and the capture and sequestration of CO₂. In December 1997 the Kyoto Protocol, which sets targets for the reduction of CO₂ emissions, was signed by 84 countries. In terms of the Kyoto Protocol, which is a

United Nations treaty, 'annex 1' countries (i.e. developed countries) are required to reduce their CO₂ emissions by an average of 7 % below 1990 levels (EIA, 1997). The 'emissions' refer to the average annual emissions between the years 2008 and 2012. As a non-annex 1 country (developing country), South Africa does not have any Kyoto obligations in terms of CO₂ reductions. This situation is, however, expected to change when the Kyoto Protocol is reviewed in 2012. The USA, which is the largest emitter of CO₂, did not ratify the treaty in its current format, mainly because developing countries such as South Africa do not have any obligations. When the treaty is reviewed in 2012 it is expected that developing countries such as South Africa, India and China will be given obligations in order to get the USA on board. Coal users in South Africa, such as Eskom and Sasol, will therefore be investigating the implementation of clean coal technologies (CCT) for power generation and liquid fuels production in the future.

1.1.3 Clean coal technologies

Clean coal technologies are defined as "technologies designed to enhance both the efficiency and the environmental acceptability of coal extraction, preparation and use". The clean coal technologies that are being developed include (Henderson, 2003):

- Ultra supercritical pulverised coal combustion
- Post-combustion capture
- Oxy-coal combustion
- Circulating fluidised bed combustion
- Integrated gasification combined cycle technology (IGCC).

The first four technologies given above will be discussed briefly, after which IGCC will be discussed in more detail.

Ultra supercritical pulverised coal combustion is regarded as a CCT since it increases the efficiency of conventional pulverised coal combustion boilers and less CO₂ is

therefore released per MW of electricity generated. The efficiency of conventional pulverised coal combustion power stations can be raised from 35 to 45 % by using ultra supercritical steam conditions of 600 °C and 25 MPa in the boiler. It is necessary to develop specialised materials of construction for ultra supercritical steam conditions.

Post-combustion capture occurs when CO₂ is removed from the flue gas of power station boilers and heating furnaces. Options for storing the captured CO₂ include geological storage, ocean storage and mineral storage. The best proven technique for separating the CO₂ from the flue gas is to scrub it with mono-ethanol amine (MEA) solution. The MEA from the scrubber is heated with steam to release high-purity CO₂. The CO₂-free amine is then recirculated to the scrubber. The disadvantages of post-combustion capture are that the equipment sizes are large due to the large flue gas volumes and the low CO₂ concentration in the flue gas (10 - 15 %).

Oxy-coal combustion uses oxygen instead of air for coal combustion in the boiler. Flue gas is recirculated to reduce the combustion temperatures in the boiler. The advantages of this method are that the flue gas stream has a high CO₂ concentration (90 %) and the flowrate of flue gas is much lower (five times) than that from conventional combustion using air. The costs of flue gas cleaning and CO₂ removal are therefore reduced significantly. Oxy-coal combustion can be retrofitted to ultra supercritical boilers, thereby achieving higher efficiencies and improved environmental performance.

Limestone and dolomite can be added to *circulating fluidised bed combustion boilers* in order to reduce the SO_x in the flue gas. The concentration of NO_x in the flue gas is also lower due to the lower combustion temperatures that are employed. Future developments will probably include adding ultra supercritical steam conditions and oxy-coal combustion to circulating fluidised bed boilers.

The flow sheets for conventional and IGCC power generation cycles are given in Figure 1.1. In a conventional cycle all the energy in the coal is used to generate steam, which is then exhausted through a steam turbine to generate electricity. The exhaust steam has to be recondensed and recycled to the boiler. Due to the large energy losses during condensation, the overall efficiency (coal to electrical power) of a conventional power station is between 33 and 38 % (Eskom, 2002). This can be raised to 45 % by increasing the temperature and pressure of the steam.

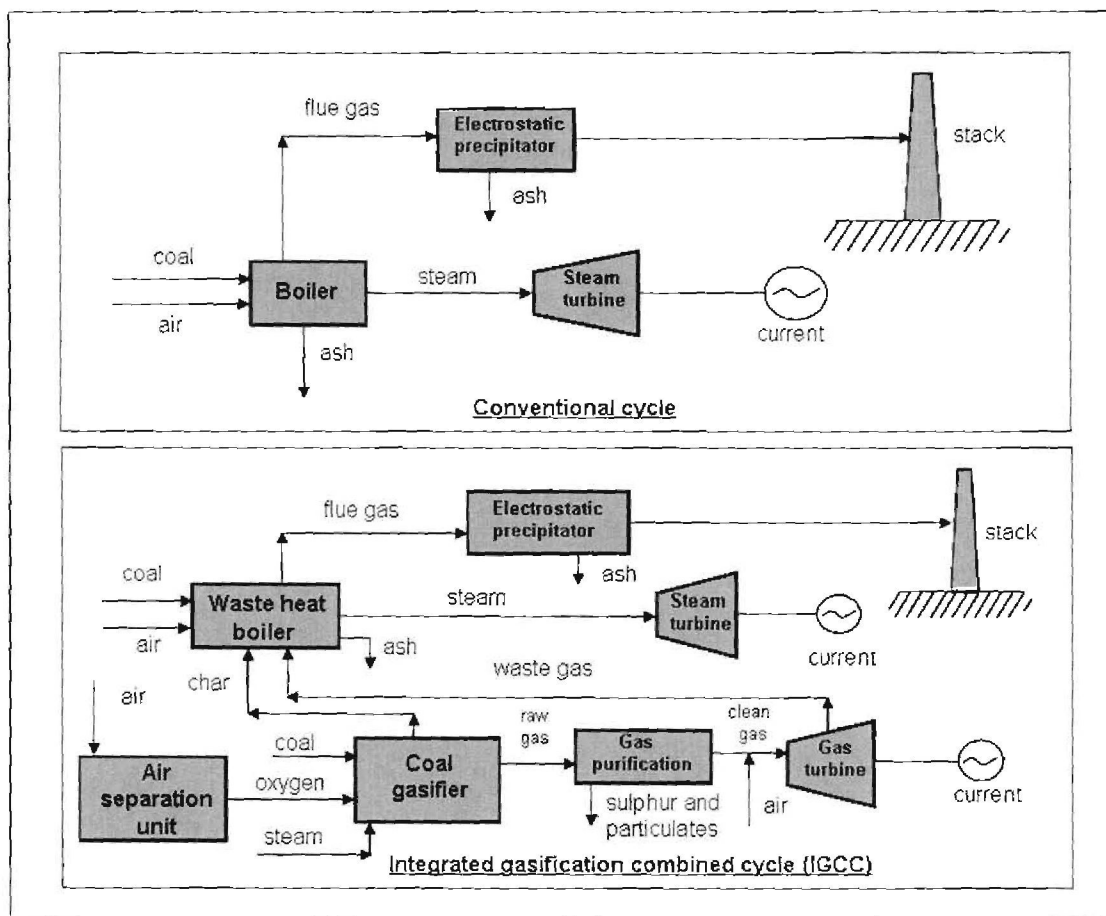


Figure 1.1: Conventional and IGCC power-generation cycles (Henderson, 2003)

In an IGCC power station a coal gasifier is incorporated into the flow sheet. During gasification coal is reacted with air and steam or oxygen and steam to produce a combustible gas ('syngas'). This gas stream is relatively easy to clean since it is under pressure and has a low volume compared with the flue gas resulting from conventional coal combustion. The cleaned gas is combusted in a gas turbine which

produces electrical power. Heat is recovered from the turbine exhaust gas by means of a conventional steam cycle. This configuration (IGCC) can produce higher efficiencies (50 %) and lower emissions than conventional power stations (Pruschek and Oeljeklaus, 1997). IGCC also has the advantage of reduced water consumption and the potential for co-production of liquid and gaseous fuels and chemicals.

1.1.4 Coal gasification

Coal gasification is a key enabling technology for IGCC plants. Coal gasification is not new to South Africa since Sasol operates 72 Lurgi gasifiers at its synfuel plants in Secunda. The Lurgi gasifier, however, is more suited to synthetic fuel and chemicals production since it cannot utilize fine coal (< 12 mm) and byproducts which include tars and oils are produced. For IGCC plants, fine coal gasification is the technology of choice (Calpine Fuels Diversity Initiative, 2006). The most well-known fine coal gasifiers are the entrained flow gasifier and the fluidised bed gasifier. These two types of gasifier are compared in Table 1.2 and Figure 1.2.

Table 1.2: Comparison of fluidised bed and entrained-flow fine coal gasifiers

	Fluidised bed	Entrained flow
Coal particle size	0.5 mm - 5 mm	< 0.5 mm
Coal moisture	Dry	Dry/slurry
Coal type	Non-caking coals	Low-ash coals
Ash in coal	< 60 %	< 30 %
Gasification agents	Air, oxygen and steam	Oxygen and steam
Temperature	850 °C - 950 °C	1 300 °C - 1 450 °C
Pressure	< 25 bar	< 30 bar
Residence time	0.5 h - 1.5 h	< 10 s
Carbon efficiency	65 % - 85 %	75 % - 90 %
Gasification efficiency	55 % - 75 %	55 % - 70 %
Commercial examples	Winkler	Texaco, Prenflo, Shell and Koppers-Totzek

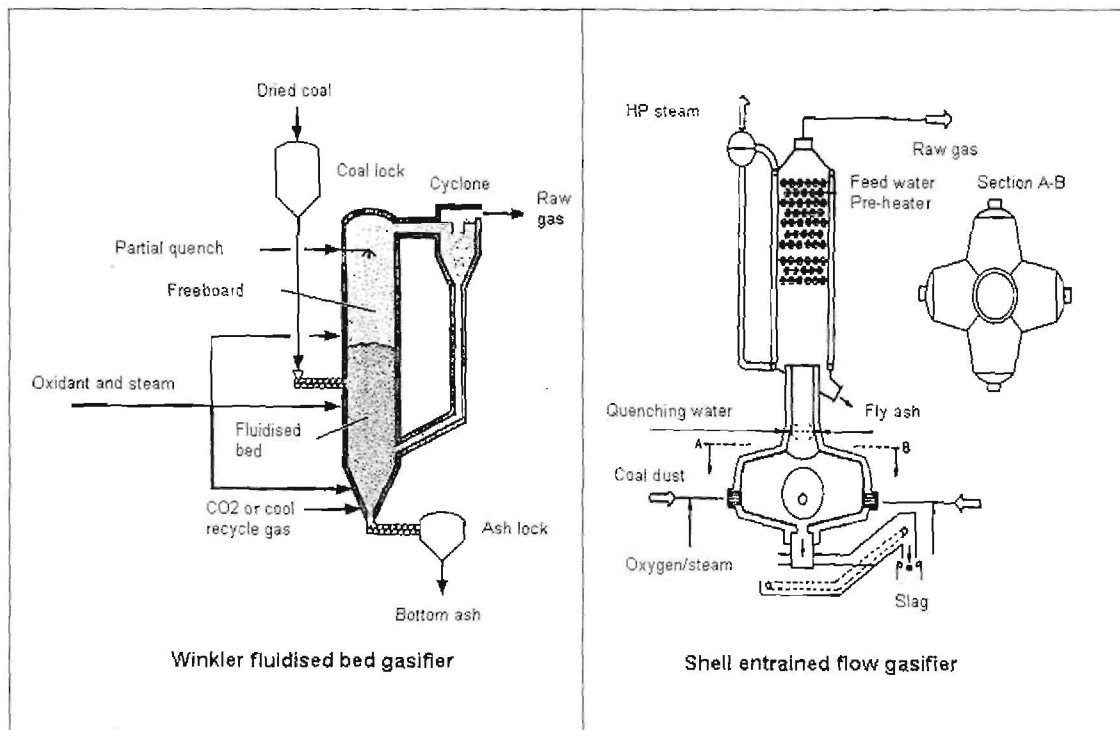


Figure 1.2: Fluidised bed and entrained-flow gasifiers (Parekh, 1982)

The only commercial example of fine coal gasification in South Africa is the six Koppers-Totzek gasifiers which were operated from 1975 to 1999 by African Explosives and Chemical Industries (AECI) at Modderfontein for ammonia production. Gas production was $\pm 100\ 000\ \text{Nm}^3/\text{h}$ containing 60 % CO. The fixed carbon conversion was between 70 and 80 % and the gasification efficiency was between 60 and 70 %. A pilot fluidised bed gasifier supplied by Krupp Engineering was operated by Highveld Steel and Vanadium Corporation in 1988. The objective of the project was to demonstrate fluidised bed gasification technology for the gasification of the discard coal produced by the surrounding mines in the Witbank area. Problems experienced by the Krupp gasifier included low carbon conversion and clinkering of the coal at the oxygen and steam nozzles in the gasifier.

The advantages of fluidised bed gasification for the gasification of South African coal include (Schiling *et al.*, 1981):

- Coals that are high in ash and low in grade can be gasified
- Fine coal (< 5 mm) can be utilised
- The heat and mass transfer rates are high
- Good temperature control can be achieved
- Lower temperature operation increases refractory life
- Limestone can be added for in bed capture of hydrogen sulphide
- As there are no moving parts in the furnace, the maintenance costs are low
- No tar and oil by-products are produced.

A potential disadvantage of fluidised bed gasification, however, is that due to the lower temperature in the gasifier, the carbon conversion is lower than entrained flow gasifiers which operate at a higher temperature. The low carbon conversion decreases the efficiency of an IGCC power station.

Coal gasification reactions occur at a much lower rate than coal combustion reactions. It is therefore important to develop an understanding of how coal properties and conditions in the gasifier affect the gasification rate and the resulting carbon conversion. This forms the basis of this investigation.

1.2 Objectives of the investigation

The objectives of the project are to:

- 1) Explore the relationship between the coal characterisation parameters, TGA results and performance of four high-ash South African coals in an air-blown, pilot-scale fluidised bed gasifier.

- 2) Assess the potential of the fluidised bed coal gasification process for incorporation into future IGCC power stations utilising high-ash South African coals.

In order to achieve the objectives, the following tasks were carried out:

- 1) Select and source four high-ash South African coals that are currently being used as power station feed.
- 2) Subject the selected coals to characterisation and thermogravimetric analysis (TGA).
- 3) Design and commission a pilot-scale fluidised bed gasifier at the CSIR.
- 4) Gasify the selected coals in the pilot-scale fluidised bed gasifier.

1.3 Scope of the investigation

The work plan for the project consisted of the activities described below.

1.3.1 Motivation for the research project

Chapter 1 gives an overview of the background and motivating factors for the research, followed by the objectives.

1.3.2 Literature review

Chapter 2 gives an overview of publications in the open literature on coal characterisation, coal gasification kinetics, fluidised bed gasification and gasifier modelling. This review includes references to results published in journals, conference proceedings and doctoral theses, and on internet websites.

1.3.3 Coal selection and characterisation

Chapter 3 contains information on the origin of the four selected coals and the criteria for their selection. The results of the detailed coal characterisation tests are given. The characterisation tests consisted of:

- Proximate analysis
- Ultimate analysis
- Petrographic analysis
- BET (Brunauer, Emmett and Teller) surface area analysis
- Hardgrove Grindability Index
- Free swelling index and Roga index
- Ash fusion temperature.

1.3.4 Laboratory thermogravimetric analysis

Laboratory TGA tests were done on the four selected coals and these are described in Chapter 4. Carbon dioxide (CO₂) was used as the reacting gas and the work consisted of:

- Measurement of the relative reactivity of chars derived from the selected coals
- Determination of the effect of temperature on the reaction rate
- Calculation of the Arrhenius activation energy (E) and grain model constants (k and β) based on the experimental data.

1.3.5 Fluidised bed gasifier pilot scale tests

The fluidised bed gasification of the four coals selected for the study is described in Chapter 5. A description of the pilot plant, together with the start-up and operating procedure that was developed for the process, is presented. The detailed results of each test are also given in this chapter.

1.3.6 Conclusion and recommendations

In Chapter 6 conclusions are drawn based on the results of this investigation. The contribution the investigation has made to the knowledge base of science and technology is given. Finally, recommendations are given for future work on gasification of South African fine coal.

CHAPTER 2 LITERATURE REVIEW

2.1 Introduction

This literature review is divided into four main sections: coal characterisation, coal gasification kinetics, fluidised bed gasification and fluidised bed gasifier modelling.

2.2 Coal characterisation

2.2.1 Coal properties

2.2.1.1 Introduction

Many analyses and indices are used for the classification of coal. The indices given below are those that were considered relevant to the current investigation, namely the fluidised bed gasification of coal.

2.2.1.2 Proximate analysis, ultimate analysis and calorific value

These analyses originated more than 100 years ago and are normally used to calculate mass and energy balances for coal utilisation processes. These are relatively simple analyses to carry out, as described by Ergun (1979).

The proximate analysis consists of determining the moisture, volatile matter, fixed carbon and ash contents. The determinations are done by measuring the percentage weight losses when coal is heated stepwise to boiling point (moisture), to 900 °C in the absence of oxygen (volatile matter), and oxidised at 900 °C (fixed carbon). The residue that is left is the ash content. It was recognised that ash determined in this way is slightly lower in weight and different in chemical composition than the original mineral matter in the coal. A simple empirical formula was developed by Ergun (1979) to relate the mineral matter content of coal to the ash determination and is as follows:

$$\text{Mineral matter (\%)} = 1.08(C_{\text{ash}}) + 0.1(S) \quad (2.1)$$

The ultimate analysis of coal involves determining the elemental carbon, hydrogen, nitrogen, sulphur and oxygen by chemical means. The carbon, hydrogen and nitrogen are determined by burning a dried sample in air and measuring the concentration of CO₂, and H₂O in the combustion products (ASTM 5373). Total sulphur is measured by using a high-temperature combustion tube furnace (ASTM D4329) and oxygen is determined indirectly by subtracting from 100 the carbon, hydrogen, nitrogen and sulphur values. No simple and reliable direct method has yet been developed to determine the oxygen in coal.

The gross calorific value of coal is determined by burning a weighed sample of coal in a calorimeter and measuring the heat that is released (ISO 1928), which includes the condensation heat of water formed. The calorific value can also be estimated from the ultimate analysis using the well-known Dulong's equation given below (Reid, 1973):

$$CV_{\text{coal}} = 0.338C + 1.442\left(H - \frac{O}{8}\right) + 0.094S \quad (2.2)$$

2.2.1.3 Petrographic analysis and rank

It has long been recognised that coal is a non-homogenous substance and that it consists of discernable components called *macerals*. The three maceral groups that are recognised are vitrinite, liptinite and inertinite (Du Cann, 2006). These are distinguished from one another by differences in reflectance, colour, morphology, shape and size. Macerals also have different chemical compositions, as shown in Table 2.1.

Table 2.1: Relative chemical composition of macerals (Du Cann, 2006)

	Carbon	Hydrogen	Oxygen
Vitrinite	high	medium	low
Liptinite	medium	high	low
Inertinite	medium	low	high

One of the most useful petrographic parameters that is used in coal utilisation is the vitrinite reflectance analysis. It has been found (Neavel, 1979) that vitrinite random reflectance is a very reliable indicator of rank, being independent of the vitrinite concentration and the ash content of the coal, but dependent on the carbon/hydrogen and carbon/oxygen ratios. Coal rank is a measure of the degree of metamorphism (coalification) that a coal has experienced and increases with maturity of the coal. The rank of coal is important for gasification research since it well known that higher-rank coals are less reactive than lower-rank coals. The inertinite content of coal has also been found to have an influence on the reactivity of coal since inertinite has a higher density which restricts the diffusion of reacting gases within the coal (Everson *et al.*, 2006).

2.2.1.3 Surface area, porosity and density measurement of coal

The internal surface area of coal consists of micropores (< 2 nm), mesopores (2 - 50 nm) and macropores (> 50 nm). Coal has a wide range of pore size distributions and the relative percentage of each type depends on the origin and rank of the coal (Gan *et al.*, 1972). The surface area and the number of active sites present influence the reactivity of the coal (Miura *et al.*, 1989). The surface area of coal chars is generally higher than that of coal due to the opening of micropores when volatiles are released. The surface area of coal and chars is most often measured using the BET (Brunauer, Emmett and Teller) method, with nitrogen as the absorbing gas. The method consists of measuring the equilibrium adsorption pressure of N₂ and relating it to the amount of N₂ absorbed and therefore to the surface area.

For cylindrical pores the porosity of coal can be calculated using equation (2.3). Equation (2.3) was derived using surface area and volume calculations (Engelbrecht, 2007).

$$\epsilon_{coal} = \frac{d_{pore} S_{BET} \rho_{coal}}{40000} \quad (2.3)$$

The bulk density of low-porosity coals ($\epsilon_{\text{coal}} < 5 \%$) can be measured using the water displacement method. (Engelbrecht, 2007).

2.2.1.4 Hardgrove Grindability Index

The Hardgrove Grindability Index (HGI) of coal is a measure of how difficult or easy it is to grind the coal to smaller sizes (ISO 5074). In general, the HGI of coal varies between 20 and 110, a lower value indicating that the coal is difficult to grind and a higher value that it is easy to grind finer. On the whole, lignite and anthracite are more resistant to grinding (i.e. have low indices) than are bituminous coals (Ode, 1963). The HGI is important for fluidised bed gasification since it could be an indicator of the amount of fines that will be generated in the gasifier due to abrasion and attrition.

2.2.1.5 Free swelling index (FSI) and Roga index (RI)

These indices are used to indicate the caking and agglomerating nature (tendency to deform and stick together) of the coal and the scales are FSI 0 - 9 and RI 0 - 90 (Thomas, 1986). Coals that have a FSI of 0 and a RI of 0 do not cake or agglomerate. To determine the FSI by the ISO 501 method, one gram of finely powdered coal (250 μm) is rapidly heated to 820 °C and the silhouette of the resulting coke button is compared with a series of standard profiles. The FSI of the sample is the number of the standard profile (0 - 9) which it most closely resembles.

To determine the RI by the ISO 335 method, a mixture of one gram of coal crushed to < 0.2 mm and 5 g of anthracite sized to between 0.3 and 0.4 mm is compacted in a crucible under a weight 6 kg for 30 seconds. After being brought to a temperature of 850 °C in 15 minutes, the coke button is weighed and screened at > 1 mm. The weight of the > 1 mm fraction is an indication of the agglomerating nature of the coal. If coal has swelling and agglomerating properties, this could potentially be problematic for fluidised bed operation since the coal particles will stick together, defluidise and clinkers will be formed in the bed.

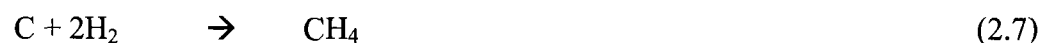
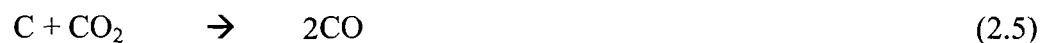
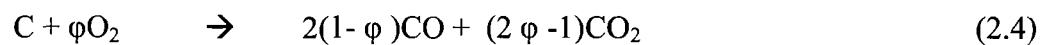
2.2.1.6 Ash fusion temperature

The melting of ash in coal is characterised by means of four temperatures (Ergun, 1979). These temperatures are the deformation temperature (DT), the softening temperature (ST), the hemispherical temperature (HT) and the fluid temperature (FT). In the ASTM method (D-27), a prepared ash sample in the form of a pyramid is heated quickly to 800 °C and then at a rate 7 to 13 °C/min to 1 600 °C. The DT is noted when the apex of the pyramid becomes rounded. The ST is recorded when the pyramid has fused down to a nearly spherical lump having the height equal to the base. The HT is noted when the height of the lump becomes one half of the length of the base. The final measurement of the fluid temperature is made when the ash fuses and spreads into a liquid layer with a height of 1 mm or less. In a fluidised bed gasifier, there is a zone of higher temperature at the bottom of the bed near the distributor. In order to prevent sintering of particles and subsequent clinker formation, the mid-bed temperature has to be maintained at 200 - 250 °C below the deformation temperature (DT) of the ash (Clark, 1979).

2.3 Coal gasification kinetics

2.3.1 Factors affecting gasification rate

Coal gasification consists of coal devolatilisation and subsequent conversion of the char that is formed. Since devolatilisation occurs at a rapid rate, coal gasification kinetics are concerned mainly with the slower char gasification reactions. The most important char gasification reactions are:



The rates of the char gasification reactions are affected by the external operating conditions surrounding the char particle and by factors related to the char particle (reactivity) (Molina and Mondragon, 1998). The external conditions include the temperature, pressure and composition of the atmosphere surrounding the char particle. The char reactivity is affected by:

- 1) Structural properties such as surface area and porosity
- 2) The concentration of active sites on the surface
- 3) The catalytic effect of the mineral matter.

The conditions used for the preparation of chars such as temperature and time has an effect on the three factors given above.

2.3.2 Relative reactivity

The relative reactivity of a particular char (relative to other chars) is often compared by using the reactivity index R_s (Zhang *et al.*, 2006 and Ye *et al.*, 1997) which can be expressed as:

$$R_s = \frac{0.5}{\tau_{0.5}} \quad (2.8)$$

with $\tau_{0.5}$ being the time (h) taken for the char to reach a fractional conversion of 0.5 at specified conditions of temperature, pressure, reacting gas composition and char particle size. Therefore if the char takes $\frac{1}{2}$ hour to reach a fractional conversion of 0.5, the reactivity index is 1.

2.3.3 Char conversion models

The rate of char conversion with CO₂ is often expressed using the rate equation given by Lu and Do (1994):

$$\frac{dX}{dt} = k_{CO_2} F(X) P_{CO_2}^\alpha \quad (2.9)$$

As the gasification reactions proceed, the char's pore structure changes continuously with the extent of reaction "which leads to variations in the effective area for reaction and, then, to variations in reactivity" (De Carvalho and Brimacombe, 1987). The structural factor F(X) is used to describe the effect of fractional char conversion (X) on the gasification rate of coal chars. Various structural factor models have been developed in order to describe the different ways in which char structure changes with the extent of reaction (Molina and Mondragon, 1998; Liliedahl and Sjöström, 1996).

A structural factor model that is often used to describe char gasification is the grain model and can be expressed as (Lu and Do, 1994):

$$F(X) = (1-X)^\beta \quad (2.10)$$

This model predicts that the gasification rate (dX/dt) will decrease from the initial rate when X = 0, to zero when X = 1.

Two special cases of the grain model are the *homogenous model* ($\beta = 1$) (also referred to as the volumetric model) and the *shrinking core model* ($\beta = 2/3$). The homogenous model assumes that the reaction takes place uniformly throughout the whole volume of the particle. The shrinking core model assumes that the reaction occurs only on the outer surface of the particle and as the reacting surface recedes a layer of ash is formed around the unreacted core of char. (Zhang *et al.*, 2006). The shrinking core

model is characteristic of “fast reactions” with the overall reaction rate being controlled by external diffusion. The homogenous model, on the other hand, is characteristic of “slow reactions” with the overall reaction rate being controlled by chemical reaction rate at the internal surface of the particle.

The *random pore model* and *random capillary model* developed by Bhatia and Perlmutter (1980) and Gavalas (1980) respectively can predict the char conversion rate if the rate increases from the initial rate to a maximum and then decreases to zero. This behaviour is often explained in terms of surface area changes, the rate increasing due to pore opening and growth and then decreasing due to pore coalescence. The equation for the *random pore model* is:

$$F(X) = (1 - X)\sqrt{1 - \Psi \ln(1 - X)} \quad (2.11)$$

$$\Psi = \frac{4\pi L_0(1 - \varepsilon_0)}{S_0^2} \quad (2.12)$$

In the above equation, Ψ is referred to as the structural factor. S_0 , L_0 and ε_0 represent the initial surface area, pore length and porosity of the particles respectively.

In equation (2.10) above, α is the reaction order with respect to the reacting gas. For reacting gas pressures of 0 to 1 bar, the reaction order is close to unity. For higher pressures, the reaction order decreases and reaches a value of 0 at pressures of 12 - 18 bar (Sha *et al.*, 1990).

The effect of temperature on gasification rate can be described by the well-known Arrhenius equation (Ye *et al.*, 1997):

$$k = k_0 \exp\left(\frac{-E}{RT}\right) \quad (2.13)$$

The addition of CO and H₂ to the reacting gases CO₂ and H₂O results in a retarding or inhibiting effect on the overall reaction rate (Goyal *et al.*, 1989 and Everson *et al.*, 2006). The reaction mechanism that explains this observation is that CO and H₂ adsorb onto the char surface, thereby blocking active sites for CO₂ and H₂O to react. It is important to consider this effect in developing rate equations for coal gasification since in practical gasifiers significant amounts of CO and H₂ are present in the reacting gas. The Langmuir–Hinshelwood-type rate equations are used to describe the intrinsic rate when CO and H₂ are present in the reacting gas mix. These equations have the form:

$$r_1 = \frac{k_1 K_{CO_2} P_{CO_2}}{1 + K_{CO_2} P_{CO_2} + K_{CO} P_{CO}} F(X) \quad (2.14)$$

$$r_2 = \frac{k_2 K_{H_2O} P_{H_2O}}{1 + K_{H_2O} P_{H_2O} + K_{H_2} P_{H_2}} F(X) \quad (2.15)$$

Njapha (2005) found that if the reactions proceed on separate sites, the overall rate is:

$$r_t = r_1 + r_2 \quad (2.16)$$

The above rate equation can be incorporated into fluidised bed gasification models that are based on fundamental kinetics. The major disadvantage of the Langmuir–Hinshelwood-type rate equations is the large number of unknown parameters involved (Kaitano, 2007).

2.4 Fluidised bed coal gasification

2.4.1 Background

Fluidised bed coal gasification has the distinction of being the first commercial application of fluidised bed technology (Kunii and Levenspiel, 1977). In 1926 the Winkler gasifier, developed by Fritz Winkler, started commercial operation in Leuna, West Germany, producing fuel gas for gas engines that compressed ammonia synthesis gas and hydrogen for tar hydrogenation (Squires, 1983). Subsequently, 63 gasifiers were constructed, mainly in Europe, Japan and India, producing fuel gas and synthesis gas for ammonia and methanol production (Parekh, 1982). The Winkler gasifier operates at atmospheric pressure using lignite as the feed coal and at a temperature of 850 °C to 950 °C. A flow diagram of the Winkler gasifier is given in Figure 1.2 (Chapter 1). After 1967 no new Winkler plants were built since at the time it was cheaper to produce methanol, ammonia and hydrogen using oil-based feedstocks.

In 1978 Reinische Braunkohlenwerke AG in Germany started development of the High-Temperature Winkler (HTW) process. In 1986 a 720 ton/day HTW demonstration plant was built in Cologne, West Germany, to produce synthesis gas for methanol production (Brungel *et al.*, 1989). Special features of the HTW gasifier include:

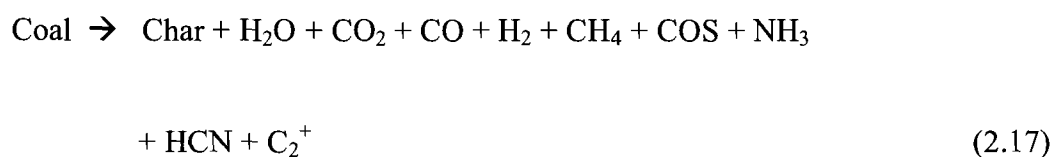
- Operating pressure : 10 bar
- Bed temperature : 1 000 °C
- Freeboard temperature : 1 100 °C
- Gasification agents : Oxygen and steam
- Coal particle size : 1 - 4 mm
- Pre-drying of lignite coal feed
- Recycling of fly ash
- Dry bottom ash-removal system

The major disadvantage of the HTW gasifier is that only reactive non-caking coals can be used as feedstock. The use of unreactive caking coals in the HTW process results in low carbon conversions and defluidisation of the bed. There are indications that the addition of dolomite and limestone to the coal could reduce the tendency of caking coals to agglomerate in the gasifier and also improve the carbon conversion (Ocampo *et al.*, 2003).

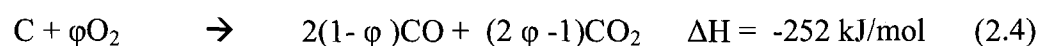
Research in the USA has concentrated on developing a fluidised bed gasifier that can gasify caking coals. This research has resulted in the development of the Kellogg Rust Westinghouse (KRW) and Institute of Gas Technology (U-gas) processes, which have an ash agglomeration zone in the gasifier (Shinnar *et al.*, 1988). The concept involves maintaining two distinct zones within the same vessel. The bottom 'hot zone' generated by a jet of steam, oxygen and coal is maintained at temperatures above the ash sintering temperature. At these temperatures the ash is sticky and agglomerates into low-in-carbon particles. The agglomerates grow in size until they defluidise and drop out of the bed through the bottom classifying throat. This type of gasifier is termed a 'Fluidised Bed Agglomerating Ash Gasifier' (FBAAG). These processes have, however, been hindered by operating problems and have not found commercial application.

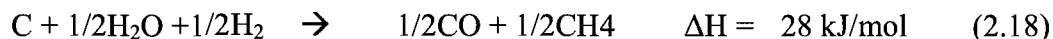
2.4.2 Chemical reactions

When coal enters the gasifier, it is first devolatilised by means of reaction (2.17).



The char that is produced by devolatilisation is converted by means of heterogeneous reactions (2.4) to (2.7) and (2.18) to (2.19) (Yan *et al.* 1999).





Homogenous gas phase reactions that take place in the dilute and emulsion phases of the fluidised bed are (Yan *et al.* 1999):



Most of the heat required for the fluidised bed gasification process, which normally operates at temperatures between 850 °C and 950 °C, is produced by means of the exothermic partial combustion reaction (2.4). The heat is required to heat the reactants (air and steam) to the bed temperature and for the endothermic reactions ((2.17), (2.5), (2.6), (2.18) and (2.21)).

2.4.3 Pilot plant investigations

Many pilot plant studies have been carried out to investigate the fluidised bed gasification of coal. The objective of pilot plant testing is to investigate the effect of operating variables such as:

- air/coal ratio
- oxygen/coal ratio
- steam/coal ratio
- coal type
- coal particle size
- bed temperature
- reactor pressure.

on gasifier performance parameters such as:

- gas yield
- gas composition
- carbon conversion
- fly ash/bed ash ratio.

Potential operating problems such as:

- blocking of coal feeding and ash-removal screw conveyors
- bed agglomeration and clinkering
- attrition and thermal shattering of coal

are also investigated.

Gutierrez and Watkinson (1982) reported that when gasifying western Canadian coal with air, gas calorific values of between 2.9 and 3.5 MJ/Nm³ were obtained. When steam was added, the calorific value increased to 4.2 MJ/Nm³. Carbon conversions of between 65 and 85 % were obtained.

Chatterjee *et al.* (1995) conclude from their work that when gasifying bituminous coal and coke-breeze, the bed temperature should be limited to 950 °C for bituminous coal and to 1 000 °C for coke-breeze to avoid ash agglomeration and defluidisation of the bed.

Jing *et al.* (2005) tested three coals of differing rank at various air/coal ratios, steam/coal ratios and temperatures, and found that “the gas yield and carbon conversion increase with air/coal ratio, steam/coal ratio, and bed temperature, while they decrease with the rise of the rank of coal”.

Zhuo *et al.* (1999) investigated the reactivity of the bed ash and cyclone ash produced from the gasifier. This information is required for the design of a secondary combustor for the combustion of the ash produced by the gasifier. They reported that

the bed ash was less reactive than the fly ash and concluded that this was because it had experienced more 'thermal annealing' during its longer stay in the gasifier.

Huang *et al.* (2003) investigated the effect of pressure (5 - 15 bar) on gasifier operation. They found that:

- Pressure has little effect on the gas composition
- Increase in pressure increases the amount of fly ash that is produced from the gasifier.

Ocampo *et al.* (2003) gasified Columbian coal mixed with limestone in a pilot fluidised bed gasifier with a diameter of 220 mm. They reported that the addition of limestone prevented clinkering of the bed and captured 25 % of the sulphur at 850 °C.

2.4.4 Future developments

Many IGCC demonstration projects are currently under construction. Three of these projects have selected fluidised bed coal gasification technology for gas production.

The Kellogg Brown and Roots (KBR) transport gasifier has been selected as the basis of the 330 MWe IGCC demonstration plant at the Stanton Energy Station in Orlando Florida, USA (Smith *et al.*, 2005). The KBR gasifiers (fluidised bed) will be fed with dry sub-bituminous Power River Basin coal and be operated in air-blown mode. Provision has also been made for post-combustion of the fly ash produced by the gasifiers.

Work on a 400 MWe IGCC demonstrator in Australia is expected to start at the end of 2007 and be completed in 2009 (Mc Farlane, 2006). The plant will be located in the Latrobe Valley, in the State of Victoria. The supplier of the fluidised bed gasifier has not been specified.

At the Vresova plant, which is located between Karlovy Vary and Sokolov in the Czech Republic, existing fixed-bed Lurgi gasifiers will be replaced by HTW fluidised bed gasifiers for the gasification of lignite to produce 400 MWe power (Bucko, 2000). The Lurgi gasifiers are being replaced to avoid the production of unwanted by-products.

2.5 Modelling of fluidised bed gasifiers

2.5.1 Introduction

The objective of fluidised bed gasifier modelling is to predict the performance of the gasifier based on given input conditions.

The input conditions usually include:

- Coal feedrate and analysis
- Air flowrate and temperature
- Steam flowrate and temperature
- Oxygen flowrate and temperature
- Gasifier pressure
- Heat losses.

The performance parameters are:

- Gasifier temperature
- Gas flowrate and composition
- Carbon conversion
- Temperature and concentration profiles inside the gasifier.

2.5.2 Models

Efforts at modelling fluidised bed gasification started in earnest in the early 1980s and many models have been developed. Models generally belong to one of the following categories (Basu, 2006):

- Equilibrium models
- Kinetic models.

Equilibrium models are developed by first setting up mass balance equations for the system. The mass balance equations (element balances) produce six equations and eight unknowns. To obtain eight equations and eight unknowns the water-gas shift reaction ($\text{CO} + \text{H}_2\text{O} \rightarrow \text{CO}_2 + \text{H}_2$) and the hydro-gasification reaction ($\text{C} + 2\text{H}_2 \rightarrow \text{CH}_4$) equilibrium equations are added to the mass balance equations (Furusawa *et al.*, 1989). Solution of the equations produces values for the eight unknowns which are the seven gas components and the product gas flow. Using the input flows and calculated output flows, the gasifier temperature can be calculated by means of an energy balance (Kovacik *et al.*, 1990). Equilibrium models cannot predict carbon conversion and profiles (temperature and concentration) inside the gasifier. For this purpose kinetic models are required.

Kinetic models are a lot more complex to set up and solve. They consist of several differential and linear equations that have to be solved simultaneously. Despite the complexity of kinetic models, they still require the combustion product distribution coefficient (φ) and the relative reactivity factor (f_0) to be adjusted to fit the experimental data. This is because there are processes such as coal devolatilisation, coal shattering and attrition that are not taken into account in these models.

Kinetic models require kinetic data for the individual gasification reactions in the gasifier. A hydrodynamic model is also required to describe the mixing in the bed (Ma *et al.*, 1988). The two-phase theory of fluidisation developed by Davidson and Harrison (1971) and Kunii and Levenspiel (1977) is used to describe the bed

hydrodynamics. It assumes that the bed consists of two phases: a bubble phase and an emulsion phase.

A model developed by Yan *et al.* (1999) predicted that 21 - 41 % of the oxygen input to the gasifier is consumed by combustible gas in the gasifier that is back-mixed to the distributor region. The remainder of the oxygen reacts with the char in the bed.

Gururanjan and Argarval (1992) reported that a relatively small proportion of the gas is produced by the slow-rate char gasification reaction. The fast coal devolatilisation and char combustion reactions have the biggest effect on gas composition and carbon conversion in the gasifier. It was concluded that most of the fixed carbon conversion occurs in the bottom part of the bed via the partial combustion reactions.

All the kinetic models have the char combustion product distribution coefficient (ϕ) as an adjustable parameter. The combustion product distribution coefficient (ϕ) gives the relative amounts of CO and CO₂ that are produced during the partial combustion reaction according to equation (2.15):

$$\phi = Y_{\text{CO}_2} + 0.5Y_{\text{CO}} \quad (0.5 < \phi < 1.0) \quad (2.17)$$

Yan and Zhang (2000) found that if homogenous gas combustion is not considered in the model, the value of ϕ has a large influence on the model predictions. However, if homogenous gas combustion is considered in the model, the value of ϕ can be set at between 0.75 and 0.85 with “negligible effect on model predictions”.

The model of Chejne and Hernandez (2002) requires the solution of 29 differential and 10 non-linear equations using the method of Gear and Adams. This model was validated using experimental data from two pilot-scale fluidised bed reactors.

The model of Yan *et al.* (1998) considers net flow between the bubble phase and the emulsion phase in the conservation equations. From this model, the calculated net flow was found to be 71 - 87 % of the feed gas flow. The net flow decreased when the rank of the coal that was used as input to the model increased.

A non-isothermal model was developed by Ross *et al.* (2005) to predict the temperature profile in the fluidised bed. This is useful since a region of higher temperature is present at the bottom of the gasifier near the distributor. It is important to know what the peak temperature is since this could indicate the possibility of clinking and agglomeration in the bed. The non-isothermal model predicted higher carbon conversions (higher temperature zone) than the isothermal model and was in better agreement with the experimental data.

The model of Luo *et al.* (1998) has two adjustable parameters, f_o (relative reactivity factor) and ϕ (combustion product distribution coefficient). For medium- to high-rank coals, a better agreement with the experimental data was obtained than for low-rank coals. An explanation for the above observation was that the actual reactivity of coal is better correlated to f_o ($f_o = 6.2(1-C_{daf})$) for medium- and high-rank coals than for low-rank coals.

CHAPTER 3 COAL CHARACTERISATION

3.1 Introduction

This chapter describes aspects concerned with characterisation of the four coals selected for the thermogravimetric analysis and fluidised bed gasification experimentation described in Chapters 4 and 5. Section 3.2 gives the criteria used for coal selection and information on the origin of the coals. The results and discussion of the various characterisation tests are presented in Section 3.3. A summary of the coal characterisation tests is given in Section 3.4.

3.2.1 Selection criteria

One of the objectives of the project was to evaluate the suitability of fluidised bed gasification of South African coals for incorporation into future IGCC plants. The coals evaluated were therefore those that would be likely feedstock to IGCC plants in South Africa in future. The criteria given below were used to select four coals:

- Low-grade coals with ash contents between 30 and 45 %
- Feed coals to existing Eskom power stations
- Estimated life of the mines producing the coals, which should be 30 - 50 years.

New Vaal, Matla, Grootegeluk and Duvha coals satisfied the above criteria and were accordingly selected for this study.

3.2.2 Background information on selected coals

Geographical, technical and historical information on the selected coals is given in Table 3.1.

Table 3.1: Information on the selected South African coals

Colliery	New Vaal	Matla	Grootegeluk	Duvha
Location of mine	Free State	Mpumalanga	Limpopo	Mpumalanga
Coal field	Sasolburg	Highveld	Waterberg	Witbank
Production rate (Mt/a) ¹	15.2	14.0	15.0	16.0
Started production	1985	1979	1985	1979
Expected lifetime (years) ¹	30 - 40	40 - 50	40 - 50	30 - 40
Coal preparation	Washed	Raw coal	Washed	Raw coal
Receiving power station	Lethabo	Matla	Matimba	Duvha
Power station rating (GWe)	3.6	3.6	3.6	3.5

¹ 2005

Table 3.1 shows that the coals selected are from three different provinces in South Africa and four different coal fields.

3.3 Coal characterisation

A representative (\pm) 1 000 kg coal sample was received from each of the four mines. The coal was used to carry out coal characterisation tests, thermogravimetric analysis and fluidised bed gasification experiments. The results obtained are discussed in relation to how the coal is expected to perform in a fluidised bed gasifier.

3.3.1 Coal characterisation parameters

3.3.1.1 Proximate, ultimate and calorific value analyses

The proximate, ultimate and calorific value analyses are the analyses most often carried out on coal samples and the results are given in Table 3.2. The analyses were carried out by Advanced Coal Technologies (Pretoria) in accordance with the methods given in Table 3.2.

Table 3.2: Proximate analysis, ultimate analysis and calorific value

		New Vaal	Matla	Grootegeluk	Duvha
Proximate analysis	Standard				
Ash content (%)	ISO 1171	40.40	33.40	34.90	32.50
Inherent moisture (%)	SABS 925	5.80	3.50	1.60	1.80
Volatile matter (%)	ISO 562	19.20	21.00	24.90	19.90
Fixed carbon (%)	By diff.	34.60	42.10	38.60	45.80
Ultimate analysis					
Carbon (%)	ISO 12902	42.58	50.66	51.96	58.70
Hydrogen (%)	ISO 12902	2.19	2.65	3.15	3.33
Nitrogen (%)	ISO 12902	0.89	1.07	0.99	1.27
Sulphur (%)	ISO 19759	0.69	0.74	1.58	1.10
Oxygen (%)	By diff.	7.54	7.97	5.85	3.14
Calorific value					
Calorific value (MJ/kg)	ISO 1928	15.07	18.60	19.80	21.10

Table 3.2 shows that the selected coals have low calorific values and high ash contents, and are therefore low in grade (Grade D). The inherent moisture and oxygen contents indicate that the coals are bituminous in rank. Although fluidised beds are known for their ability to process high-ash coals, the high ash content could have a negative impact on the efficiency of the gasifier.

3.3.1.2 Petrographic analysis

The petrographic analysis was carried out Petrographics SA (Pretoria) in accordance with the ISO 7404-3 method. The maceral contents and vitrinite random reflectance of the selected coals are shown in Table 3.3.

Table 3.3: Petrographic analysis

	New Vaal	Matla	Grootegeeluk	Duvha
Vitrinite (% daf ¹)	23	38	52	13
Liptinite (% daf)	3	5	7	4
Total inertinite (% daf)	74	57	41	83
Vitrinite random reflectance (%)	0.53	0.64	0.68	0.75

¹ Dry ash free

From Table 3.3 it can be seen that the vitrinite random reflectance values are between 0.53 and 0.75 %. According to the classification system by Du Cann (2006) shown in Figure 3.1, the coals are bituminous in rank and low to medium in vitrinite content.

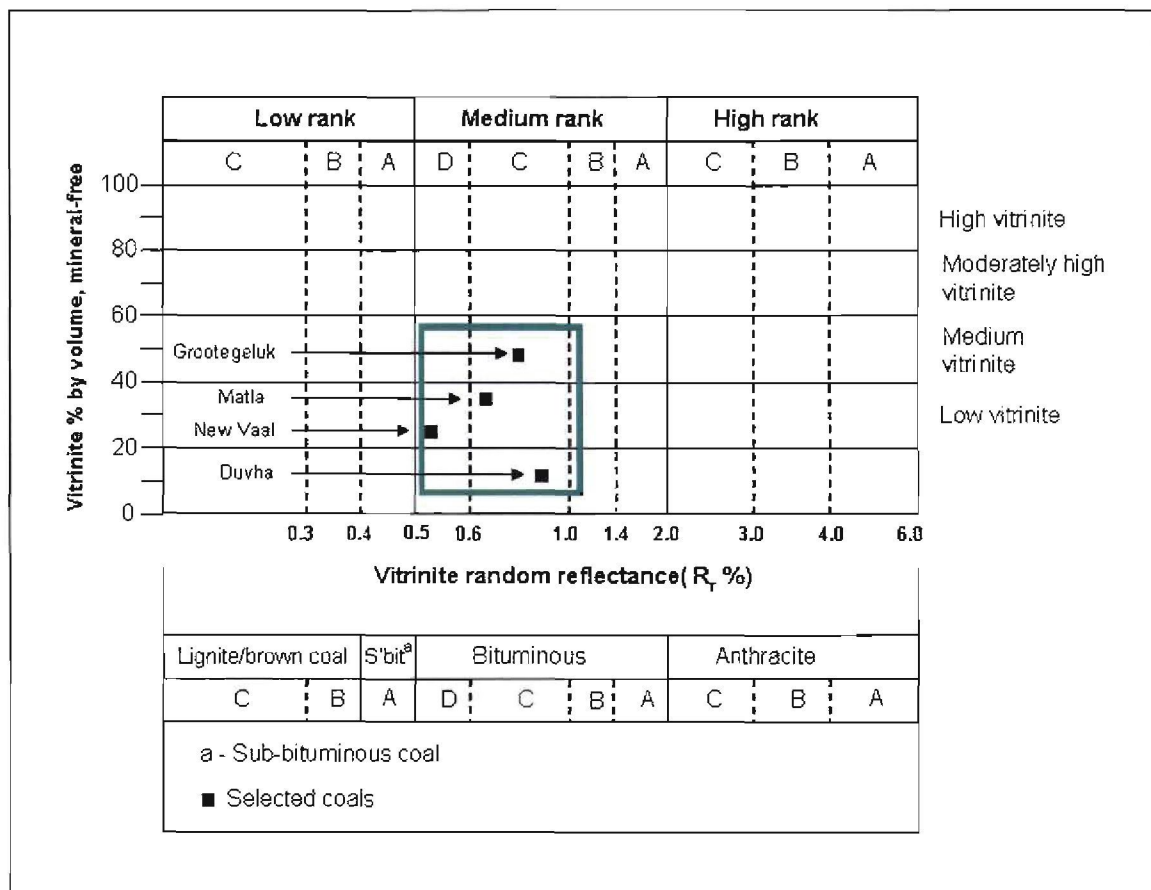


Figure 3.1: Rank classification system using vitrinite random reflectance

New Vaal coal has the lowest rank parameter, being closer to the sub-bituminous coals, and Duvha has the highest rank parameter, being closer to the semi-anthracite coals. Pinheiro (1999) reported that 95 % of South African coals fall within the green square shown in Figure 3.1. The selected coals are therefore representative of the variation in rank and vitrinite content within South African coals.

3.3.1.2 Structural and physical properties

The structural and physical properties of the selected coals are given in Table 3.4.

Table 3.4: Structural and physical properties

	New Vaal	Matla	Grootegeluk	Duvha
BET surface area (m ² /g) ¹	7.01	2.08	0.38	0.17
Bulk density (kg/m ³) ²	1 700	1 620	1 570	1 577
BET pore diameter (nm) ¹	11.3	15.4	101.1	16.5
BET Porosity (%) ³	3.4	1.3	1.5	0.1
Hardgrove grindability index ⁴	66	51	47	60

¹ Carried out by Protechnik Laboratories (Pretoria) using the BET method

² Measured by the CSIR (Pretoria) using the method referenced in Section 2.2.1.3

³ Calculated using BET surface area, BET pore diameter and bulk density (equation (2.3))

⁴ Measured by Advanced Coal Technologies (Pretoria) using the ISO 5074 method

From Table 3.4 it can be seen that the surface area and porosity of the coals decrease with increasing rank. The higher-rank coals have experienced more extensive coalification (pressure and time) and therefore have lower surface areas and porosities. Table 3.4 also shows that the pores are in the mesopore (2-50 nm) and macropore range (> 50 nm). The hardgrove grindability index (HGI) shows no clear relationship with the rank of the coal.

3.3.1.3 Caking properties

Table 3.5 shows that only the Grootegeluk coal is weakly caking. It has been found by other investigators (Du Cann, 2006) that high-ash, high-inertinite and low-volatile bituminous coals tend to be non-caking in nature. Severe agglomeration of coal in a fluidised bed gasifier is therefore not expected to occur.

Table 3.5: Free swelling index and Roga index of selected coals

	New Vaal	Matla	Grootegeluk	Duvha
Free swelling index (FSI) ¹	0	0	1	0
Roga index (RI) ²	0	0	10	0

¹ Measured by Advanced Coal Technologies (Pretoria) using the ISO 501 method

² Measured by Advanced Coal Technologies (Pretoria) using the ISO 335 method

3.3.1.4 Ash melting temperatures and ash analysis

The ash melting temperatures and analysis of the ash were determined by SABS (Pretoria) and are given in Table 3.6 together with the measurement methods that were used.

Table 3.6 shows that the ash softening temperatures (ST) of the selected coals are all above 1 400 °C. Clinkering of the coals in a fluidised bed gasifier, which normally operates below 1 000 °C, is therefore not expected to occur. The ash analysis shows that the ash consists mainly of SiO₂ and Al₂O₃, and that the ash melting temperature increases with increasing Al₂O₃ content.

3.4 Summary of coal characterisation tests

The proximate analysis shows that the selected coals have low calorific values and high ash contents, and are therefore low in grade.

Table 3.6: Ash melting temperatures and analysis of the ash

	New Vaal	Matla	Grootegeeluk	Duvha
Ash melting temperature	In accordance with ASTM D 27			
DT (°C)	1 600	1 400	1 350	1 460
ST (°C)	1 600	1 450	1 410	1 500
HT (°C)	1 600	1 480	1 480	1 560
FT (°C)	1 600	1 500	1 500	1 600
Ash composition	In accordance with ASTM D 3862			
SiO ₂ (%)	56.7	48.2	62.5	55.2
Al ₂ O ₃ (%)	31.7	26.4	21.8	28.6
FeO ₃ (%)	2.61	4.33	8.22	5.22
P ₂ O ₅ (%)	0.25	0.98	0.33	0.64
TiO ₂ (%)	1.55	1.51	0.92	1.66
CaO (%)	2.50	9.71	2.35	3.11
MgO (%)	0.76	1.93	0.83	1.07
K ₂ O (%)	0.44	0.77	0.87	0.90
Na ₂ O (%)	0.19	0.46	0.18	0.10

The petrographic analysis shows that the coals are high in inertinite and medium to low in vitrinite content. The vitrinite random reflectance, which is regarded as a reliable rank parameter, shows that the coals selected are representative of the variation of rank within South African bituminous coals.

Structural and physical analyses of the coals show that the higher rank coals have lower surface areas and porosities due to the more extensive coalification (pressure and time) it has been subjected to.

The characterisation tests also show that the coals have low caking properties and high ash fusion temperatures. Agglomeration and clinkering of the char in a fluidised bed gasifier is therefore not expected to occur at temperatures below 975 °C.

CHAPTER 4 THERMOGRAVIMETRIC ANALYSIS

4.1 Introduction

In this chapter the carbon dioxide–char gasification reaction is investigated for each coal using a thermogravimetric analyser (TGA). Experiments using the TGA analyser were carried out in order to determine the relative gasification reactivity of chars, derived from the selected coals, in CO₂ and to determine the grain model parameters (k and β) for each char. A brief description of the experimental apparatus and operating procedures is given in Sections 4.2 and 4.3. The experimental programme is discussed in Section 4.4, while the experimental results are presented and discussed in Section 4.5. Finally, the results are summarised in Section 4.6.

4.2 Experimental apparatus

Thermogravimetric analysis is a semi-batch experiment which involves placing a pre-weighed sample in a reaction chamber and then exposing the sample to predetermined conditions of temperature, pressure and reacting gas concentration flowing through the reaction chamber. The main advantages of the TGA are that:

1. The mass of the coal sample is continuously recorded during the reaction period, which enables instantaneous conversion levels and reaction rates to be calculated; these can be used for reaction rate modelling.
2. Since the gas flowrate to the apparatus is large compared with the sample mass, the concentration of the reacting gas at the gas-solid surface is very close to that of the feed gas composition and can be easily manipulated.

The TGA used was a Bergbau-Forschung GmbH7 model supplied by Deutsche Montan Technologie (DMT), Germany. This TGA can handle particles with diameters between 1 and 5 mm and sample masses up to 2 g at temperatures up to 1 000 °C and pressures up to 10 MPa.

A schematic representation of the apparatus is shown in Figure 4.1 and a photograph in Figure 4.2. The apparatus shown consists of a gas supply system, the TGA (reactor and microbalance), a pressure control system and a data acquisition interface. A detailed description of the TGA is given by Kaitano (2007).

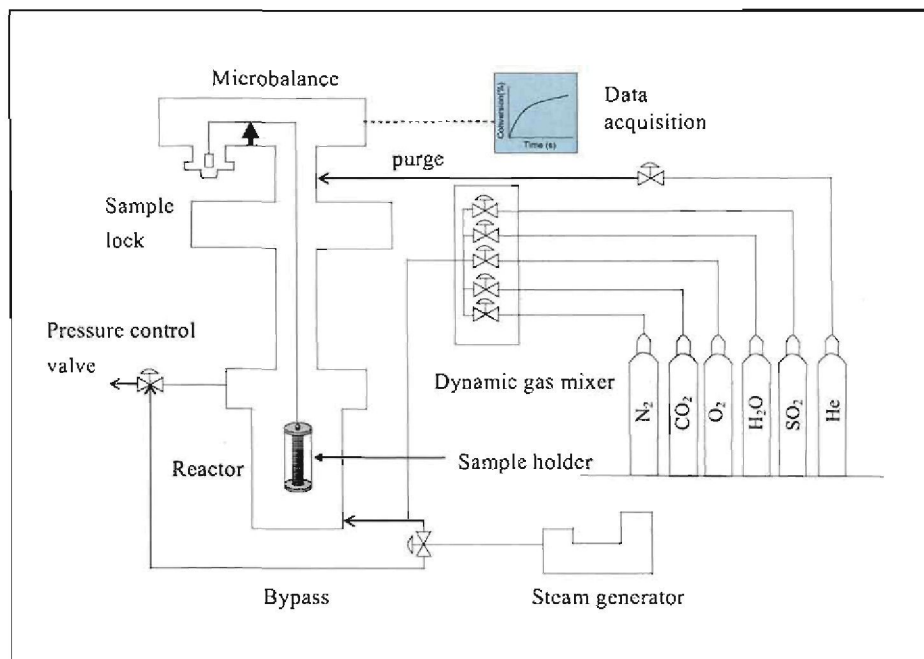


Figure 4.1: Schematic representation of the apparatus

4.3 Experimental procedure

Coal samples received from New Vaal, Matla, Grootegeluk and Duvha collieries were screened ($0.85 \text{ mm} < d_p < 1.2 \text{ mm}$) into representative batches for the TGA experiments. For each experiment $\pm 100 \text{ mg}$ of the screened sample was loaded into the basket of the TGA. The TGA was heated to the operating temperature before the sample basket was loaded to the upper section of the reaction chamber which is at a low temperature ($< 50 \text{ }^\circ\text{C}$). Before lowering the sample basket into the hot zone, the reaction chamber was flushed with reacting gas (CO₂) in order to purge oxygen from the system. The data logging computer programme was started and the sample basket was lowered into the reaction zone of the TGA. The mass loss of the sample was recorded by the data acquisition system and the experiment was continued until no further mass loss was observed. The reaction data (time, temperature and mass) was copied to an Excel[®] file for data processing.

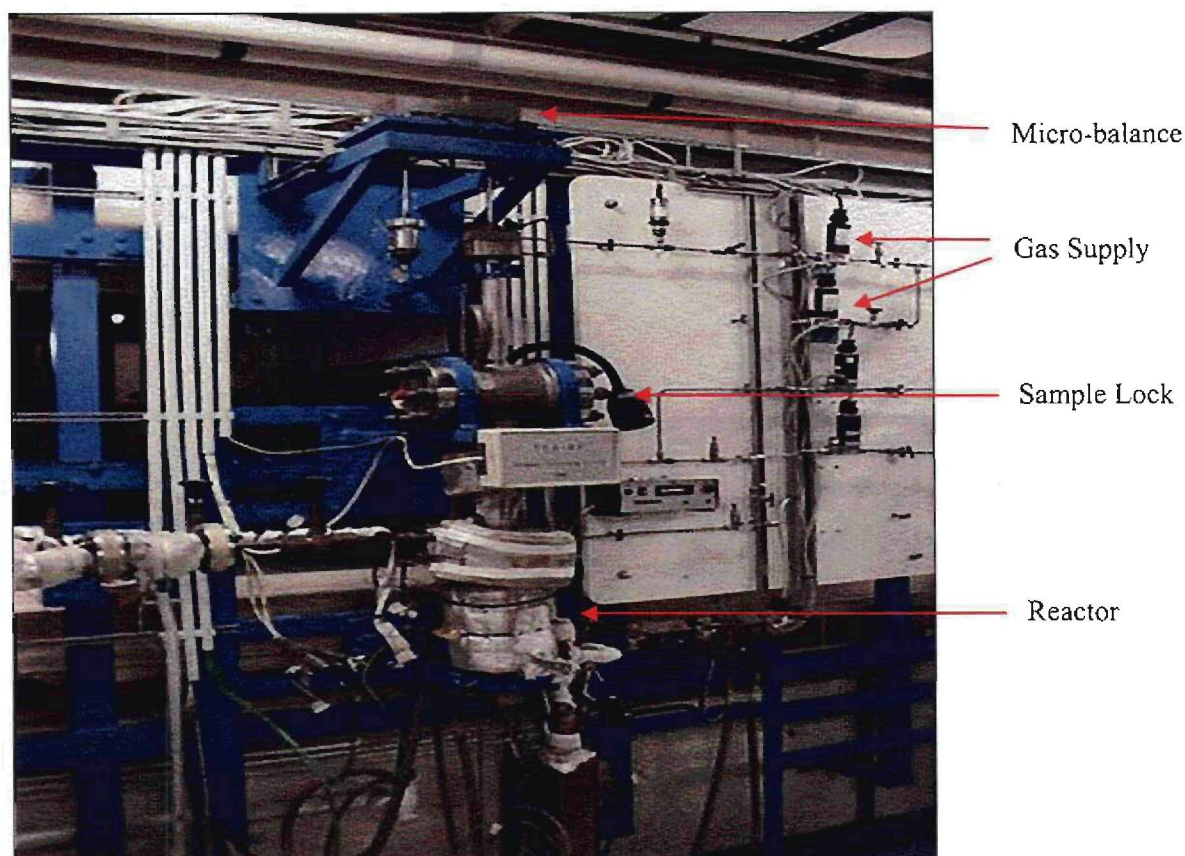


Figure 4.2: Photograph of the thermogravimetric analyser (Kaitano, 2007)

4.4 Experimental programme

The reaction conditions used for the gasification experiments are given in Table 4.1.

Table 4.1: Reaction conditions used for gasification experiments

Coal	Pressure (kPa)	Particle size (mm)	CO ₂ concentration (mole %)	Temperatures (°C)
New Vaal	87.5	0.85 - 1.20	100	875, 900, 925, 950
Matla	87.5	0.85 - 1.20	100	875, 900, 925, 950
Grootegeeluk	87.5	0.85 - 1.20	100	875, 900, 925, 950
Duvha	87.5	0.85 - 1.20	100	875, 900, 925, 950

For each test, the coal sample mass was (\pm) 100 mg and the CO₂ flowrate was 1 800 ml min⁻¹(STP). The tests were carried out at ambient pressure which was assumed to be approximately 87.5 kPa (absolute).

4.5 Results and discussion

4.5.1 Normalisation of experimental data

The experiment on Matla coal at 925 °C is used in this Section to demonstrate how the experimental data were processed in order to obtain plots of char conversion vs. time for each coal and temperature. The results of all the experiments are given in Section 4.5.2.

Data obtained from a thermogravimetric analyser are in the form of mass as a function of time, as shown in Figure 4.3 for Matla coal at 925 °C. The sample mass decreases rapidly during the first minute or two of the experiment during which time the coal is pyrolysed (devolatilised). During the second stage, the fixed carbon is converted. The fixed carbon conversion rate gradually decreases from its initial value until a stage is reached where no further loss in mass is observed. The mass loss during the pyrolysis and carbon reaction stages agrees within $\pm 3\%$ with the volatile matter and fixed carbon content of the coal. The residue obtained after the experiment agrees within $\pm 5\%$ with the ash content of the coal (Table 3.2).

The first four minutes of the TGA experiment is shown in Figure 4.4. It can be seen from the plot of mass loss as a function of time that pyrolysis was complete within 1.2 minutes. An accurate estimate of the time required to complete pyrolysis (breakpoint), can be obtained by fitting a polynomial equation (6-th order) to the first four minutes of the experimental data given in Figure 4.4. The breakpoint is obtained by calculating the time at which the first derivative of mass ($m_i(t)$) as a function of time ($\frac{d(m_i(t))}{dt}$), attains a constant value (Engelbrecht, 2007).

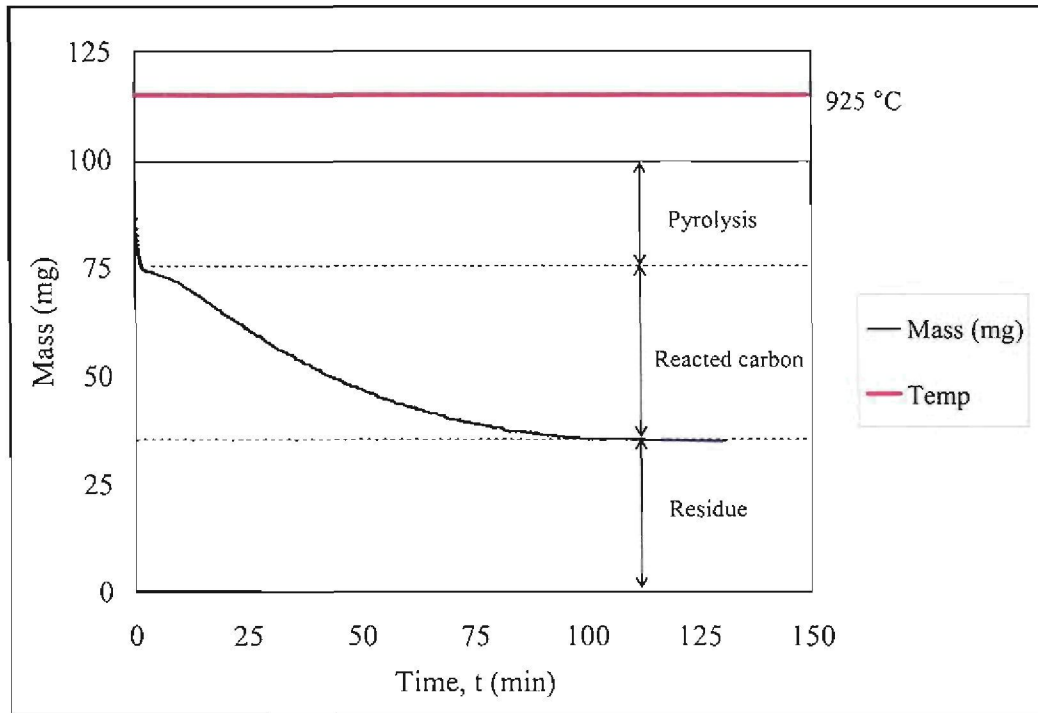


Figure 4.3: Isothermal gasification of Matla coal at 925 °C in 100 % CO₂ at 87.5 kPa

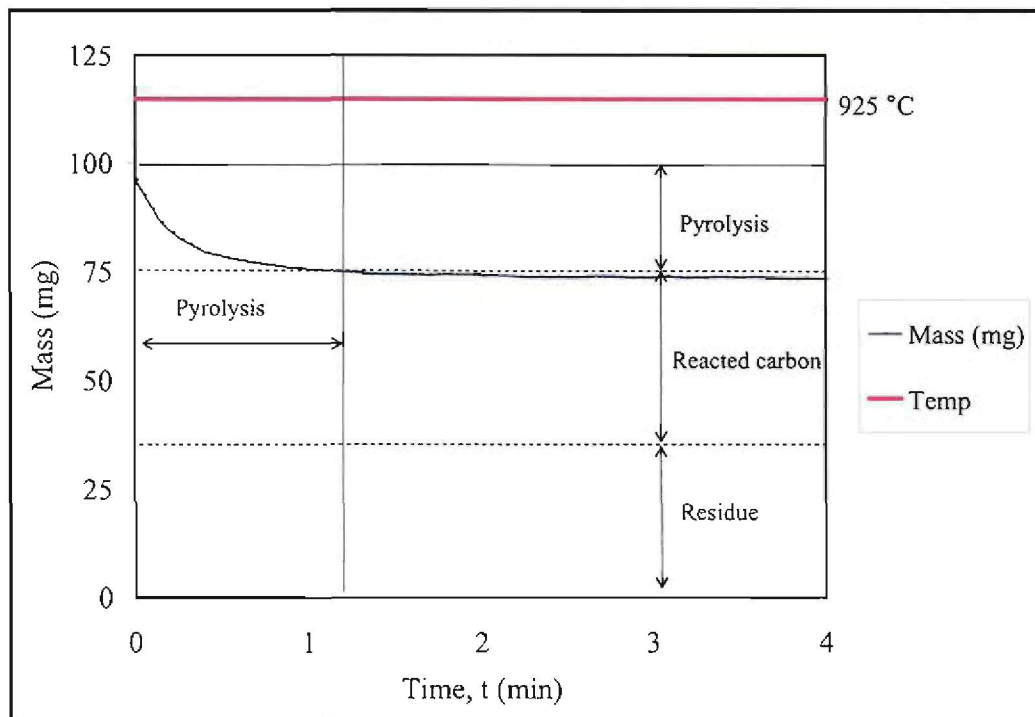


Figure 4.4: Initial isothermal gasification of Matla coal at 925 °C in 100 % CO₂ at 87.5 kPa

The char (reacted carbon) conversion stage, shown in Figure 4.5, was obtained by excluding the mass loss data of the coal pyrolysis stage. For the other experiments the coal pyrolysis time was typically between 0.5 and 2 minutes.

The experimental data shown in Figure 4.5 were normalised by expressing the char conversion variation on an ash-free basis according to equation (4.1) (Kaitano, 2007)

$$X = \frac{m_0 - m_t}{m_0 - m_{\text{ash}}} \quad (4.1)$$

A typical normalised result derived from the data in Figure 4.5 is shown in Figure 4.6.

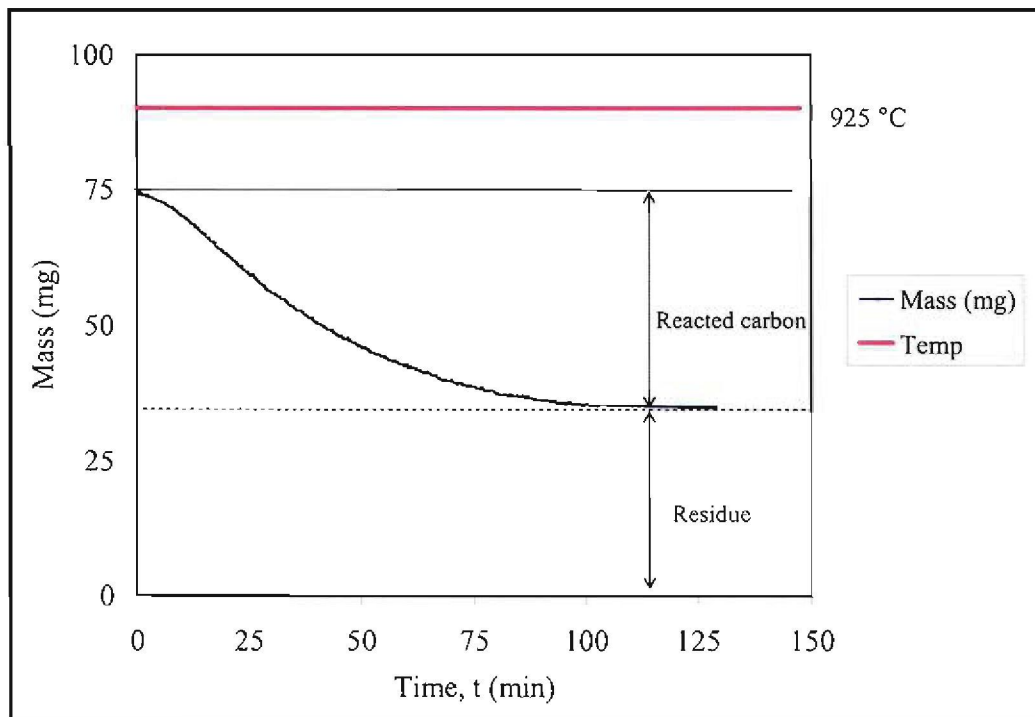


Figure 4.5: Isothermal gasification of Matla char at 925 °C in 100 % CO₂ at 87.5 kPa

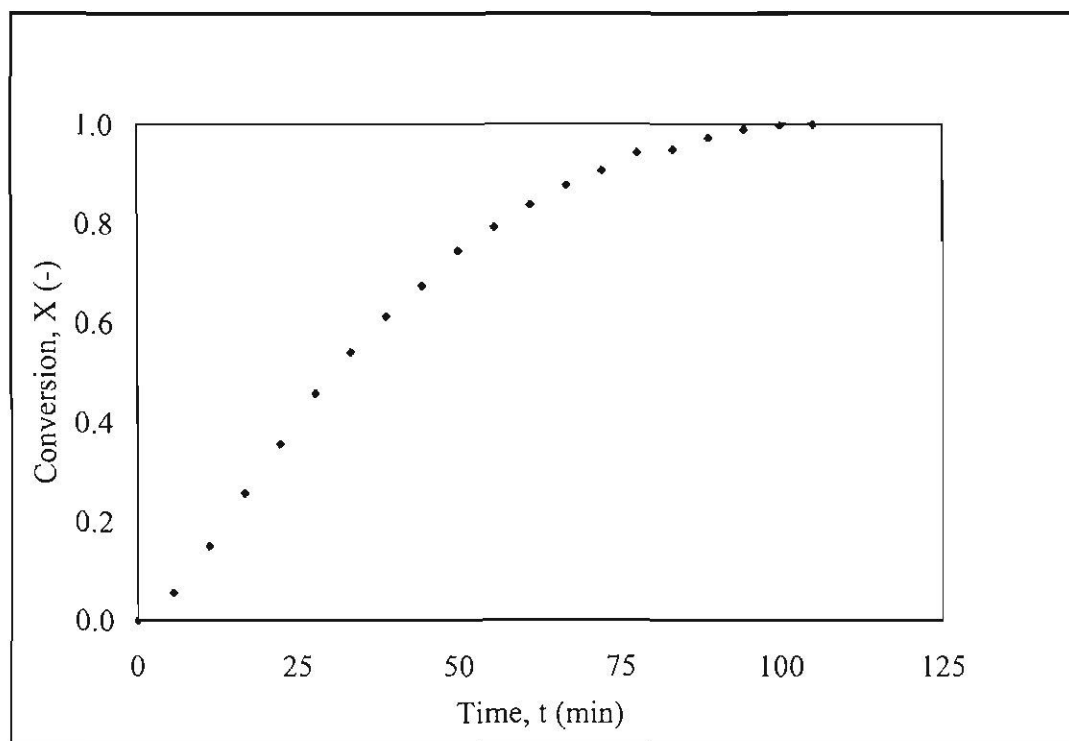


Figure 4.6: Conversion of Matla char at 925 °C in 100 % CO₂ at 87.5 kPa

For each test, twenty data points were used for the calculation of R_s , k and β given in Sections 4.5.2 and 4.5.3. Twenty data points was considered to be sufficient since using eighty data points resulted in a difference of less than $\pm 3\%$ in the calculated values of R_s , k and β which is within the repeatability of the experiments ($\pm 5\%$).

During the tests on Grootegeluk coal it was observed that the char formed a dense cake in the basket of the TGA. This can be attributed to the caking properties of Grootegeluk coal as shown in Table 3.5. Caking of char could have resulted in diffusion effects since the test at 925 °C produced a similar result to that of the test at 950 °C. The tests on Grootegeluk coal were therefore repeated using char prepared in the apparatus shown in Appendix A.1. The resulting char did not cake in the basket of the TGA as experienced with the experiments that used Grootegeluk coal directly in the TGA.

4.5.2 Gasification reactivity

The relative gasification reactivity at 950 °C of the chars derived from the selected coals is shown in Figure 4.7. The relative gasification reactivities at 875, 900 and 925 °C are given in Appendix A.2.

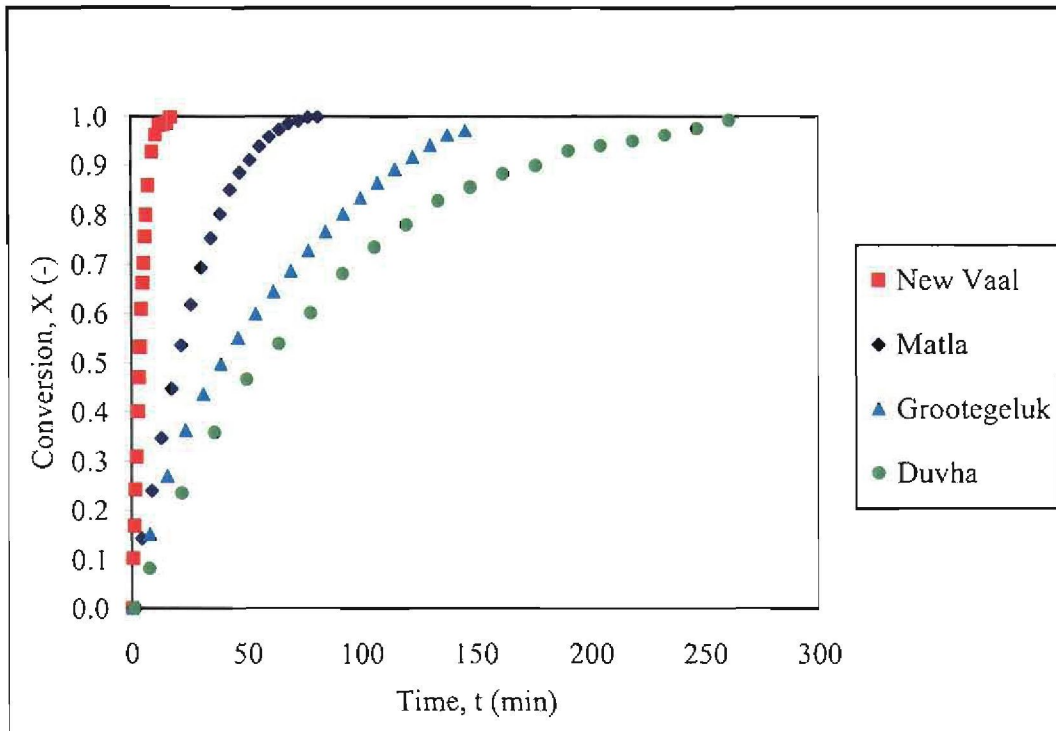


Figure 4.7: Relative char gasification reactivity at 950 °C in 100 % CO₂ at 87.5 kPa

The relative reactivity of char (relative to other chars) is often compared by using the reactivity index R_s (Zhang *et al.*, 2006 and Ye *et al.*, 1997) given in Section 2.3.2, equation (2.8):

$$R_s = \frac{0.5}{\tau_{0.5}}$$

with $\tau_{0.5}$ being the time (h) taken for the char to reach a fractional conversion of 0.5.

The reactivity indices calculated from Figure 4.7 and Appendix A.2 are given in Table 4.2 for each char.

Table 4.2: Reactivity indices (h^{-1}) of chars at 875, 900, 925 and 950 °C in 100 % CO₂ at 87.5 kPa

Char	Temperature (°C)				Rank parameters of parent coal	
	875	900	925	950	Vitrinite random reflectance (%)	C (%) Dry ash free
New Vaal	2.75	3.80	5.63	8.92	0.53	79.1
Matla	0.51	0.65	0.99	1.56	0.64	80.2
Grootegeeluk	0.14	0.27	0.40	0.75	0.68	81.8
Duvha	0.13	0.21	0.34	0.52	0.75	84.7

Table 4.2 shows that the reactivity index of the chars decreases with increase in rank of the coal, as indicated by the vitrinite random reflectance and carbon content (daf) of the parent coals. A similar result was obtained by Kwon *et al.* (1988) who used a TGA to measure the reactivity of Chinese, Canadian and Australian coals with carbon contents (daf) between 70 and 90 %. The higher rank coals (Grootegeeluk and Duvha) have lower porosities and surface areas (Table 3.4), and since the CO₂ gasification rate of char is controlled by chemical reaction at the char surface, the reactivity indices of these chars are lower. The orders of magnitude of the reactivities obtained by Kwon *et al.* (1988) are similar to those reported in Table 4.2 at 900 °C for the Matla, Grootegeeluk and Duvha coal chars. The reactivity of the New Vaal coal char, however, is orders of magnitude higher than those achieved by Kwon *et al.* (1988) at 900 °C. The reactivity index of New Vaal coal char (bituminous coal) has the same order of magnitude as South Australian lignite (Bowman's coal) as reported by Ye *et al.* (1997).

4.5.3 Evaluation of experimental data against the grain model

The experimental data were evaluated against the grain model described in Chapter 2. Equation (2.9) and (2.10) given in Chapter 2, Section 2.3.3, reduces to equation (4.2) since the CO₂ concentration was fixed at 100 % for this investigation.

$$\frac{dX}{dt} = k(1 - X)^\beta \quad (4.2)$$

Equation (4.3) and (4.4) are the integrated forms of equation (4.2) and expresses the conversion as a function of time:

$$X = 1 - [1 - (1 - \beta)kt]^{1/(1-\beta)} \quad (\text{for } \beta \neq 1) \quad (4.3)$$

$$X = 1 - e^{-kt} \quad (\text{for } \beta = 1) \quad (4.4)$$

The model parameters k and β were calculated by regression using the experimental data for New Vaal char, as shown in Figure 4.8. Evaluations of the grain model for the Matla, Grootegeluk and Duvha chars are given in Appendix A.3. The grain model parameters for each char and temperature is given in Table 4.3.

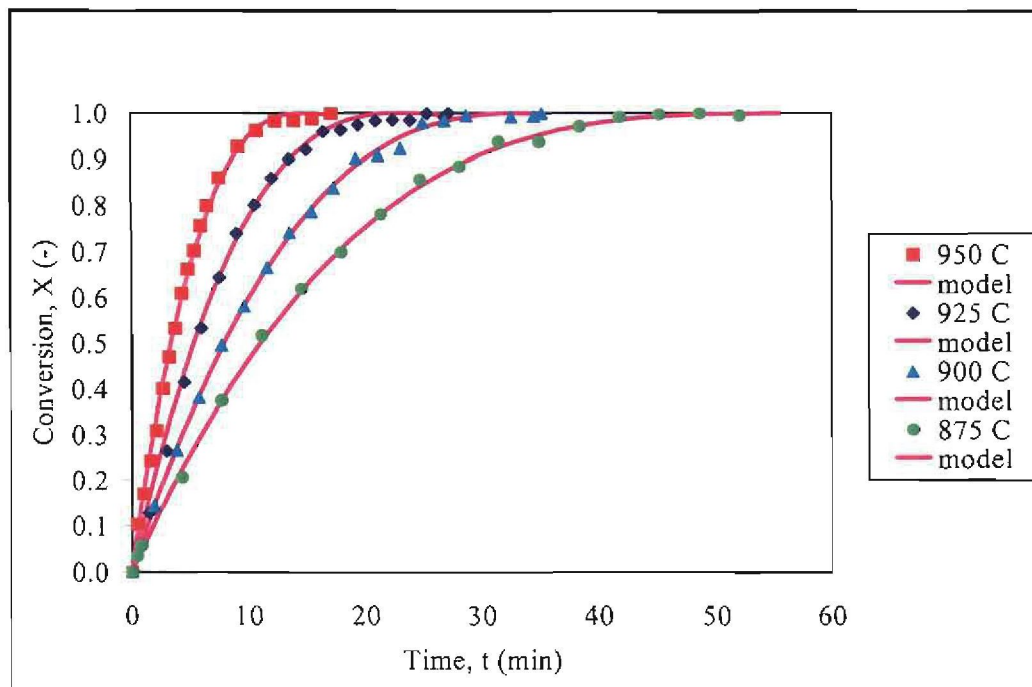


Figure 4.8: Grain model for New Vaal char at 87.5 kPa in 100 % CO₂

Table 4.3: Grain model parameters k and β for selected chars

Char	Temperature (°C)							
	875		900		925		950	
	k^1 min ⁻¹	β^2	k min ⁻¹	β	k min ⁻¹	β	k min ⁻¹	B
New Vaal	0.0571	0.69	0.0773	0.62	0.1147	0.62	0.1810	0.63
Matla	0.0098	0.47	0.0127	0.48	0.0194	0.49	0.0316	0.63
Grootegeeluk	0.0031	0.91	0.0061	0.93	0.0090	0.92	0.0166	0.88
Duvha	0.0028	0.80	0.0043	0.71	0.0073	0.83	0.0116	0.87

¹ The estimated error in the calculation of k is $\pm 5\%$; based on the repeatability of the TGA experiments ($\pm 5\%$)

² The estimated error in the calculation of β is $\pm 10\%$; based on the repeatability of the TGA experiments ($\pm 5\%$)

Table 4.3 shows that each char has a characteristic structural parameter β . The variation of β with temperature could be due to errors associated with the experimental data.

The experimental data suggest that the New Vaal char reacts according to the shrinking core model ($\beta = 2/3$) which is a special case of the grain model. The shrinking core model assumes that the reaction occurs at the external surface of the particle and gradually moves to the middle of the particle, leaving an ash layer behind. The other special case of the grain model is the homogenous model ($\beta = 1$) which assumes that the gasification reaction occurs 'uniformly' throughout the particle volume. (Ye *et al.*, 1997). The results indicate that the Grootegeeluk char reacts predominantly according to the homogenous model, whereas for the Duvha char, the reaction takes place via both models simultaneously (shrinking reacted core model).

The char conversion rate (dX/dt) shown in Figure 4.9 was calculated using the experimental data shown in Figure A.3a (Appendix A.3). The grain model plot shown in Figure 4.9 was calculated using equation (4.2) and the values of k and β for Matla char at 925 °C given in Table 4.3. The experimental data plot given in Figure 4.9 shows that the char conversion rate reaches a maximum value at a conversion of ≈ 0.18 . This could indicate pore growth and increases in surface area, followed by collapse of the pores and a decrease in surface area as the reaction proceeds to completion. This result was confirmed by a test done at the University of Pretoria using a Mettler 851e TGA (Appendix A.4). The results show that only the Matla char exhibits a maximum in the char conversion rate at a conversion of ≈ 0.21 . The lower value of β ($\beta \approx 0.5$) obtained for Matla char is indicative of a higher char conversion rate at lower conversion levels, with a rapid decrease in the conversion rate at higher conversion levels. The random pore model of Bhatia and Perlmutter (1980) is often used to describe experimental data that shows a maximum conversion rate at lower conversion levels. Since only the Matla char exhibited this behaviour and the maximum rate was only $\pm 15\%$ higher than the initial rate, the random pore model was not applied to model the experimental data.

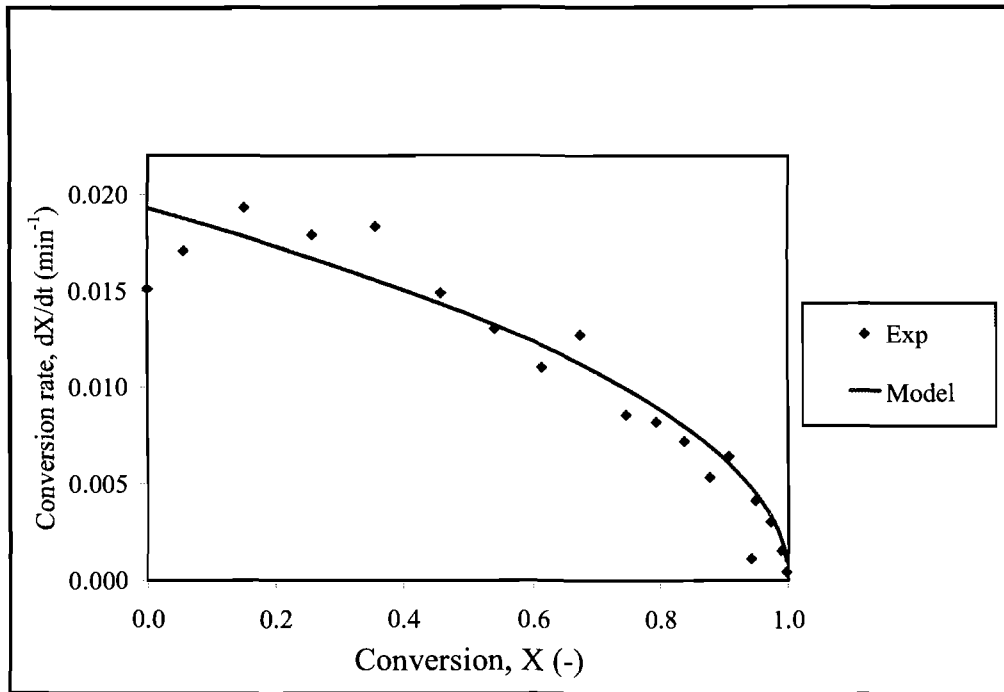


Figure 4.9: Conversion rate of Matla char in 100 % CO₂ at 925 °C

4.5.4 Arrhenius activation energy

The variation of the reaction rate constant (k) with temperature shown in Table 4.3 can be described by the Arrhenius equation (4.5) also given in Chapter 2, Section 2.3.3:

$$k = k_0 \exp\left(\frac{-E}{RT}\right) \quad (4.5)$$

The Arrhenius equation can also be written as:

$$-\ln(k) = \left(\frac{E}{R}\right) \cdot \left(\frac{1}{T}\right) - \ln(k_0) \quad (4.6)$$

By plotting $-\ln k$ as a function of $1/T$, E is obtained from the slope and $\ln(k_0)$ from the intercept of the linear graph. The Arrhenius plot for each char is given in Figure 4.10. The Arrhenius constants were calculated from Figure 4.10 and are given in Table 4.4.

Table 4.4: Arrhenius activation energy (E) and pre-exponential factor (k_0)

Char	E (kJ/mol)	$\ln(k_0)$ (s^{-1})	Correlation Coefficient (R^2)
New Vaal	180 (± 14)	11.82 (± 1.40)	0.9884
Matla	184 (± 20)	10.44 (± 2.04)	0.9765
Grootegeluk	252 (± 16)	16.54 (± 1.63)	0.9919
Duvha	222 (± 9)	13.29 (± 0.88)	0.9970

The uncertainty in the calculated values of E and $\ln(k_0)$, given in Table 4.4, are obtained from the slope-error and intercept-error of the linear regression equations (Draper and Smith, 1966).

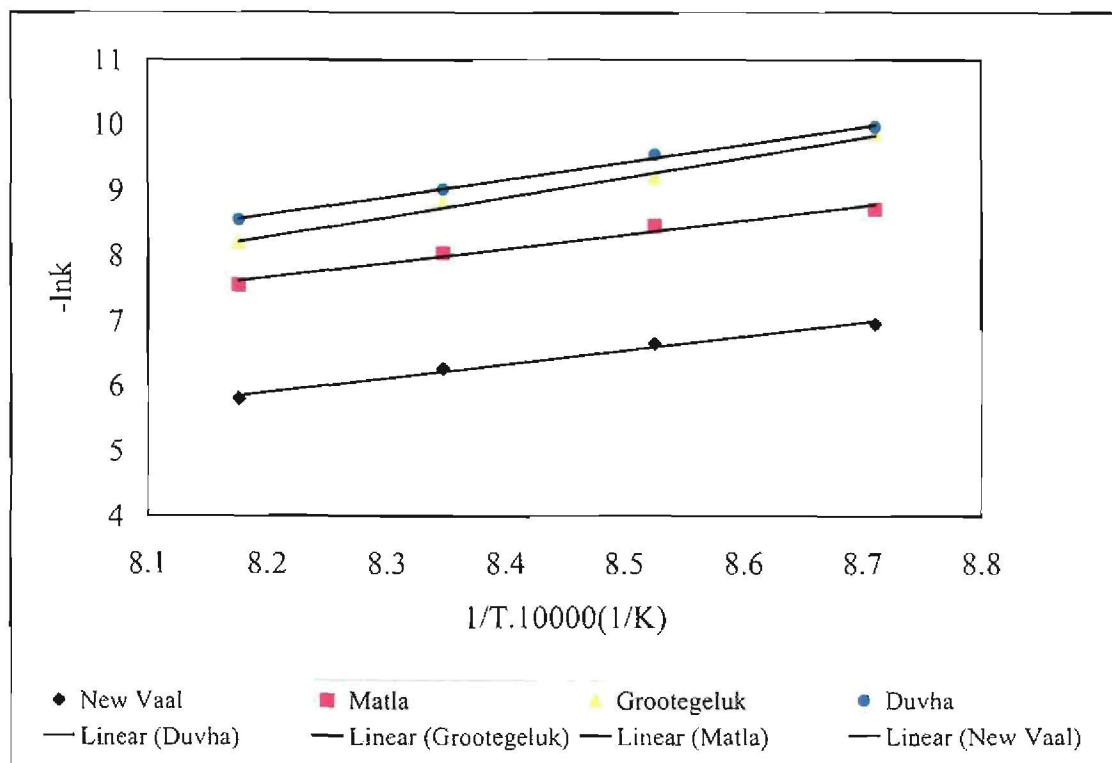


Figure 4.10: Arrhenius plots for New Vaal, Matla, Grootegeluk and Duvha chars

Kaitano (2007) investigated the gasification of a high-ash South African bituminous coal char in 100 % CO₂ at 87.5 kPa and reported an activation energy of 266 kJ/mol. An activation energy of 183 kJ/mol was obtained by Ochoa *et al.* (2001) for the gasification of Argentinean bituminous coal char in 70 % CO₂ at 100 kPa between 900 and 1160 °C.

4.6 Summary of TGA tests

The carbon dioxide gasification of four high-ash South African coal chars was studied in the temperature range between 875 and 950 °C, with 100 % carbon dioxide at an absolute pressure of 87.5 kPa, with 1 mm coal particles. It was found that the gasification rate increased with increasing temperature and decreasing rank of the parent coal. Other investigators obtained similar results for the CO₂ gasification of coal chars.

It was found that the grain model can be used to describe the char conversion, with each char having a characteristic structural parameter, β . The β parameter describes how the char structure changes during the conversion process.

The effect of temperature on the reaction rate constant can well be described by the Arrhenius equation, and the values of the activation energy are consistent with the literature on CO₂ gasification for high-ash coal chars.

CHAPTER 5 PILOT-SCALE FLUIDISED BED GASIFICATION

5.1 Introduction

In this chapter the fluidised bed gasification of each coal is investigated using a pilot-scale fluidised bed gasifier. In Section 5.2 the fluidised bed gasifier pilot plant and its operation are described in detail. The experimental programme and the test results are presented in Sections 5.3 and 5.4. Finally, a summary of the fluidised bed gasification tests is given in Section 5.5.

5.2 Pilot-scale fluidised bed coal gasifier

A pilot-scale fluidised bed gasifier (FBG) at the CSIR was used to investigate the gasification performance of the four selected coals in terms of carbon conversion and gas quality. The main advantages of the pilot FBG are that:

- (1) The conditions that coal particles are exposed to, such as heat-up time, gas atmosphere and attrition in the bed, are representative of a large-scale FBG.
- (2) Since the operation is continuous, gas produced by the FBG can be sampled and analysed online.

The FBG tests, however, require large coal samples (350 kg per test) and the furnace takes ± 15 h to heat up and stabilise at the required operating conditions.

5.2.1 Plant and process description

A flow diagram of the FBG pilot plant is given in Figure 5.1 and a photograph is also shown in Figure 5.2. The pilot plant, previously used for fluidised bed combustion (FBC) trials, was retrofitted in order to carry out the test programme on the four selected coals. Specifications of the FBG pilot plant are given in Table 5.1.

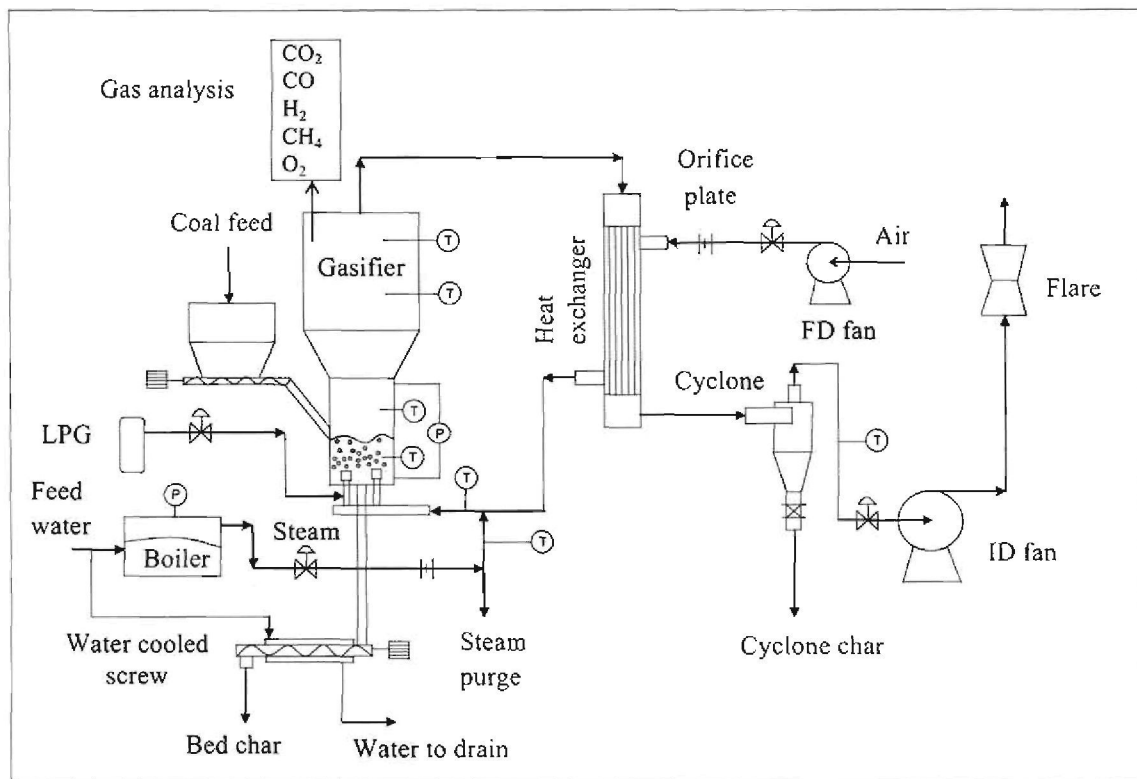


Figure 5.1: Flow diagram of the FBG pilot plant

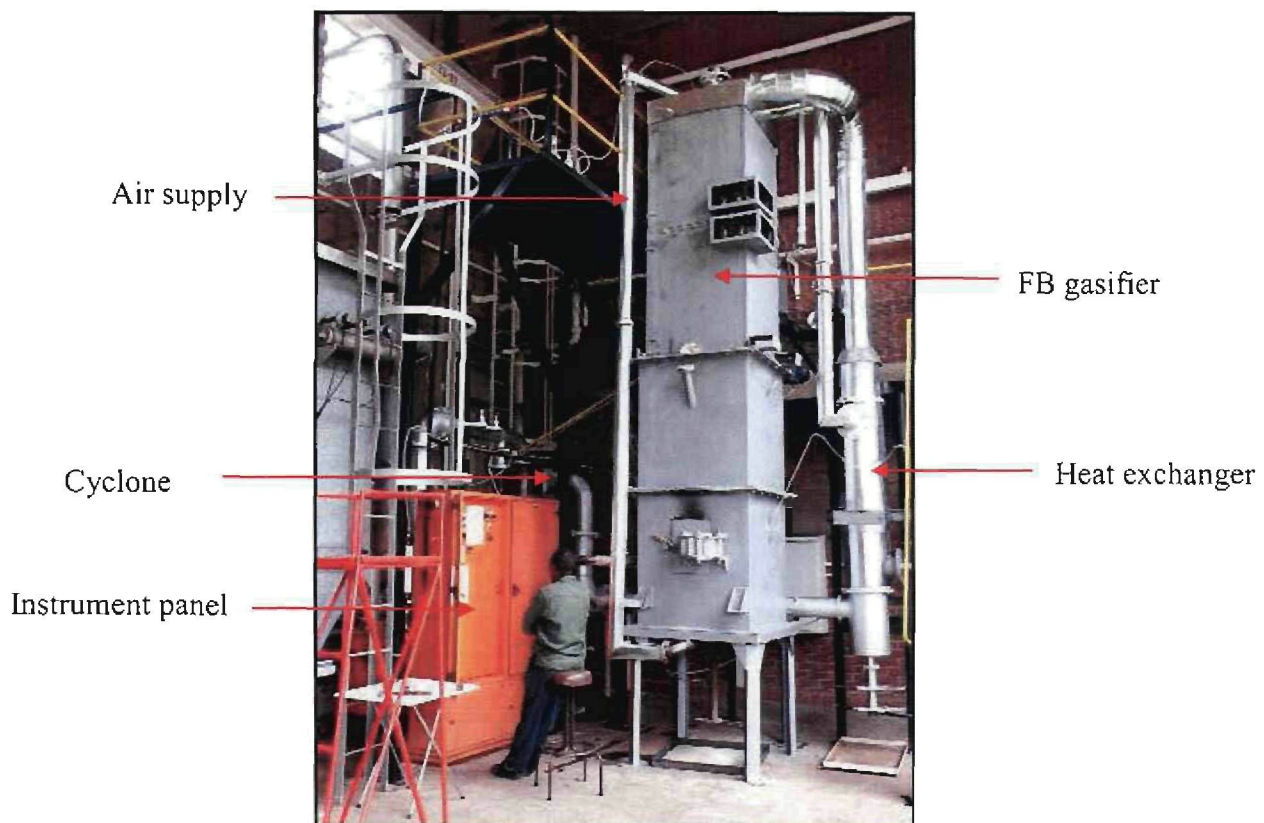


Figure 5.2: Photograph of the FBG pilot plant

Table 5.1: Specifications of the FBG pilot plant

Operating pressure	Atmospheric
Bed dimensions (m)	0.2 × 0.2 (square)
Freeboard dimensions (m)	0.55 × 0.55 (square)
Furnace height (m)	4 (2 m bed & 2 m freeboard)
Fluidised bed height (m)	< 0.6
Coal feedrate (kg/h)	18 - 30
Coal particle size (mm) (d_{50})	1 - 2.5
Coal CV (MJ/kg)	> 10
Air flowrate (Nm ³ /h)	40 - 60
Steam flowrate (kg/h)	5 - 12
Bed temperature (°C)	850 - 950
Air temperature (°C)	155 - 210
Fluidising velocity (m/s)	1.5 - 2.5

Coal, air and steam are the input streams to the process which produce the output streams of gas and char (ash). Coal is fed to the gasifier by means of a screw conveyor at a height of 1.5 m above the distributor. Steam is generated in an electrode boiler and is mixed with preheated air before introduction into the gasifier via the distributor. The gas produced during the gasification process is used to preheat the air, using a shell-and-tube heat exchanger. Char is removed from the bed (bed char) by means of a water-cooled screw conveyor and from the gas (cyclone char) by means of a cyclone which is placed after the gas cooler. The de-dusted gas is combusted (flared) before it is vented to atmosphere.

5.2.1.1 Fluidisation

In a fluidised bed coal gasifier, the char particles are suspended (fluidised) by the gas stream flowing upwards in the furnace. In order for the bed to be ‘well fluidised’, the recommended gas velocity in the bed is greater than three times the minimum fluidising velocity (U_{mf}) of the char particles. The minimum fluidising velocity can be obtained by solving equation (5.1) for U_{mf} (Geldart, 1986).

$$1.75\rho_g U_{mf}^2 + \frac{150(1-\epsilon)\mu}{d_p} U_{mf} = (\rho_{char} - \rho_g)gd_p \epsilon^3 \quad (5.1)$$

Calculated values of U_{mf} as a function of char particle size (d_p) and density (ρ_s) are given in Appendix B.1.

5.2.1.2 FBG distributor

An important component of an FBG is the gas distributor. The distributor distributes the fluidising gas (air and steam) uniformly across the bed area to provide ‘smooth’ fluidisation of the bed. In order to distribute the gas uniformly across the bed, it is essential to design the distributor so that the gas passing through it has a sufficiently high pressure drop. It is recommended that the ratio of distributor pressure drop to bed pressure drop should be greater than 0.30 ($\Delta P_D/\Delta P_B > 0.30$). Diagrams of the FBG gas distributor and details of the nozzle are given in Figures 5.3 and 5.4.

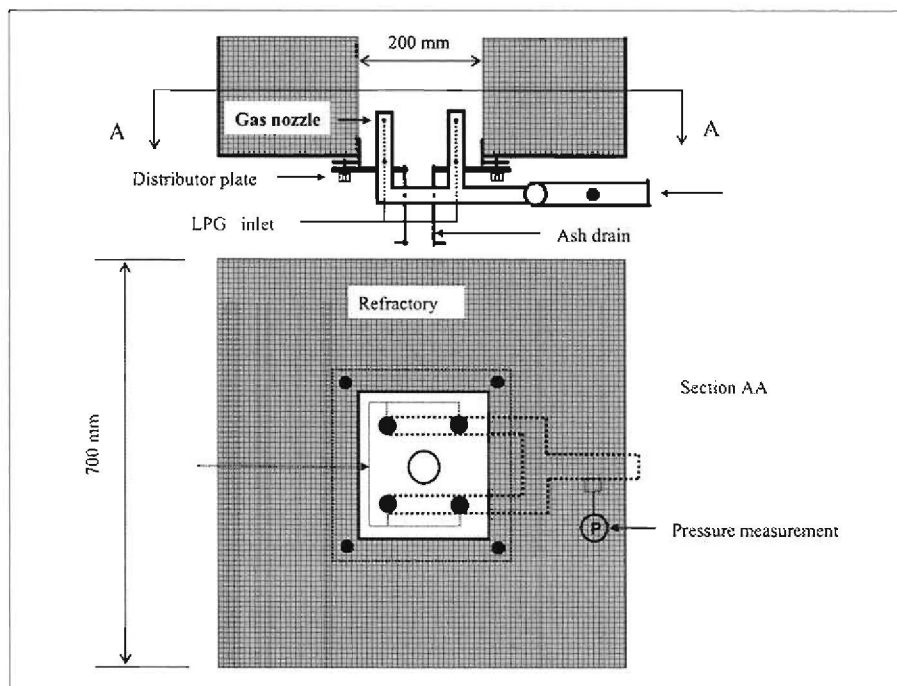


Figure 5.3: FBG distributor layout

5.2.1.3 Furnace details

The internal dimensions of the FBG and the location of the thermocouples and pressure probes are given in Figure 5.5. Figure 5.5 shows that the FBG has a 0.2 m x 0.2 m bed section, which expands to a 0.55 m x 0.55 m freeboard section.

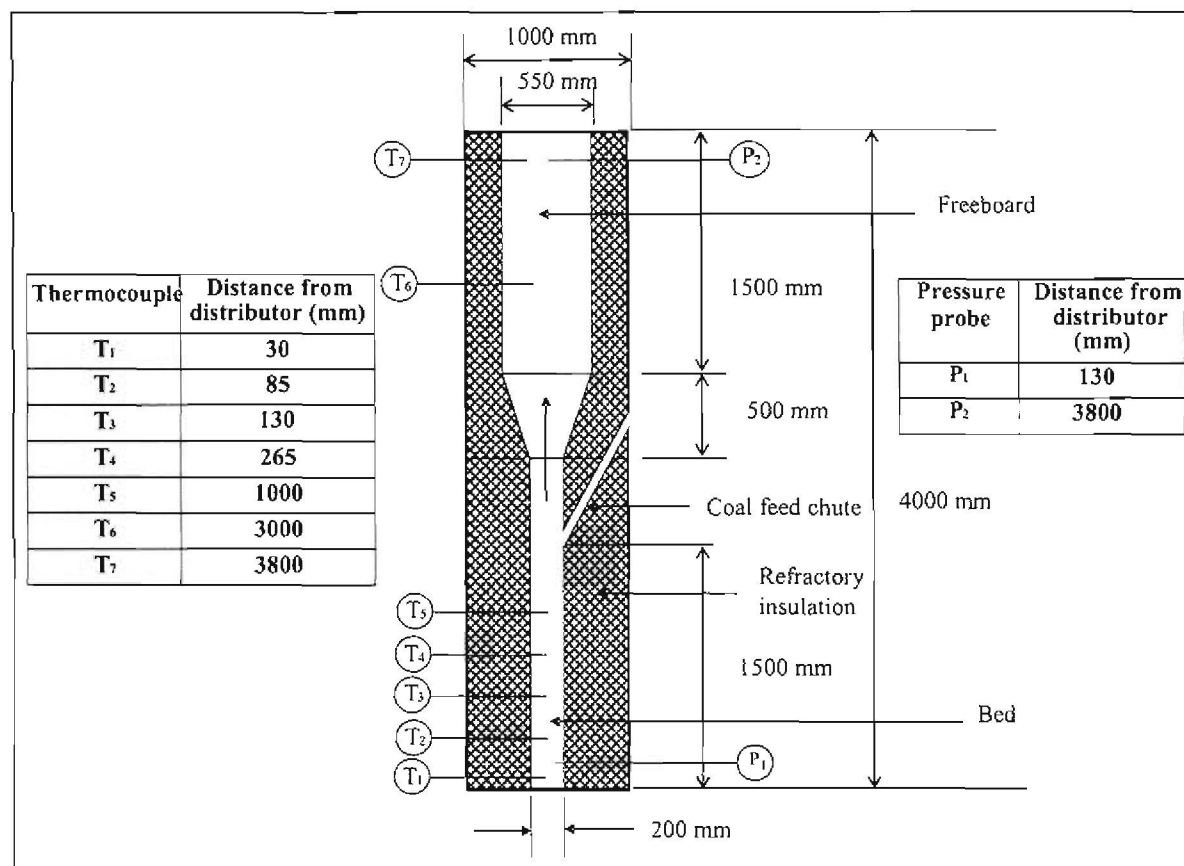


Figure 5.5: Dimensions of the FBG furnace

Coal particles that enter the furnace via the coal feed chute drop into the fluidised bed section and start the conversion to gas and char. The char particles move rapidly up and down between the gasification and combustion zones in the bed. The combustion zone is limited to the lower 10 - 15 % of the bed above the air and steam distributor and is rich in oxygen. Reaction (2.4) occurs predominantly in the combustion zone, resulting in temperatures that are higher (up to 150 °C) than the mid-bed temperature. Reactions (2.5) to (2.19) occur predominantly in the bed above the combustion zone.

Due to the fluidising action of the bed, the char particles experience attrition and break down into smaller particles. When the particles are small enough, they are entrained into the freeboard section (upper part) of the furnace. Due to the expanded nature of the freeboard, the gas velocity decreases and the particles fall back to the bed, resulting in internal circulation of particles between the bed and the freeboard. Further breakdown of the char particles results in their terminal falling velocity (U_t) being lower than the freeboard velocity and they are elutriated from the furnace. A significant proportion of the char particles (40 - 60 %) is not elutriated from the furnace and these are drained from the bottom of the bed in order to maintain a constant fluidised bed height.

5.2.2 FBG start-up and control

The FBG is started up by adding 15 kg of silica sand (0.4 - 0.85 mm) to the furnace. The silica sand is fluidised by starting the forced-draught (FD) and induced-draught (ID) fans. LPG is injected into the fluidised silica sand bed via the nozzles shown in Figure 5.4. The LPG is ignited by means of a pilot flame which is inserted through the furnace door and directed down towards the bed. When the bed temperature reaches 650 °C, coal addition to the furnace is started. When the temperature reaches 850 °C, LPG injection is stopped, the pilot flame (lance) is removed and the furnace door is closed. The temperature is further increased by coal addition and the furnace is operated in combustion mode (excess air) at 925 °C for 6 h. Operation in combustion mode is required for thermal soaking of the refractories and heating of the freeboard. After 6 h, the coal flowrate is increased \pm fourfold and steam is added to produce reducing conditions (oxygen deficient) in the furnace. The furnace is operated for a further 6 h to allow the bed carbon content and freeboard temperature to stabilise.

During heat-up and the test period, the airflow is set at a fixed value which is high enough to maintain good fluidisation and low enough to minimise elutriation of fine char from the furnace ($3xU_{mf} < U < 10xU_{mf}$). The bed temperature is controlled by increasing or decreasing the steam flow. If the steam flow drops below a minimum value (determined by the air/steam ratio), the air/coal ratio is adjusted. A minimum steam flow is required in order to prevent hot spots in the bed. The bed height is

controlled by removing char from the bed via the bed extraction screw. The gauge pressure in the furnace is controlled at - 20 mmH₂O (- 200 Pa) by adjusting the valve before the ID fan. Once stable conditions have been achieved, operating data are recorded and samples are collected for a period of 3 to 4 h.

5.2.3 Measurements and analyses

5.2.3.1 Coal feedrate

The coal screw feeder was calibrated by measuring the rotational speed of the screw shaft and measuring the mass of coal fed in a given time period. During the tests, the coal feedrate is determined by measuring the rotational speed of the screw shaft and using Figure B.3 in Appendix B.3, which gives the coal feedrate as a function of rotational speed. The accuracy of the coal feedrate measurement is estimated to be ± 1.0 kg/h based on the accuracy of the scale used for the measurement of the coal mass during calibration of the coal screw feeder.

5.2.3.2 Airflow

The airflow was measured using a sharp-edged orifice plate with pressure tappings at one pipe diameter (D_p) upstream of the orifice plate and half a pipe diameter ($D_p/2$) downstream of the orifice plate. A formula was derived to calculate the airflow using British Standard 1042, 1964, which gives the airflow as a function of the pressure drop over the orifice plate, the temperature and the absolute pressure of the air. The formula and plot of airflow as a function of pressure drop are given in Appendix B.4. The accuracy (tolerance) of the airflow measurement is given by British Standard 1042, 1964 and is ± 1.5 Nm³/h.

5.2.3.3 Steam flow

The steam flow was also measured using an orifice plate. Since the steam is close to its saturation point, the method given in the British Standard 1042 is not accurate to within 5 %. The orifice plate was therefore calibrated by measuring the pressure drop across it and measuring the mass of steam that flowed through it in a given time period. The mass of steam was determined by diverting the steam to a drum filled

with crushed ice and then measuring the increase in the mass of the drum and its contents. The calibration curve for the steam flow orifice plate is given in Appendix B.5. The accuracy of the steam flow measurement is estimated to be ± 1.0 kg/h based on the accuracy of the scale used for the measurement of the condensed steam mass during calibration of the steam orifice plate.

5.2.3.4 Gas analysis

Specifications of the continuous online gas analysers used are given in Table 5.2.

Table 5.2: Specification of gas analysers

Gas	Supplier	Model	Measurement method	Accuracy
CO	Servomex	4210	Infrared	± 0.25 %
H ₂	Servomex	K1550	Thermal conductivity	± 0.50 %
CH ₄	Servomex	4210	Infrared	± 0.10 %
CO ₂	Fuji Electric	ZAJ	Infrared	± 0.25 %
O ₂	Hartman and Braun	Magnos 3K	Paramagnetic	± 0.25 %

5.2.3.5 Temperature and pressure

The process temperatures and pressures are measured by means of type K thermocouples and low-pressure gauges. The locations of the temperature and pressure gauges are shown in Figure 5.1 and Figure 5.5. Due to the bubbling action of the bed, the bed pressure drop reading fluctuates by ± 150 Pa.

5.2.3.6 Char flows and char analysis

The mass flowrate of char from the bed and cyclone is determined by collecting and weighing the char produced by the bed and cyclone during the test period. The carbon in the bed and cyclone char is determined by placing 50 g samples in a muffle oven for a period of 6 h. The resulting mass loss allows the carbon in the char to be calculated. Tyler screens are used to determine the size analysis of both the bed and cyclone char. To reduce sampling errors, four samples of the bed char and cyclone char are taken for each test. The standard deviation of the carbon in ash measurements

is 1.0 % . The char flowrate error is estimated to be 0.2 kg/h (based on the accuracy of the scale used to weigh the bed and cyclone char produced).

5.3 Experimental programme

Coal gasification tests were carried out on the pilot FBG in order to determine for each coal:

- The fixed carbon conversion
- The analysis and calorific value of the gas produced
- The relative amounts and analyses of the bed char and cyclone char
- The temperature profile in the bed.

Table 5.3: Operating conditions for fluidised bed gasification tests

Coal	Bed temperature (°C)	Mean residence time of char (min)	Mean particle size (mm) ¹	Fluidising velocity (m/s)	Absolute pressure (kPa)	Gasification agents
New Vaal	922 & 947	35 - 37	2.4&1.2	1.9 - 2.2	90	Air & steam
Matla	925 & 949	36 - 37	1.6	1.9 - 2.2	90	Air & steam
Grootegeeluk	927 & 953	45 - 46	1.9	1.9 - 2.2	90	Air & steam
Duvha	927 & 949	35 -36	1.7	1.9 - 2.2	90	Air & steam

¹ - d_{50} (PSD's are given in Appendix B.8)

Temperatures of ± 925 °C and ± 950 °C were selected for the tests since it is suggested in the literature (Chatterjee *et al.*, 1995) that temperatures above 975 °C could result in clinkering and agglomeration of the bed. The TGA tests (Chapter 4) indicated that temperatures below 900 °C would result in very low carbon conversions.

The *char residence times* given in Table 5.3 were the practical maximum limit for the apparatus since increasing the bed height further would have resulted in excessive 'slugging' of the bed (Geldart, 1986). Slugging occurs when the bubble diameter

increases to the diameter of the reactor. This phenomenon can result in reactants (oxygen and steam) bypassing the bed in the bubble phase without reacting with the char.

The variation in *mean coal particle size* between the different tests shown in Table 5.3 resulted from the crushing procedure (cone crusher) used for preparing the samples received from the mines (< 20 mm). Since the gasification reactions are chemical reaction rate controlled and not diffusion controlled for particles less than 2.8 mm the variation in mean coal particle size is not expected to have a significant effect on the results (Hanson *et al.*, 2001 and Ye *et al.*, 1997).

For the tests, the *fluidising velocity* was maintained between 1.9 and 2.2 m/s. From Appendix B.1 and the mean char particle sizes shown in Table 5.3, it can be seen that the fluidising velocity is greater than three times U_{mf} , which will result in complete fluidisation of the bed as explained in Section 5.2.1.1. If the fluidising velocity is too high, this will result in excessive carry-over of unconverted char to the cyclone.

5.4 Fluidised bed gasification test results

The results of the eight fluidised bed gasification tests are summarised in Table 5.4. The values shown in this table are average values obtained during 3 hours of stable operation. Figures 5.6 and 5.7 shows an example of the temperature and gas concentration profiles during the test period for Matla coal at 925 °C.

Test 1 was carried out before installation of the gas analysers and no gas readings (NR) are therefore available. The fluidising velocity, gas calorific value, residence time, fixed carbon conversion and char elutriated (shaded values in Table 5.4) are calculated values based on the experimental data. The calculations are given in Appendix B.6.

Table 5.4 and Figure 5.6 shows that the temperature at the top of the gasifier (T_7) is ± 190 °C lower than the bed temperatures (T_1 and T_3). The high ratio of surface area to volume of the FBG results in high heat losses, which is unfortunately a disadvantage

suffered by most small fluidised bed pilot plants. Large-scale fluidised beds have a smaller difference ($\pm 30\text{ }^{\circ}\text{C}$) between the bed and freeboard temperatures since the heat losses are a much lower percentage of the total heat input.

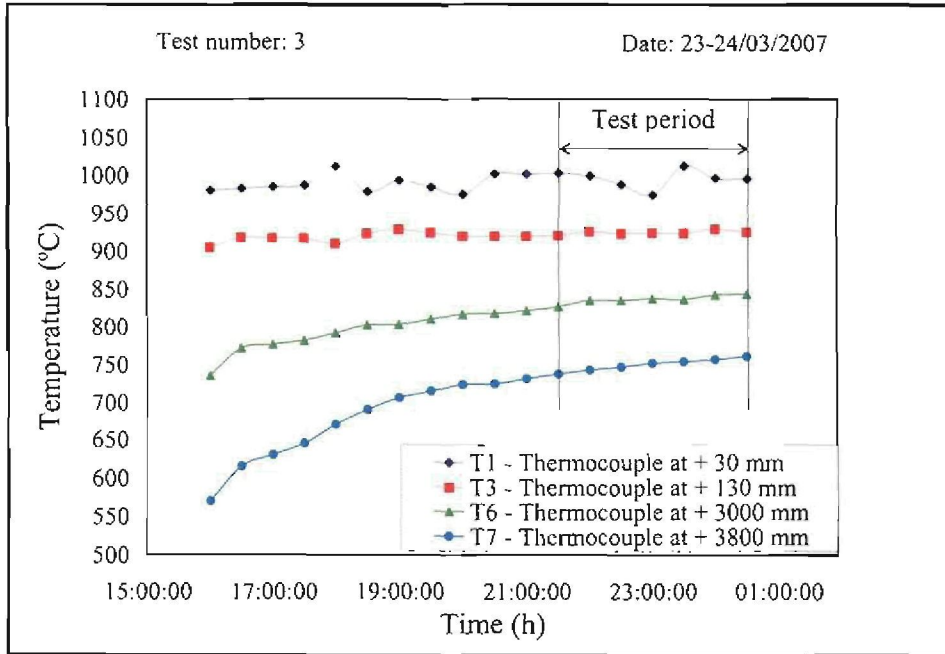


Figure 5.6: Gasifier temperature profiles for Matla coal at 925 °C

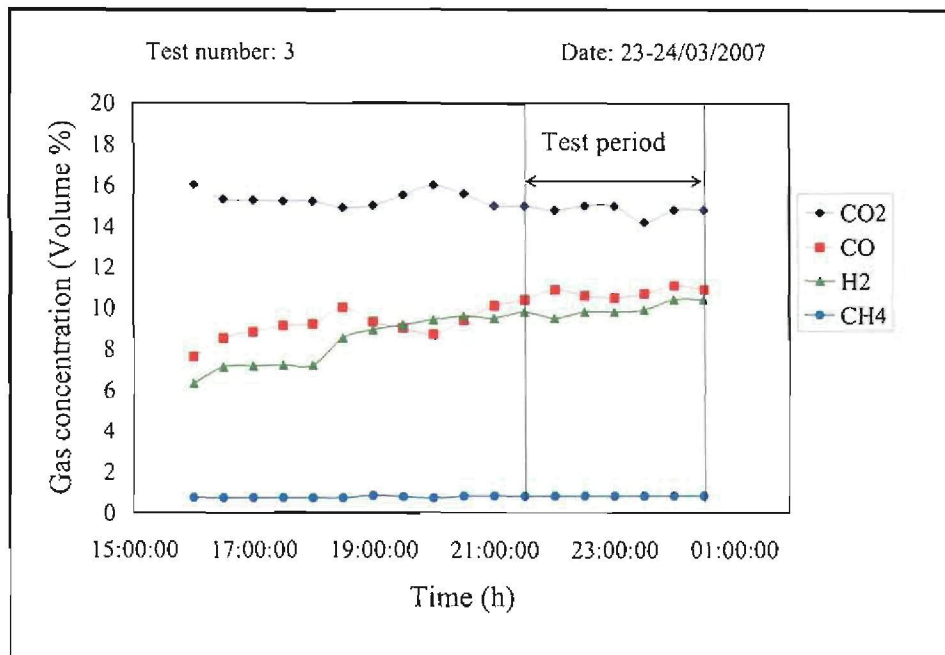


Figure 5.7: Gas concentration profiles for Matla coal at 925 °C

Table 5.4: Summary of fluidised bed gasification tests at 90 kPa absolute pressure

Test number	New Vaal		Matla		Grootegeeluk		Duvha	
	1	2	3	4	5	6	7	8
Coal feedrate (kg/h)	28.7	23.9	27.0	24.3	23.0	23.0	26.4	26.4
Airflow (Nm ³ /h)	52.2	47.0	50.6	50.9	48.5	47.8	47.5	47.8
Steam flow (kg/h)	9.1	5.8	8.5	8.5	10.2	10.0	10.9	9.0
Air and steam temp. (°C)	202	159	190	185	173	178	176	186
Oxygen: carbon molar ratio	0.48	0.52	0.42	0.47	0.46	0.45	0.34	0.35
Steam: carbon molar ratio	0.50	0.38	0.41	0.46	0.57	0.56	0.47	0.39
Coal particle size – d ₅₀ (mm) ¹	2.4	1.2	1.6	1.6	1.9	1.9	1.6	1.6
Fluidising velocity (m/s)	2.2	1.9	2.1	2.2	2.1	2.1	2.1	2.1
Mid-bed temperature (°C) T ₃	922	947	925	949	927	953	927	949
Lower bed temperature (°C) T ₁	967	948	995	972	948	978	921	954
FBG exit temperature (°C) T ₇	750	720	752	756	742	764	761	773
Dry gas composition								
CO (%)	NR ²	11.1	10.8	11.6	8.7	10.2	8.8	9.9
H ₂ (%)	NR	8.6	10.0	9.6	9.4	9.5	8.5	9.3
CH ₄ (%)	NR	0.7	0.8	0.7	1.1	1.1	0.8	0.7
CO ₂ (%)	NR	15.8	14.8	14.6	15.0	14.9	15.3	15.0
N ₂ + others ³ (%) ⁴	NR	63.7	63.5	63.4	65.7	64.2	66.5	65
O ₂ (%)	NR	0.1	0.1	0.1	0.1	0.1	0.1	0.1
Gas calorific value ⁵ (MJ/Nm ³)	-	2.8	3.0	3.0	2.7	2.9	2.5	2.7
Bed pressure drop (Pa) (P ₁ -P ₂)	2664	2115	2553	2259	2553	2553	2455	2456
Char residence time (min)	36.7	36.6	37.4	37.6	45.1	45.1	35.7	35.7
Carbon in bed char (%)	2.8	1.4	24.3	20.8	26.8	26.4	38.6	33.9
Bed char particle size (mm)	1.1	0.6	1.2	1.0	0.8	1.0	0.9	1.2
Carbon in cyclone char (%)	19.5	15.5	32.3	27.8	31.0	27.0	41.6	43.2
Cycl. char particle size (mm)	0.07	0.08	0.05	0.07	0.07	0.07	0.06	0.08
Char elutriated to cyclone (%)	60.6	66.6	53.8	55.6	51.1	51.6	58.3	59.9
Fixed carbon conversion ⁶ (%)	82.7	85.9	68.2	74.0	63.2	67.0	52.0	53.7

¹ d₅₀ – 50 % of the coal mass is less than the d₅₀ size (PSD is given in Appendix B.8)

² NR - no reading

³ Others are < 0.4 % and include H₂S, NH₃, HCN and C₂⁺

⁴ (N₂ + others) by difference

⁵ The estimated error in the calculated gas calorific value is given in Appendix B.6.2

⁶ The estimated error in the calculated fixed carbon conversion is given in Appendix B.6.4

5.4.1 Fixed carbon conversion

Figure 5.8 shows that the fixed carbon conversion of the lower-rank coals is higher than for the higher-rank coals. A similar result was obtained by Jing *et al.* (2005) who gasified three Chinese bituminous coals of differing rank in a fluidised bed gasifier. It can also be seen that increasing the temperature from 925 °C to 950 °C increased the fixed carbon conversion by an average of 3.6 %.

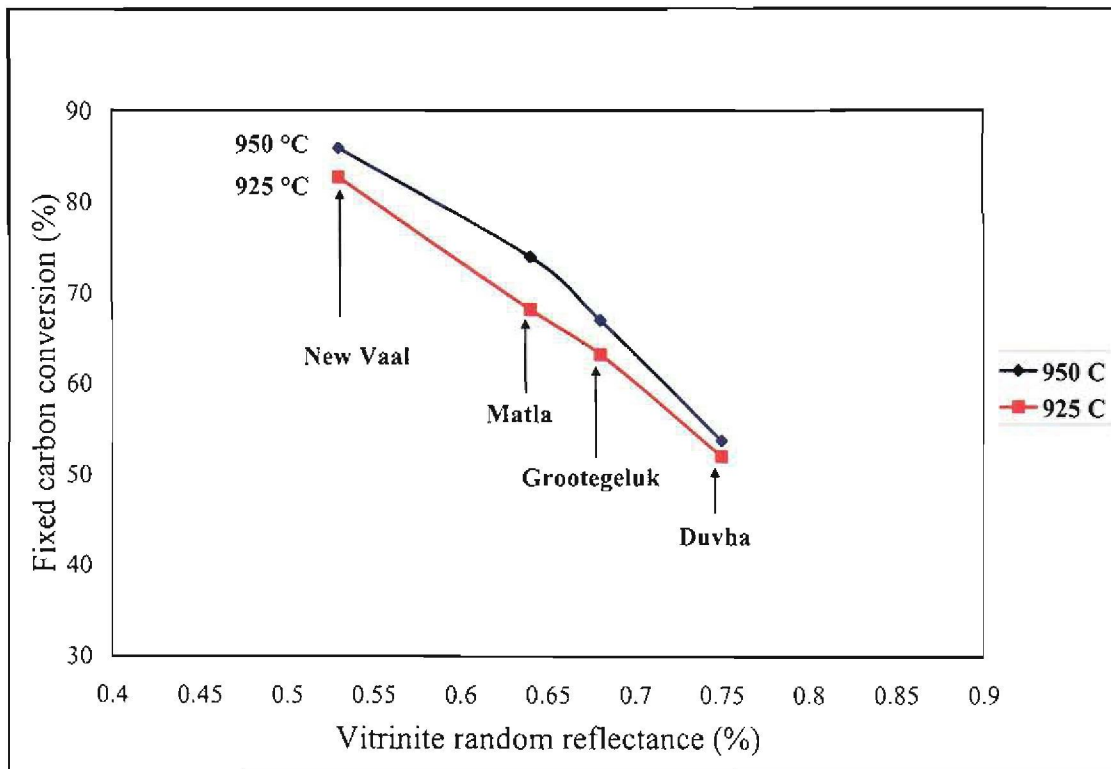


Figure 5.8: Fluidised bed gasifier fixed carbon conversion

Using the fixed carbon conversion and residence time data in Table 5.4 for each coal and temperature, the reactivity index (R_s) of the coal in the FBG was calculated using equation (2.8) and these indices are presented in Table 5.5. Calculation of the estimated time required to achieve 50 % conversion in the FBG is given in Appendix B.7 (Table B.7.1).

Table 5.5: Reactivity index (R_s) of coals in the FBG and TGA (h^{-1})

Coal	Temperature (°C)			
	925		950	
	TGA	FBG ¹	TGA	FBG
New Vaal	5.63	1.74	8.92	1.88
Matla	0.99	1.20	1.56	1.34
Grootegeeluk	0.40	0.94	0.75	1.05
Duvha	0.34	0.86	0.52	0.93

¹ The estimated error in the calculation of R_s in the FBG is given Appendix B.7

Table 5.5 shows that the order of ranking of reactivities of the different coals in the TGA and FBG are the same (New Vaal highest and Duvha lowest). In the FBG, however, the variation in the reactivity index is significantly lower than in the TGA. A possible explanation for this observation is that in the FBG a large percentage (50 - 60 %) of the fixed carbon is converted by the fast partial combustion reaction (equation (2.4)) (Yan and Zhang, 2000). In the TGA all the fixed carbon is converted by means of the CO_2 -char gasification reaction (equation (2.5)). The combustion rate of 1 - 2 mm bituminous coal particles in a fluidised bed combustor at temperatures above 900 °C is under external diffusion control and is less dependent on the reactivity of the coal (Brunello *et al.*, 1996). Since the factors that affect external diffusion, such as oxygen concentration, temperature, particle size and fluidising velocity, were nearly constant for each coal tested in the FBG, the fixed carbon conversion rate by partial combustion would be nearly constant, resulting in a lower variation in the measured reactivity index.

5.4.2 Calorific value

The calorific value of the gas given in Table 5.4 is plotted in Figure 5.9 as a function of the coal rank parameter (R_r) and temperature. The calorific value of the gas is comparable ($\pm 10\%$) to that obtained by other investigators (Jing *et al.*, 2005, Ocampo *et al.*, 2002 and Gutierrez and Watkinson, 1982) who investigated the air-blown fluidised bed gasification of bituminous coal using small pilot plants.

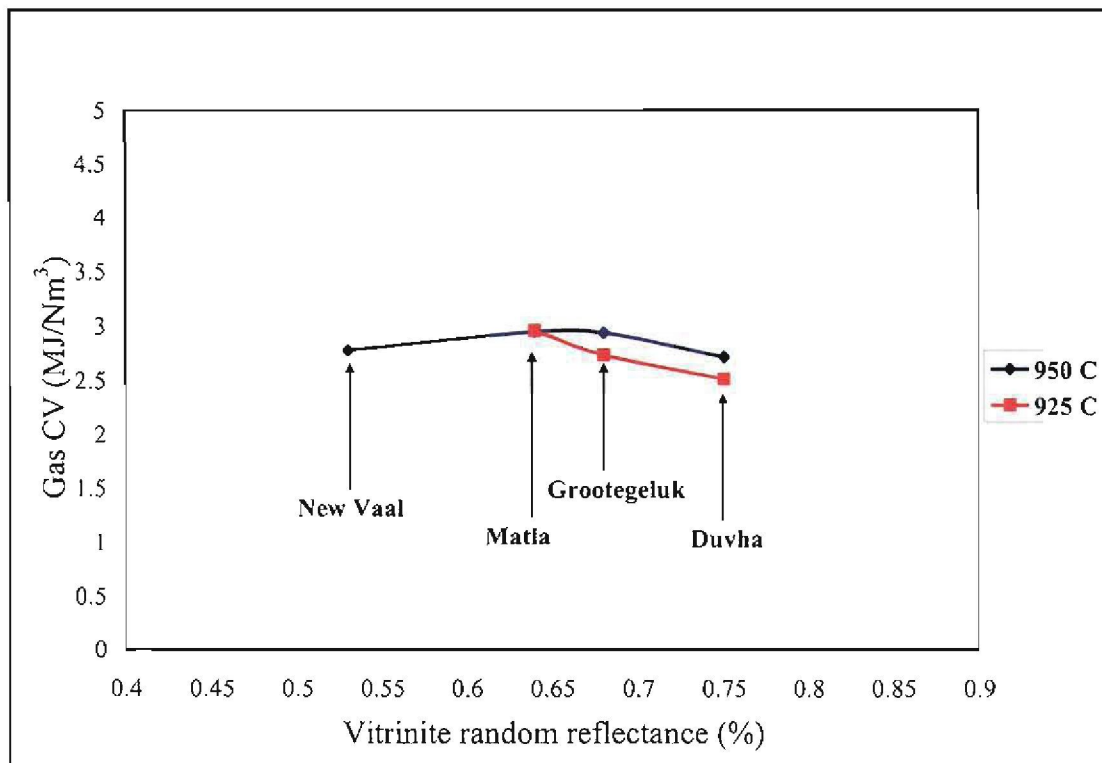


Figure 5.9: Gas calorific value as a function of vitrinite random reflectance (R_r)

The disadvantage of a small pilot plant is that the heat losses are high as a percentage of the total heat input. In order to maintain the bed temperature above 900 °C, without external heating, a high air/coal ratio is required. This reduces the calorific value of the gas due to nitrogen dilution. The high ash content of the coals tested also has a negative impact on the calorific value since the ash has to be heated to the bed temperature by means of char combustion which produces a high CO_2 concentration in the gas ($\pm 15\%$).

Figure 5.9 shows that although New Vaal coal has the highest reactivity (lowest rank), it produced a calorific value that is similar to that of the lower-reactivity coals. This trend was also observed by Gururanjan and Argarval (1992) who concluded that the volatile matter content of the coal has a greater effect on the calorific value of the gas than the char reactivity.

5.4.3 Char fines generation and elutriation

Table 5.4 shows that the particle size of the bed char is lower than that of the feed coal. This is a result of thermal shattering and attrition of the coal in the bed which results in the generation of fines that are eventually elutriated from the gasifier. The particle size distributions, appearance and relative amounts of the coal, bed char and cyclone char are shown in Appendices B.8 and B.9.

The relationship between the percentage cyclone char and the Hardgrove Grindability Index (HGI) is given in Figure 5.10 for each coal and temperature.

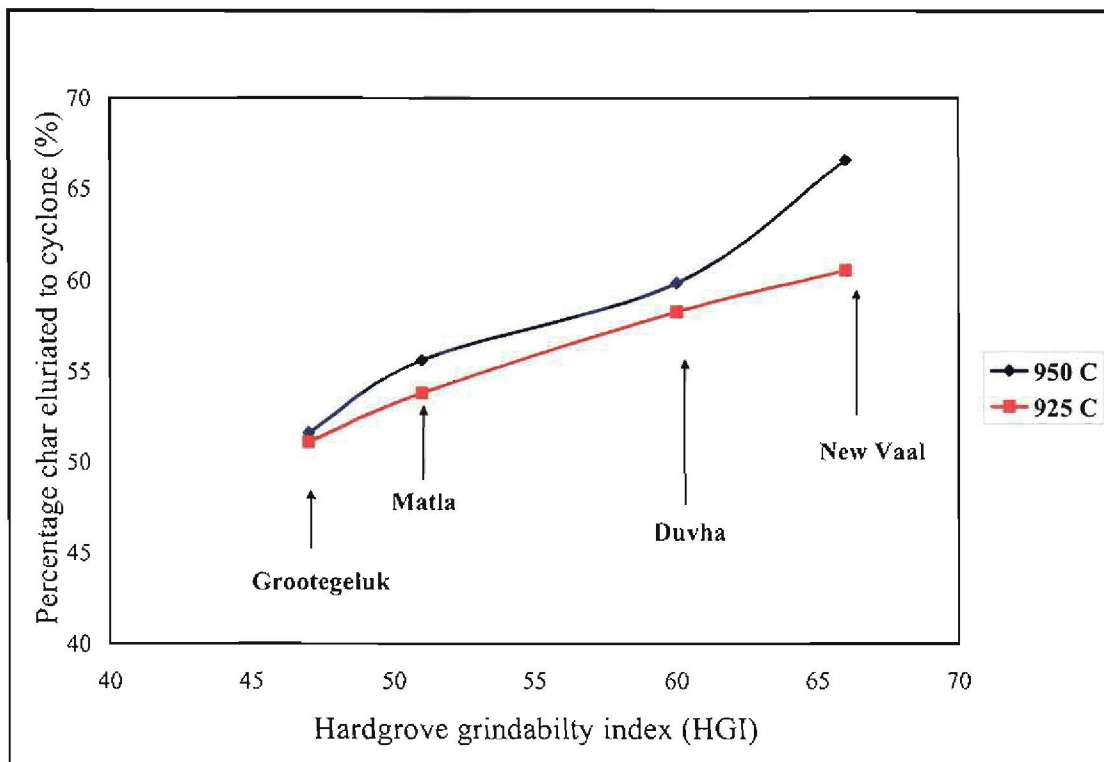


Figure 5.10: Char fines generated as a function of HGI

Figure 5.10 shows that the char fines generated and elutriated increase with the grindability of the coal and with the temperature. Since the fly-ash (cyclone char) has a higher carbon in char, as shown in Table 5.4, the generation of fines has a negative impact on the total fixed carbon conversion.

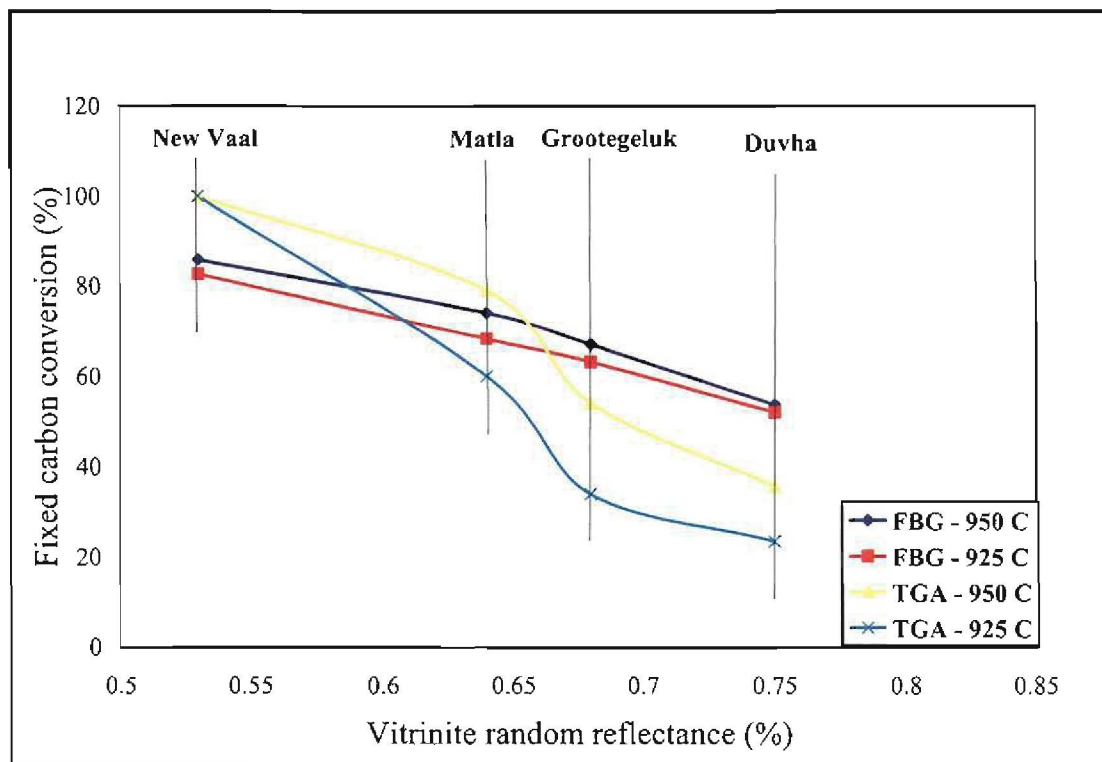


Figure 5.11: Comparison of fixed carbon conversion in the FBG and TGA

The negative effect of fines generation in the FBG on fixed carbon conversion is illustrated in Figure 5.11 which compares the fixed carbon conversion in the FBG and the TGA at the residence times given in Table 5.4 for each coal and temperature. It can be seen that complete conversion of the New Vaal char was achieved in the TGA whereas in the FBG the conversion was significantly lower at $\pm 84\%$. The fines generated are entrained to the freeboard of the FBG where they are not exposed to oxygen but to the freeboard gas which contains $\pm 12\% \text{CO}_2$, $\pm 10\% \text{H}_2\text{O}$, $\pm 9\% \text{CO}$, $\pm 8\% \text{H}_2$ and the balance N_2 . The freeboard gas produces a low conversion rate of char due to the low concentrations of CO_2 and H_2O and also due to the inhibiting effect of CO and H_2 on the reaction rate (Goyal *et al.*, 1989 and Everson *et al.*, 2006).

Using the experimental data and least squares regression, a correlation was developed to predict the amount of cyclone char that would be produced by the gasifier. This is given by equation (5.3) for values of U from 1.9m/s to 2.2m/s and values of d_p from 1.2 mm to 2.4 mm.

$$\text{Elutriated char (\%)} = A_E = 3.13(HGI)^{0.69}(U)^{0.33}(d_p)^{-0.19} \quad (5.3)$$

In equation (5.3), d_p is the mean particle size (d_{50}) of the feed coal. A similar correlation was used by Rhinehardt *et al.* (1987) to predict the carry-over of fines from a fluidised bed gasifier.

Char particles taken from the bed of the gasifier are shown in Appendix B.10. These images show that the New Vaal coal reacts via the shrinking core model and the Duvha coal reacts via the homogenous model as predicted by the TGA experiments (Chapter 4).

5.4.4 Bed agglomeration and clinkering

Table 5.4 and Figure 5.6 shows that the temperature close to the distributor (T_1) is higher than the temperature in the middle of the bed (T_3). This is a result of oxygen reacting with the char and with back-mixed combustible gas close to the air distributor (Ross *et al.*, 2005). Ciesielczyk and Gawdzik (1994) reported that the maximum temperature is limited to the bottom 10 % of the bed and is up to 200 °C higher than the uniform bed temperature in the middle of the bed. The maximum temperature increase observed during the pilot plant tests was ± 70 °C (Test 3). The lower maximum temperature could be due to heat losses through the bottom of the distributor (see Figure 5.3).

Due to the non-caking nature of the coals tested, bed agglomeration and defluidisation of the bed did not occur during any of the tests. The same result was achieved by Gutierrez and Watkinson (1982) who gasified non-caking Canadian coal in an air-blown fluidised bed gasifier.

Upon inspection of the bed after Test 1, small clinkers were observed on the distributor as shown in Appendix B.11. This could be due to segregation of the particles to the bottom and corners of the bed as a result of the larger coal particle size used for this test.

5.5 Summary of fluidised bed gasification tests

The atmospheric pressure air-blown fluidised bed gasification of four high-ash South African coals was investigated at temperatures of 925 °C and 950 °C.

The results show that the fixed carbon conversion achieved in the gasifier correlates well with the rank parameter (R_r) of the coal. Although the order of reactivities in the fluidised bed gasifier and the TGA are the same, the variation in the reactivity index in the fluidised bed gasifier is significantly lower than in the TGA. This was attributed to the large amount of fixed carbon that is converted by means of the partial combustion reaction, the rate of which is less sensitive to the reactivity of the char.

Due to its higher ash content and lower volatile matter content, the New Vaal coal did not produce a higher gas calorific value than the other coals, despite having a much higher char reactivity.

The carbon conversions and calorific values obtained are consistent with published literature on air-blown fluidised bed gasification of high-ash coals in small pilot plants.

The low fixed carbon conversions and calorific values obtained are the result of the inherent disadvantages of a small pilot plant gasifier, which include high heat losses and low residence times of bed and cyclone char. Other factors, not directly related to the size of the gasifier, that reduce the carbon conversion and calorific value of the gas are the generation of fines in the gasifier and the dilution of the gas with nitrogen (air-blown).

No agglomeration and defluidisation of the bed were observed during the fluidised bed gasification tests. This is consistent with the literature which suggests that only coals with high FSI and RI indices (caking coals) are prone to agglomeration in a fluidised bed gasifier.

A region of higher temperature was observed above the gas distributor of the pilot FBG; this has also been reported by other investigators who studied the fluidised bed gasification of coal. Since the maximum temperature increase was only 70 °C, melting and sintering of the char in the bed did not occur.

CHAPTER 6: GENERAL CONCLUSIONS AND RECOMMENDATIONS

6.1 General conclusions

This dissertation presents results concerning the characterisation of four typical high-ash South African coals, followed by thermogravimetric analysis and fluidised bed gasification tests. The conclusions drawn from this investigation are the following:

- 1) There are significant differences in gasification characteristics between different high-ash South African bituminous coals.
- 2) The rank parameter of the coal (R_r) is a reliable indicator of the reactivity of the coal and of the fixed carbon conversion achievable in a fluidised bed gasifier.
- 3) Although the order of ranking of reactivities of the different coals in the fluidised bed gasifier and the TGA are the same, the variation in the reactivity index in the fluidised bed gasifier is significantly lower than in the TGA. This can be attributed to the large amount of fixed carbon that is converted by means of the partial combustion reaction, the rate of which is less sensitive to the reactivity of the char.
- 4) The low fixed carbon conversions and calorific values obtained are the result of the inherent disadvantages of a small pilot plant gasifier, which include high heat losses and low residence times of bed and cyclone char. Other factors, not directly related to the size of the gasifier, that reduce the carbon conversion and calorific value of the gas are the generation of fines in the gasifier and the dilution of the gas with nitrogen (air-blown).

- 5) The low free swelling (FSI) and Roga (RI) indices, together with the high ash fusion temperature (AFT) of the coals tested, prevented agglomeration, clinkering and de-fluidisation of the bed.
- 6) The amount of fines generated in the gasifier and the resulting elutriation rate of fly-ash from the gasifier can well be described by the hardgrove grindability index (HGI) of the feed coal.
- 7) Due to the low reactivity of most South African bituminous coals, a secondary char combustion stage may be required after the fluidised bed gasifier, in order to achieve overall carbon conversions in excess of 95 %.

6.2 Contributions to the knowledge base of coal science and technology

A experimental relationship was established between coal characterisation parameters, TGA measurements and performance in a fluidised bed gasifier for typical high-ash South African coals. This information, which has not been reported in the published literature, could be useful in selecting South African coals for IGCC power stations based on fluidised bed gasification.

6.3 Recommendations for future investigations

The following recommendations are proposed for further work on the fluidised bed gasification of South African coal:

- 1) In order to achieve acceptable IGCC plant efficiencies ($> 45\%$), a gas calorific value and fixed carbon conversion of at least 4.25 MJ/Nm^3 and 75% respectively are required (Smith *et al.*, 2005). The fixed carbon conversion and gas calorific value achieved in the pilot-scale fluidised bed gasifier can possibly be improved by:

- a. Increasing the height of the fluidised bed
- b. Increasing the height of the furnace
- c. Recycling cyclone char to the bed
- d. Increasing the air and steam pre-heat temperatures
- e. Enriching the gasification air with oxygen
- f. Reducing heat losses.

The effect of the above optimisation steps can be investigated by:

- a. Modifying the pilot-scale fluidised bed gasifier
 - b. Developing a simulation model for the fluidised bed gasification process.
- 2) Since most applications of fluidised bed gasifiers, such as IGCC plants, operate at pressures up to 2.5 MPa, gasification research work under pressurised conditions is recommended. As mentioned in Section 2.3.3, the rate of the gasification reaction increases with pressure up to ± 1.5 MPa, after which no further increase in rate is observed. Since the coal residence time decreases linearly with an increase in pressure, the fixed carbon conversion is likely to be lower at higher pressures. It is therefore essential to carry out TGA and pilot plant tests at higher pressures.
- 3) Control of the high-temperature region above the distributor is critical for trouble-free operation of a fluidised bed coal gasifier. It is therefore recommended that a better understanding of the effect of operating conditions on the temperature distribution in this region be obtained by inserting additional thermocouples into the lower 20 % of the bed. The simulation model referred to above should also be extended to incorporate the high-temperature region.

REFERENCES

- BASU, P. (2006). Chapter 3. In: *Combustion and Gasification in Fluidised Beds*. Boca Raton, London, New York: CRC Taylor and Francis, 97-98.
- BHATIA, S.K. AND PERLMUTTER, D.D. (1980). A random pore model for fluid-solid reactions: I. Isothermal, kinetic control. *AICHE Journal* 26: 379-386.
- BRITISH STANDARD 1042. (1964). Methods for the measurement of fluid flow in pipes. Part 1. Orifice plates, nozzels and venturi tubes. British Standards Institution.
- BRUNDEL, N., LAMBERTZ, J. AND THEIS, K.A. (1989). Stages of Development of the HTW Process Regarding its Suitability for Combined-cycle Plants. Rheinische Braunkohlenwerke AG report.
- BRUNELLO, S., FLOUR, I., MAÏSSA, P. AND BRUYET, B. (1996). Kinetic study of char combustion in a fluidised bed. *Fuel* 75:536-544.
- BUCKO, Z. (2000). HTW fluidised bed gasification for 400 MWe IGCC power plant, Vresova – Czech Republic. Paper presented at the Gasification Technologies Conference, San Francisco, California, 9-11 October 2000.
- Calpine Fuels Diversity Initiative. (2006).
www.netl.doe.gov/publications/proceedings/02/turbines/Izzo.pdf
- CHATTERJEE, P.K., DATTA, A.B. AND KUNDU, K.M. (1995). Fluidised bed gasification of coal. *The Canadian Journal of Chemical Engineering* 73: 204-210.
- CHEJNE, F. AND HERNANDEZ, J.P. (2002). Modelling and simulation of coal gasification process in fluidised bed. *Fuel* 81:1687-1702.
- CIESIELCZYK E. AND GAWDZIK, A. (1994). Non-isothermal fluidised bed gasifier model for char gasification taking into account bubble growth. *Fuel* 73:105-111.
- CLARK, E.L. (1979). Major technical issues facing low and medium Btu gasification. In: PELOFSKY, A.H. (Ed), *Coal Conversion Technology*, ACS Symposium Series 110, 183-195.
- DAVIDSON, J.F. AND HARRISON, D. (1971) *Fluidization*. London and New York: Academic Press.
- DE CARVALHO, R.J. AND BRIMACOMBE, J.K. (1987). Relationship between reactivity and surface area changes during the Boudouard reaction for low-rank Western Canadian coals. Paper presented at the Pyrometallurgy 87 Symposium, London, England, September.
- DU CANN, V.M. (2006). A brief introduction to some basic aspects of Coal and Organic Petrology. South African Bureau of Standards report.

DRAPER, N.R. AND SMITH, H. (1966). Chapter 1. In: Applied Regression Analysis. New York, Chichester, Brisbane, Toronto: John Wiley & Sons, 18-24.

EIA. 1997. Kyoto report. <http://www.eia.doe.gov/oiaf/kyoto/kyotobtxt.html>

ENGELBRECHT, A.D. (2007) Clean Coal technology - Fine coal gasification progress report. CSIR report, DMS number 133570.

ERGUN, S. (1979) Coal classification and characterization. In: WEN, C.Y. AND SANLEE L.E., (Eds), Coal Conversion Technology, Chapter 1, Massachusetts: Addison-Wesley, 1-56.

Eskom. 2002. Generation and transmission. <http://www.eskom.co.za>

EVERSON, R.C., NEOMAGUS, H.W.J.P., KASAINI, H. AND NJAPHA, D. (2006). Reaction kinetics of pulverised coal-chars derived from inertinite-rich coal discards: Gasification with carbon dioxide and steam. *Fuel* 85: 1076-1082.

FURUSAWA, T., ADSCHIRI, T. AND BOONAMUAYVITAYA, V. (1989). Thermodynamic analysis of coal gasifier performance. American Chemical Soc. Fuel Chemistry Preprints, Vol. 34.

GAN, H., NANDI, S.P. AND WALKER, P.L. (1972). Nature of the porosity in American coals. *Fuel* 51:272.

GAVALAS, G.R. (1980a). A random capillary model with application to char gasification at chemically controlled rates, *AIChE Journal* 26(4): 577.

GELDARDT, S. (1986). Single particles, fixed and quiescent beds In: Gas Fluidization Technology, Chapter 2, New York, Brisbane, Toronto, Singapore: Wiley, 26.

GOEDE, G.F. (2004). CO₂ capture and storage (sequestration): Progress and status. Fossil Fuel Foundation Indaba, Johannesburg, South Africa, 11 November 2004.

GOYAL, A., ZABRANSKY, R.F. AND REHMAT, A. (1989). Gasification kinetics of Western Kentucky bituminous coal char. *Industrial Eng. Chem. Res.* 28:1767-1778.

GURURANJAN, V.S. AND ARGARWAL, P.K. (1992). Mathematical model of fluidized bed coal gasifiers. *Chem. Engng Res. Des. Trans.* 70A: 211-237.

GUTIEREZ, L.A. AND WATKINSON, A.P. (1982). Fluidized bed gasification of some Western Canadian coals. *Fuel* 61:133-138.

HANSON, S., PATRICK, J.W. AND WALKER, A. (2001). The effect of coal particle size on pyrolysis and steam gasification. *Fuel* 81:531-537.

HENDERSON, D. (2003). Clean Coal Technologies. *IEA Clean Coal Centre Report: CCC/74*, ISBN 92-9029-389-6.

- HIETKAMP, S., GOLDING, A., ENGELBRECHT, A.D. AND SCHOLES, B. (2004). Potential for the sequestration of carbon dioxide in South Africa. CSIR report.
- HUANG, J., FANG, Y., CHEN, H. AND WANG, Y. (2003). Coal gasification characteristic in a pressurized fluidised bed. *Energy and Fuels* 17:1474-1479.
- JING, B., ZHONG, Z., HUANG, Y. AND XIAO, R. (2005). Air and steam coal partial gasification in an atmospheric fluidized bed. *Energy & Fuels* 19:1619-1623.
- JOHNSON, J.L. (1979). Chapter 1. In: *Kinetics of Coal Gasification*, New York: Wiley.
- KAITANO, R. (2007). Characterisation and reaction kinetics of high ash chars derived from inertinite-rich coal discards. Doctoral thesis. North-West University, South Africa.
- KOVACIK, G., OGUZTORELI, M., CHAMBERS A. AND OZUM B. (1990). Equilibrium calculation in coal gasification. *Int. J Hydrogen Energy* 15(2):125-131.
- KUNII, D. AND LEVENSPIEL, O. (1977). Industrial Applications. In: *Fluidisation Engineering*, Chapter 2, New York: Krieger Publishing Co.
- KWON, T-W., KIM, S.D. AND FUNG, D.P.C. (1988). Reaction kinetics of char-CO₂ gasification. *Fuel* 67:530-535.
- LILIEDAHL, T. AND SJÖSTRÖM, K. (1996). Modelling of char - gas reaction kinetics. *Fuel* 76:29-37.
- LU, G.Q. AND DO, D.D. (1994). Comparison of structural models for high ash char gasification. *Carbon* 32(2):247 -263.
- LUO, C-H., AOKI, K., UEMIYA, S. AND KOJIMA, T. (1998). Numerical modelling of a jetting fluidized bed gasifier and the comparison with the experimental data. *Fuel Processing Technology* 55:193-218.
- MA, R.P., FELDER, R.M. AND FERREL, J.F. (1988). Modelling a pilot-scale fluidised bed coal gasification reactor. *Fuel Processing Technology* 19:265-290.
- MC FARLANE, I. (2006). 400 MW integrated drying gasification combined-cycle plant to demonstrate technology at Latrobe Valley, TCE, April, 7.
- MIURA, K., HASHIMOTO, K. AND SILVESTON, P.L. (1989). Factors affecting the reactivity of coal chars during gasification, and indices representing reactivity. *Fuel* 68:1461.
- MOLINA, A. AND MONDRAGON, F. (1998). Reactivity of coal gasification with steam and CO₂. *Fuel* 77:1831-1839

- NEAVAL, R.C. (1979). Origin, petrography, and classification of coal. In: ELLIOTT, M.A., Chemistry of Coal Utilization, Chapter 3, New York: Wiley, 91-158.
- NJAPHA, D. (2003). Determination of the kinetic models and associated parameters for the low temperature combustion and gasification of high-ash coal chars. Doctoral thesis. North-West University, South Africa.
- OCAMPO, A., ARENAS, E., CHEJNE, F., ESPINEL, J., LONDONO, C., AGUIRRE, J. AND REREZ, J.D. (2003). An experimental study on gasification of Columbian coal in a fluidised bed. *Fuel* 82:161-164.
- OCHOA, J., CASSANELLO, M.C., BONELLI, P.R. AND CUKIERMAN, A.L. (2001). CO₂ gasification of Argentinean coal chars: a kinetic characterization. *Fuel Processing Technology* 74: 161-176.
- ODE, W.H. (1963). Coal analysis and mineral matter. In: LOWRY, H.H., Chemistry of Coal Utilization – Supplementary Volume, Chapter 5, New York: Wiley, 202-231.
- PRÉVOST, X.M. AND MSIBI, M.D. (2005) IN: DUVAL, J.A.G., South African Minerals Industry 2005-2006, Department of Minerals and Energy report, 42-50
- PAREKH, R.D. (1982). Handbook of gasifiers and gas treatment systems. DOE Contract Report, DOE/ET/10159-T2 DE83 004846, September.
- PINHEIRO, H.J., PRETORIUS, C.C., BOSHOFF, H.P. AND BARKER, O.B. (1999). A techno-economic and historical review of the South African coal industry in the 19th and 20th centuries and analysis of coal product samples of South African collieries 1998-1999. Coal Bulletin 113. Issued by South African Bureau of Standard (SABS) and the Department of Minerals and Energy (DME).
- PRUSCHEK, R. AND OELJEKLAUS, G. (1997). The role of IGCC in CO₂ abatement. *Energy Conversion Management*, 38:153-158.
- RECK, R.A. AND HOAG, K.J. (1996). A comparison of greenhouse gas mitigation options. *Energy* 22:115-120.
- REID, W.T. (1970). In: PERRY, H. AND CHILTON, H. Chemical Engineers Handbook, Fifth Edition, Section 9, Heat Generation and Transport, McGraw-Hill, Kogakusha, 9.3-9.7.
- RHINEHART, R.R., FELDER, R.M. AND FERREL, J.K. (1987). Coal gasification in a pilot-scale fluidized bed reactor. 3. Gasification of Texas lignite. *Ind. Eng. Chem. Res.* 26: 2048-2057.
- ROSS, D.P., YAN, H-m., ZHONG, Z. AND ZHANG, D-k. (2005). A non-isothermal model of a bubbling fluidised bed coal gasifier. *Fuel* 84:1469-1481.
- SCHILING, H.D, BONN, B. AND KRAUSS, U. (1981). Chapter 6. In: Coal Gasification-Existing Processes and New Developments. London: Graham & Trotman, 85-95.

- SHA, X.Z., CHEN, Y.G., CAO, J., YANG, Y.M. AND REN, D.Q. (1990). Effects of operating pressure on coal gasification, *Fuel* 69: 656-659.
- SHINNAR, R., AVIDAN, A.I. AND WENG, L. (1988). Evaluation of Fluidized bed Coal Gasification – Present Status and Future Developments Problems, Task III, DOE Contract report, DOE/MC/21259—2573 DE88 001075, February.
- SMITH, P.V., SALAZAR, N., DAVIS, M.D., NELSON, J.M., LEONARD, R., AND BREUALT, R.W. (2005). KBR transport gasifier. Paper presented at the Gasification Technologies Conference, San Francisco, California, 9-12 October.
- SMITH J.M. AND VAN NESS, H.C., In: Introduction to Chemical Engineering Thermodynamics, McGraw Hill Chemical Engineering Series, Tosho Printing Co. Ltd. Tokyo, Japan., 1975, Chapter 4, Heat effects, 104-114, Chapter 9, Chemical-reaction equilibria, 389- 398.
- SQUIRES, A.M. (1983). Three bold exploiters of coal gasification. In: HOWARD, J.R. (Ed), Fluidized Beds – Combustion and Applications, Chapter 8, London and New York: Applied Science, Winkler, Godel and Porta, 277-304.
- THOMAS, K.M. (1986). Characterisation of coal for gasification processes. In: FIGUEIREDO, J.L. AND MOULIJN, J.A., Carbon and Coal Gasification, Dordrecht: Martinus Nijhoff Publishers, 421-453.
- WINKLER, H. (2006). Energy policies for sustainable development in South Africa-Options for the future, Energy Research Centre, University of Cape Town, April 2006.
- YAN, H.-M., HEIDENREICH, C. AND ZHANG, D.K. (1999). Modelling of bubbling fluidised bed coal gasifiers. *Fuel* 78:1027-1047.
- YAN, H-m. AND ZHANG, D-k. (2000). Modelling of fluidised bed coal gasifiers: Elimination of the combustion product distribution coefficient by considering homogeneous combustion. *Chem. Engng Proc.* 39: 229-237.
- YAN, H-m., HEIDENREICH, C. AND ZHANG, D-k. (1998). Mathematical modelling of a bubbling fluidised bed coal gasifier and the significance of ‘net flow’. *Fuel* 77:1067-1079.
- YE, D.P., AGNEW, J.B. AND ZHANG, D.K. (1997). Gasification of South Australian low-rank coal with carbon dioxide and steam: Kinetics and reactivity studies. *Fuel* 77:1209-1219.
- ZHANG, L., HUANG, J., FANG, Y. AND WANG, Y. (2006). Gasification reactivity and kinetics of typical Chinese anthracite chars with steam and CO₂. *Energy & Fuels* 20:1201-1210.

REFERENCES

ZHUO, Y., MESSENBOCH, R., COLLOT, A-G., MEGARITIS, A., PATERSON, N., DUGWELL, D.R. AND KANDIYOTI, R. (1999). Conversion of coal particles in pyrolysis and gasification: Comparison of conversion in a pilot scale reactor gasifier and bench scale test equipment. *Fuel* 79:793-802.

APPENDIX A: THERMOGRAVIMETRIC ANALYSIS

Appendix A.1: Char preparation apparatus for Grootegeluk coal

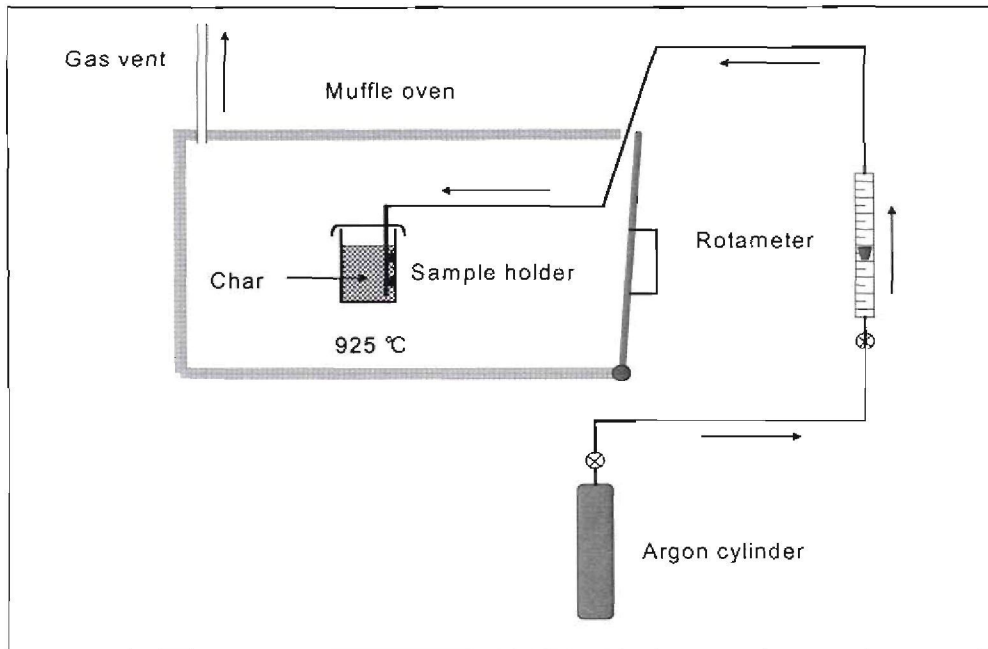


Figure A.1: Char preparation apparatus for Grootegeluk coal

Appendix A.2: The relative char gasification reactivities at 925, 900 and 875 °C

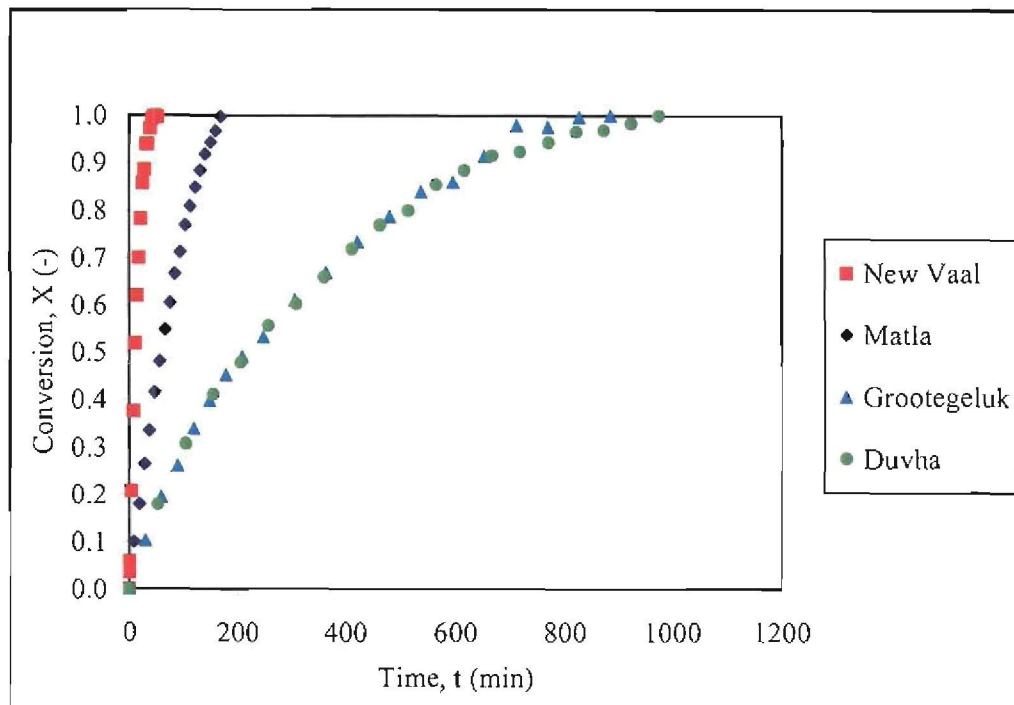


Figure A.2a: Relative char gasification reactivity at 875 °C in 100 % CO₂ at 87.5 kPa

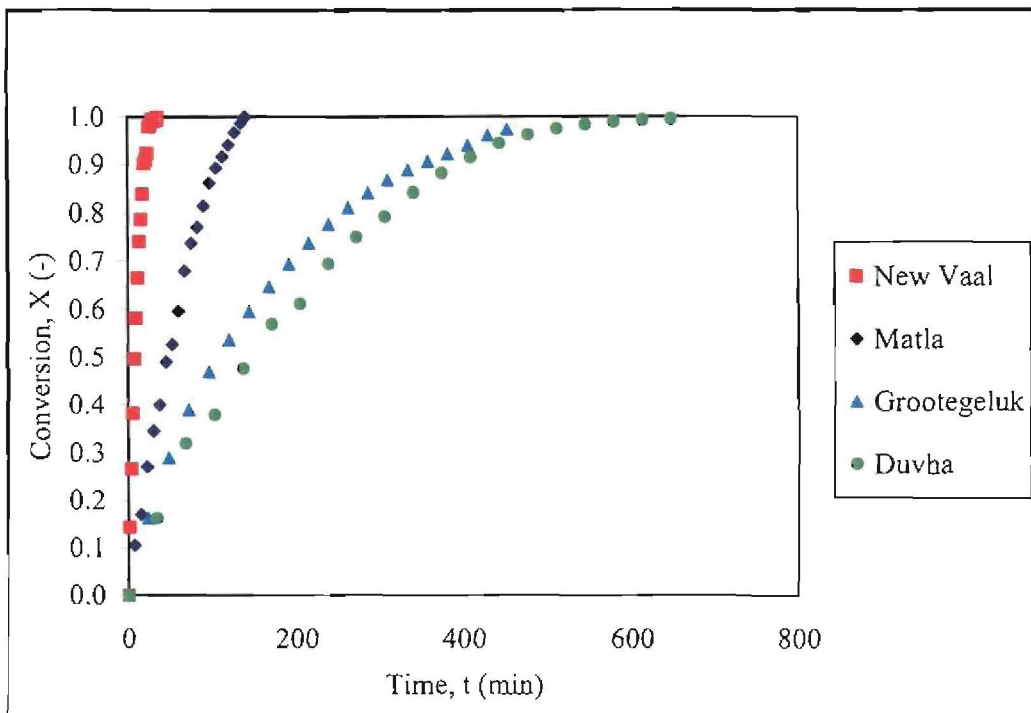


Figure A.2b: Relative char gasification reactivity at 900 °C in 100 % CO₂ at 87.5 kPa

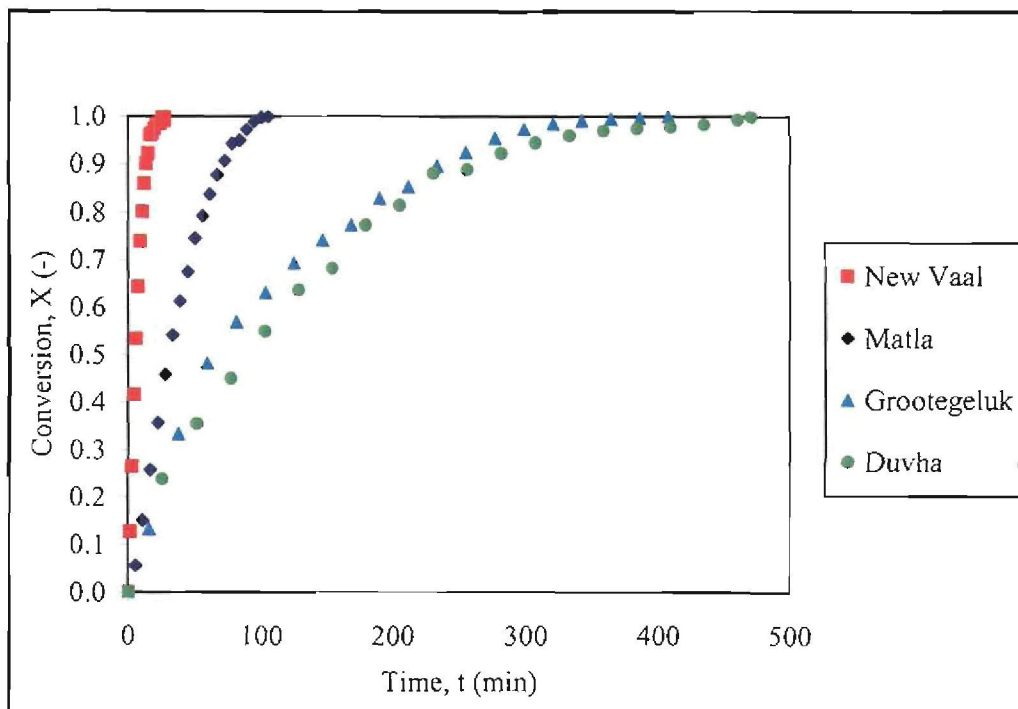


Figure A.2c: Relative char gasification reactivity at 925 °C in 100 % CO₂ at 87.5 kPa

Appendix A.3: Evaluation of grain model for Matla, Grootegeluk and Duvha chars

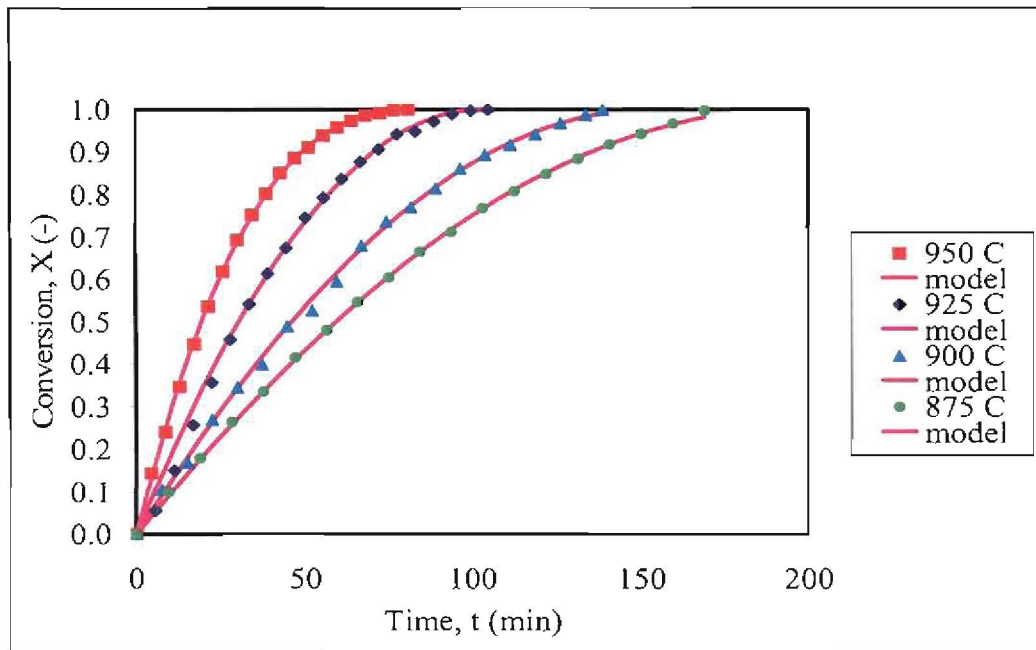


Figure A.3a: Grain model for Matla char at 87.5 kPa in 100 % CO₂

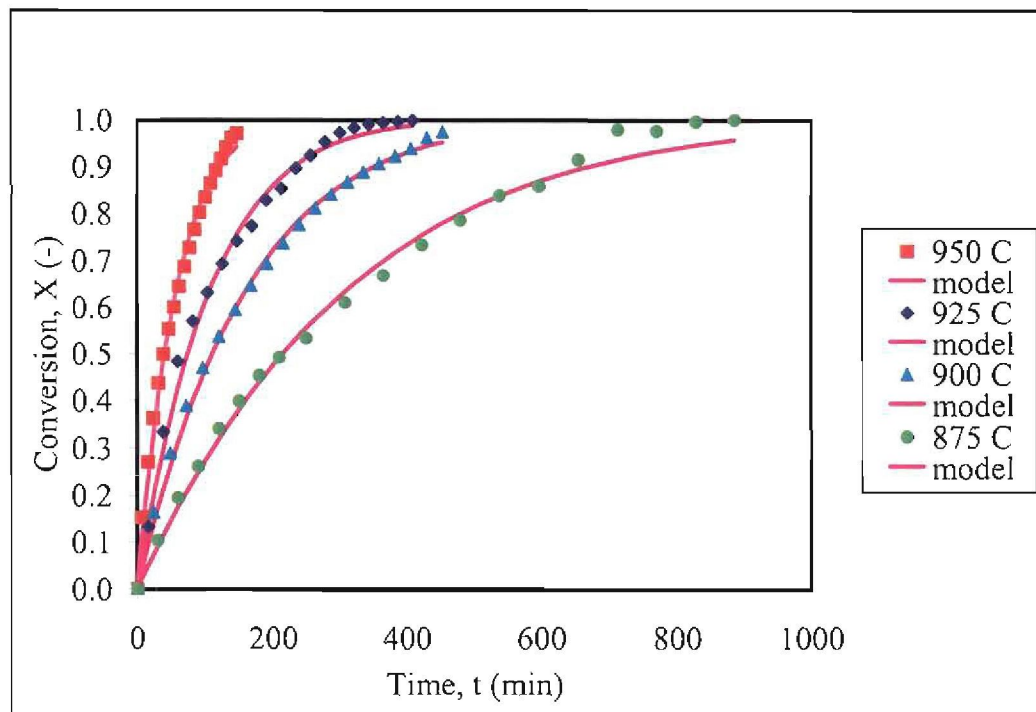


Figure A.3b: Grain model for Grootegeluk char at 87.5 kPa in 100 % CO₂

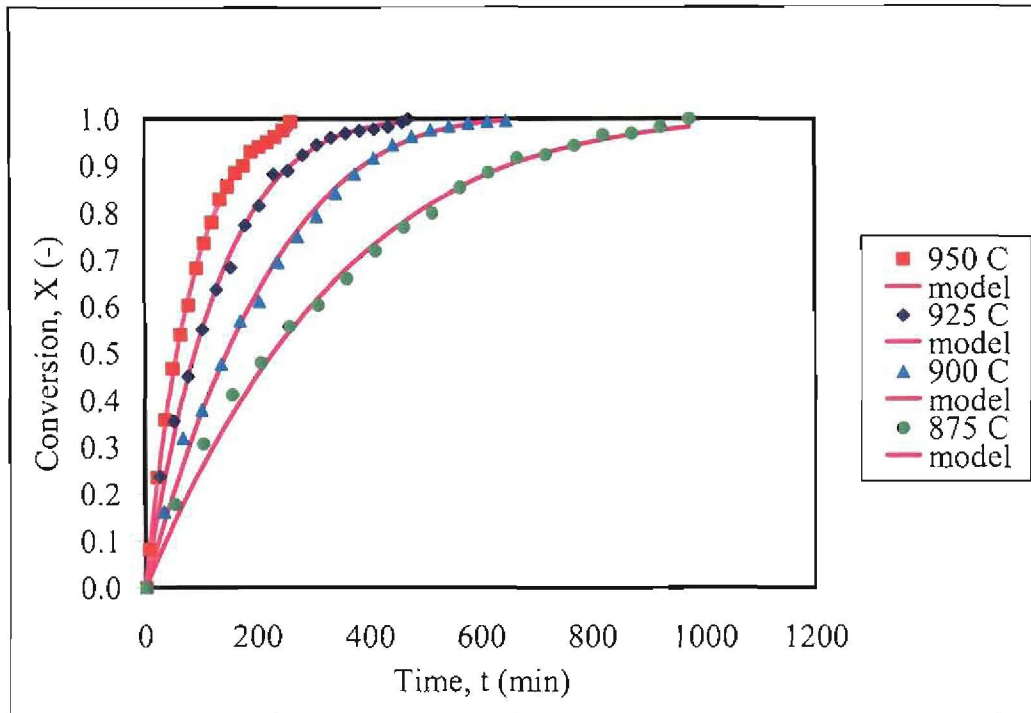


Figure A.3c: Grain model for Duvha char at 87.5 kPa in 100 % CO₂

Appendix A.4: Conversion rate of chars

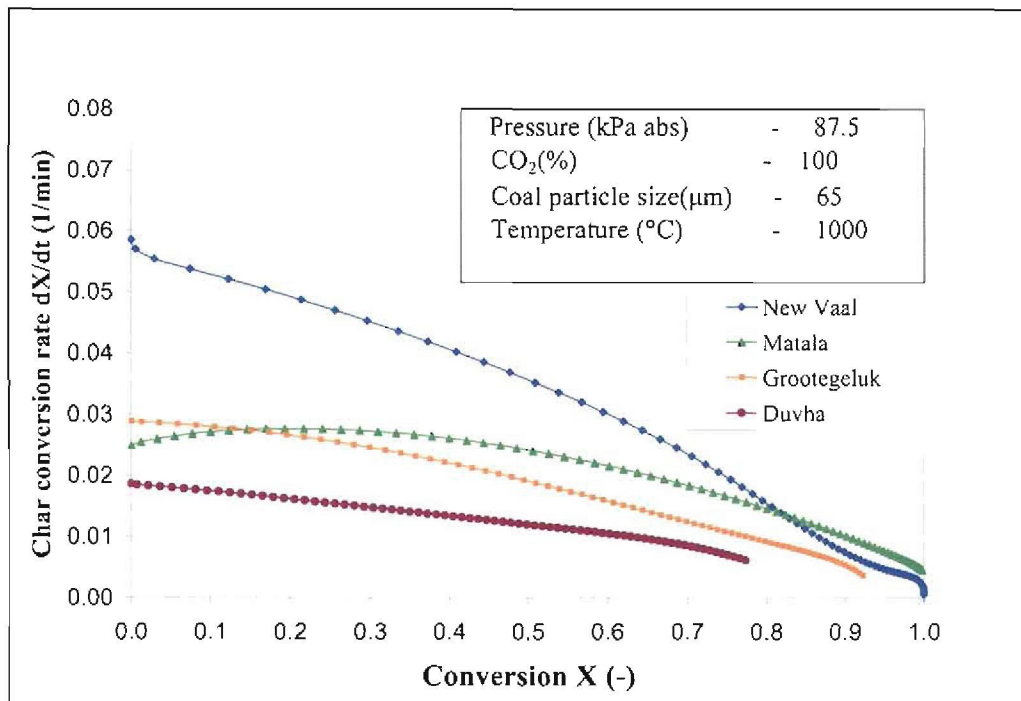
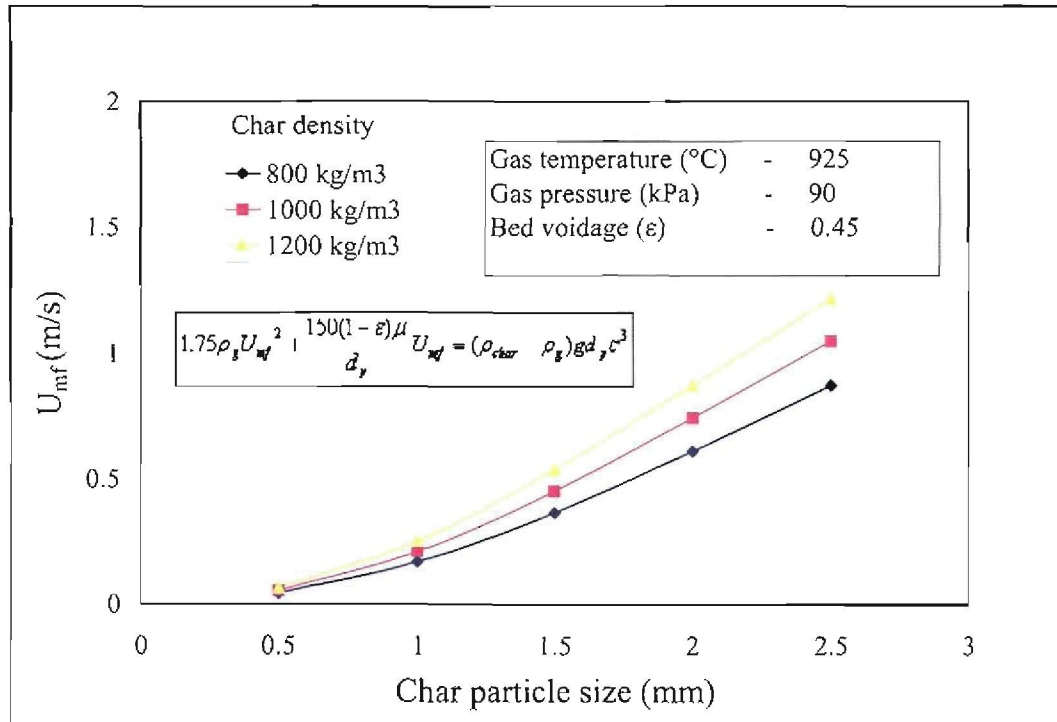


Figure A.4a: Conversion rate of chars at 1 000° C and 87.5 kPa

APPENDIX B: PILOT-SCALE FLUIDISED BED GASIFICATION

Appendix B.1: Calculated values of U_{mf} as a function of char particle sizeFigure B.1: U_{mf} as a function of char particle size for various char densities

Appendix B.2: Distributor pressure drop

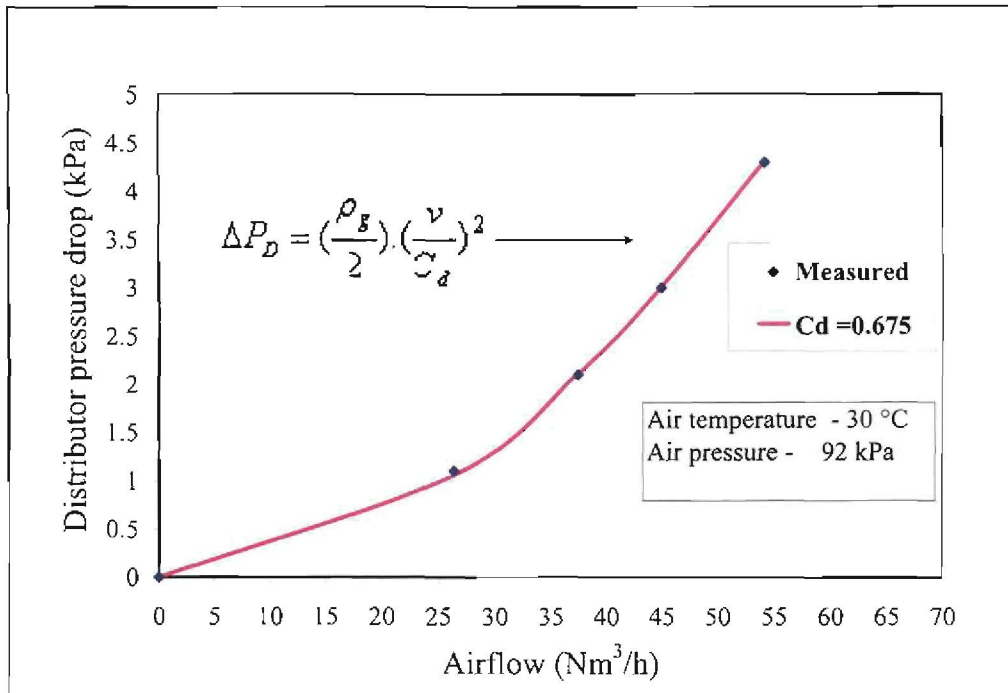


Figure B.2: Distributor pressure drop as a function of airflow

Appendix B.3: Coal feeder calibration curves

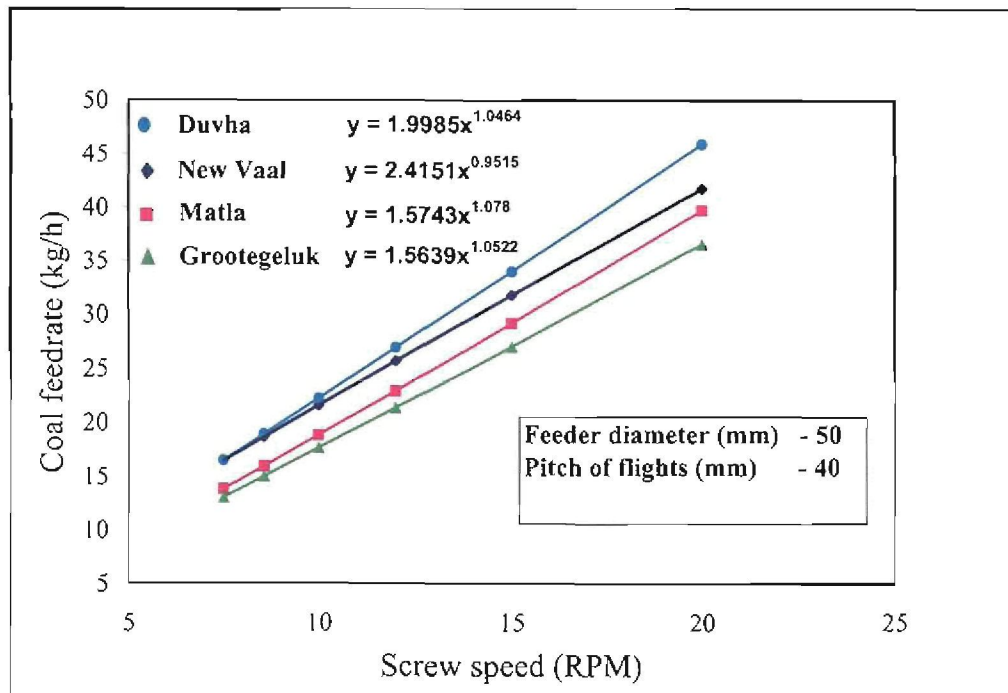


Figure B.3: Coal feeder calibration and calculation formulae

Appendix B.4: Airflow calculation

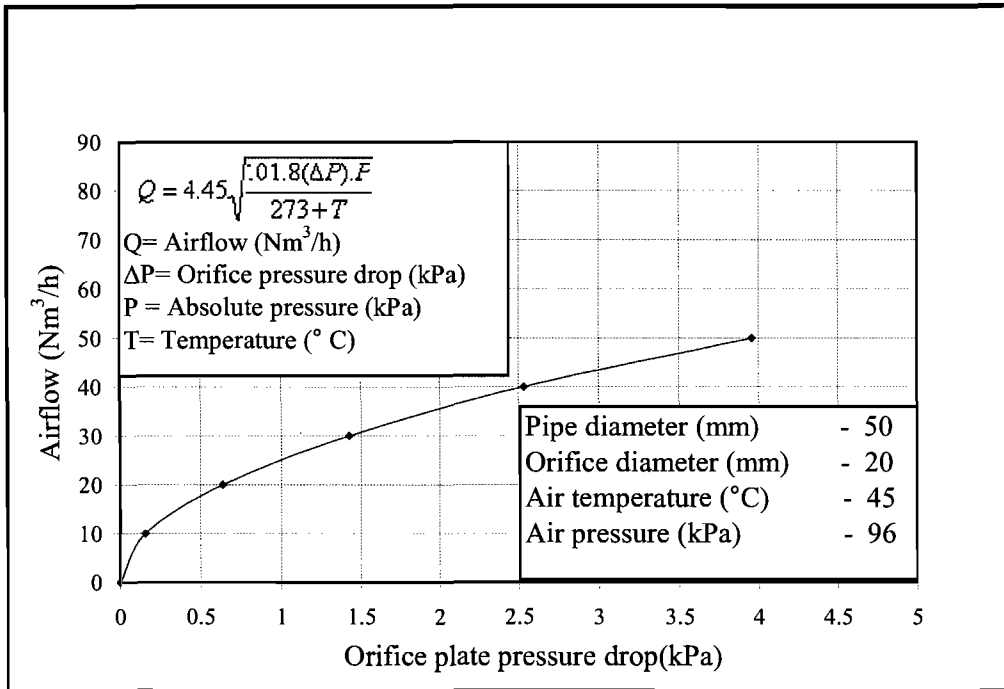


Figure B.4: Airflow orifice calibration curve

Appendix B.5: Steam flow calibration curve

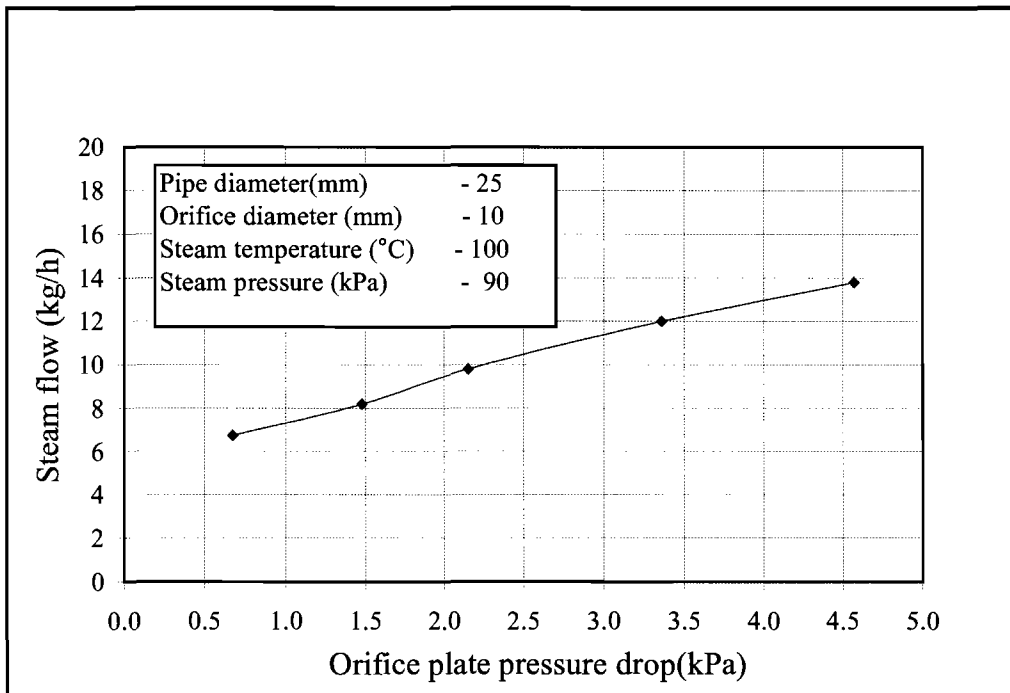


Figure B.5: Steam flow orifice calibration curve

Appendix B.6: Calculation of fluidising velocity, gas calorific value, residence time, fixed carbon conversion and elutriated char percentage

Appendix B.6.1: Calculation of fluidising velocity (U)

Note:

- Normal (N) conditions are 101.325 kPa and 273 °C
- 1 Nm³ contains 44.64 gmoles of an ideal gas

$$\text{Total gas flow to bed (Nm}^3/\text{h)} = NQ_{\text{total}} = Q_{\text{air}} + \frac{G_{\text{steam}} \cdot 1000}{(18)(44.64)} = Q_{\text{air}} + 1.245 \cdot G_{\text{steam}}$$

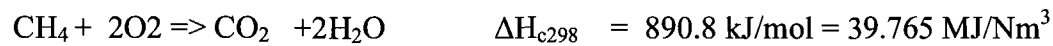
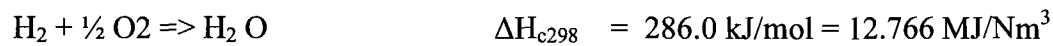
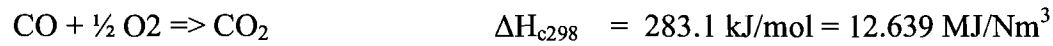
$$\text{Total flow to bed at bed conditions (m}^3/\text{h)} = Q_{\text{total}} = NQ_{\text{total}} \left(\frac{101.325}{P_B} \right) \left(\frac{T_B + 273}{273} \right)$$

$$\Rightarrow U(\text{m/s}) = \frac{Q_{\text{total}}}{3600 \cdot A_B} = \frac{(Q_{\text{air}} + 1.245 G_{\text{steam}}) \left(\frac{101.325}{P_B} \right) \left(\frac{T_B + 273}{273} \right)}{3600 \cdot A_B} \quad (\text{B.6.1})$$

The accuracy of the calculated fluidising velocity (U) is associated with errors in the measurement of Q_{air} , G_{steam} , T_B and P_B . Using the tolerances given in Section 5.2.3 and equation (B.6.1) the accuracy of the calculated U is estimated to be ± 0.1 m/s.

Appendix B.6.2: Calculation of gas calorific value (CV)

The gross calorific value of the gas can be calculated from the gross heat of combustion of the following combustion reactions (Smith and Van Ness, 1975):



$$\Rightarrow \boxed{CV(\text{MJ} / \text{Nm}^3) = 0.12639.V_{\text{CO}} + 0.12766.V_{\text{H}_2} + 0.39765.V_{\text{CH}_4}} \quad (\text{B.6.2})$$

V_{CO} = CO concentration of the gas (volume %)

V_{H_2} = H₂ concentration of the gas (volume %)

V_{CH_4} = CH₄ concentration of the gas (volume %)

The accuracy of the calculated calorific value (CV) is associated with errors in the measurement of V_{CO} , V_{H_2} , and V_{CH_4} . Using the tolerances given in Section 5.2.3.4. and equation (B.6.2) the accuracy of the calculated CV is estimated to be ± 0.15 MJ/kg.

Appendix B.6.3: Residence time calculation of bed char

Bed pressure drop (Pa) = $\Delta P_B = P_1 - P_2$ (see Figure 5.5 and Table 5.4)

$$\Delta P_B = \frac{M_1 g}{A_B} \quad (\text{B.6.3a})$$

where:

M_1 = Bed mass above pressure probe (kg) (above P_1)

g = Gravitational constant (m/s^2) = 9.81

A_B = Bed area (m^2) = 0.04

$$\Rightarrow M_1 = \frac{\Delta P_B A_B}{g} = \frac{\Delta P_B}{245.5} \quad (\text{B.6.3b})$$

Bed mass below pressure probe = M_2 (below P_1)

$$M_2 = A_B (1 - \varepsilon) \rho_{char} H \quad (\text{B.6.3c})$$

where:

ε = Bed voidage at bed velocity = 0.63 (bed velocity > $3 \times U_{mf}$)

ρ_{char} = Char density (kg/m^3) = 1 200 kg/m^3

H = Distance from distributor to pressure probe P_1 = 0.130 m

$$\Rightarrow M_2 = 2.31 \text{ kg}$$

$$\text{Total bed mass (kg)} = M_t = M_1 + M_2 = \frac{\Delta P_B}{245.5} + 2.31 \quad (\text{B.6.3d})$$

$$\text{Residence time of char (min)} = t = \frac{M_t}{G_{char}} \cdot 60 \quad (\text{B.6.3e})$$

$$G_{char} = \frac{G_{coal}(C_{ash} + C_{fixed})}{100} \quad (\text{B.6.3f})$$

where:

- G_{coal} = Coal feedrate (kg/h)
 C_{ash} = Ash in coal (%)
 C_{fixed} = Fixed carbon in coal (%)

The accuracy of the calculated char residence time (t) is mainly associated with errors in the measurement of ΔP_B and G_{coal} . Using the tolerances given in Section 5.2.3 and equations (B.6.3a) to (B.6.3f), the accuracy of the calculated residence time (t) is estimated to be ± 3 min.

Appendix B.6.4: Calculation of fixed carbon conversion and percentage char elutriated

The following measured values are used to calculate the fixed carbon conversion (C_{FIXEDCON}) and percentage char elutriated (A_E):

$$\text{Coal feedrate (kg/h)} = G_{\text{coal}} = a \quad (\text{measured})$$

$$\text{Fixed carbon in coal (\%)} = C_{\text{fixed}} = b \quad (\text{measured})$$

$$\text{Ash in coal (\%)} = C_{\text{ash}} = c \quad (\text{measured})$$

$$\text{Bed char flowrate (kg/h)} = G_{\text{BC}} = d \quad (\text{measured})$$

$$\text{Carbon in bed char (\%)} = C_{\text{BC}} = e \quad (\text{measured})$$

$$\text{Carbon in elutriated char (\%)} = C_{\text{EC}} = f \quad (\text{measured})$$

The elutriated char flowrate could not be accurately measured since a certain percentage bypasses the cyclone and cannot be collected. The elutriated char flowrate is therefore determined by means of an ash balance.

$$\text{Elutriated char flowrate (kg/h)} = G_{\text{EC}} = g \quad (\text{calculated})$$

$$ac = d.(100-e) + g.(100-f) \quad (\text{ash balance}) \quad (\text{B.6.4a})$$

$$\Rightarrow g = \frac{ac - d(100 - e)}{100 - f} \quad (\text{B.6.4b})$$

The fixed carbon conversion is calculated by means of a carbon balance

$$\text{Fixed carbon conversion (\%)} = C_{\text{FIXEDCON}} = h \quad (\text{calculated})$$

$$h = \frac{(ab - (ed + fg)).100}{ab} \quad (\text{B.6.4c})$$

The percentage elutriated char is calculated from the bed and elutriated char flowrates.

$$\text{Percentage elutriated char (\%)} = A_E = i \quad (\text{calculated})$$

$$i = \frac{g \cdot 100}{d + g} \quad (\text{B.6.4d})$$

The calculated values (shaded rows) for each test are given in Table B.6.4.1.

Table B.6.4.1: Calculation of fixed carbon conversion and elutriated char

Test number	New Vaal		Matla		Grootegeeluk		Duvha	
	1	2	3	4	5	6	7	8
Coal feedrate (kg/h)	28.7	23.9	27.0	24.3	23.0	23.0	26.4	26.4
Fixed carbon in coal (%)	34.60	34.60	42.10	42.10	38.60	38.60	45.80	45.80
Fixed carbon feedrate (kg/h)	9.93	8.27	11.37	10.23	8.88	8.88	12.09	12.09
Ash in coal (%)	40.40	40.40	33.40	33.40	34.90	34.90	32.50	32.50
Ash feedrate (kg/h)	11.59	9.66	9.02	8.12	8.03	8.03	8.58	8.58
Bed char flowrate (kg/h)	5.25	3.62	5.84	4.78	5.52	5.30	6.00	5.68
Carbon in bed char (%)	2.80	1.40	24.30	20.80	26.80	26.40	38.60	33.90
Carbon in bed char (kg/h)	0.15	0.05	1.42	0.99	1.48	1.40	2.32	1.93
Ash in bed char (kg/h)	5.10	3.57	4.42	3.79	4.04	3.90	3.68	3.75
Ash in elutriated char (kg/h)	6.49	6.09	4.60	4.33	3.99	4.13	4.90	4.83
Carbon in elutriated char (%)	19.50	15.50	32.30	27.80	31.00	27.00	41.60	43.20
Carbon in elutriated char (kg/h)	1.57	1.12	2.19	1.67	1.79	1.53	3.49	3.67
Fixed carbon conversion (%)	82.7	85.9	68.2	74.0	63.2	67.0	52.0	53.7
Char elutriated (%)	60.6	66.6	53.8	55.6	51.1	51.6	58.3	59.9

The accuracy of the calculated fixed carbon conversion (C_{FIXEDCON}) is mainly associated with errors in the measurement of G_{coal} , G_{BC} , C_{BC} and C_{EC} . Using the tolerances given in Section 5.2.3 and equation (B.6.4a) to (B.6.4d), the accuracy of the calculated fixed carbon conversion is estimated to be $\pm 2.5\%$.

Appendix B.7: Calculation of reactivity index (R_s) in the fluidised bed gasifier

The reactivity index is calculated using equation (2.8) given in Section 2.3.2

$$R_s = \frac{0.5}{\tau_{0.5}} \quad (2.8)$$

The time to reach 50 % conversion ($\tau_{0.5}$) in the FBG is estimated from equation (4.3) and from the pilot plant data given in Table B.7.1.

$$X = 1 - [1 - (1 - \beta)k't]^{1/(1-\beta)} \quad (4.3)$$

Table B.7.1: Pilot plant data and calculated values of k' , $\tau_{0.5}$ and R_s

	New Vaal		Matla		Grootegeeluk		Duvha	
Test number	1	2	3	4	5	6	7	8
Bed temperature (°C)	922	947	925	949	927	953	927	949
Fixed carbon conversion (X)	0.827	0.859	0.682	0.74	0.632	0.670	0.520	0.537
Residence time (min)	36.7	36.6	37.4	37.6	45.1	45.1	35.7	35.7
Structural parameter (β)	0.64	0.64	0.52	0.52	0.92	0.92	0.80	0.80
Rate constant (k') (min^{-1})	0.035	0.038	0.024	0.026	0.021	0.024	0.019	0.020
Time to 50 % conversion (h)	0.288	0.266	0.418	0.372	0.530	0.478	0.581	0.539
Reactivity index (R_s) (h^{-1})	1.74	1.88	1.20	1.34	0.94	1.05	0.86	0.93

The apparent reaction rate constant can be calculated using the rearranged version of equation (4.3) and the conversion residence time data in Table B.7.1:

$$k' = \frac{1 - (1 - X)^{1-\beta}}{t(1 - \beta)} \quad (\text{B.7.1})$$

Finally the estimated time to reach 50 % conversion (required for equation (2.8)) is calculated using equation (B.7.2) with the calculated values of k' and setting the conversion (X) equal to 0.5.

$$\tau_{0.5} = \frac{1 - (1 - X)^{1-\beta}}{k' (1 - \beta)} \quad (\text{B.7.2})$$

The accuracy of the calculated value of the reactivity index (R_s) in the FBG is mainly associated with the accuracy of the calculated value of fixed carbon conversion (± 2.5 %) and the residence time (± 3 min) and is estimated to be $\pm 0.2 \text{ h}^{-1}$.

Appendix B.8: Particle size distributions of coal, bed char and cyclone char

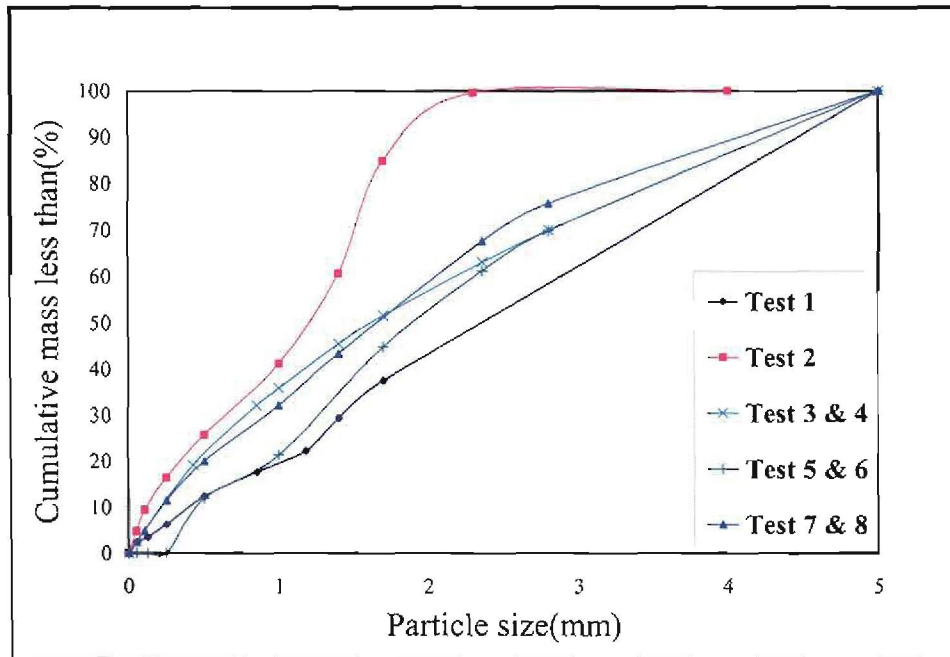


Figure B.8a: Particle size distribution of coal

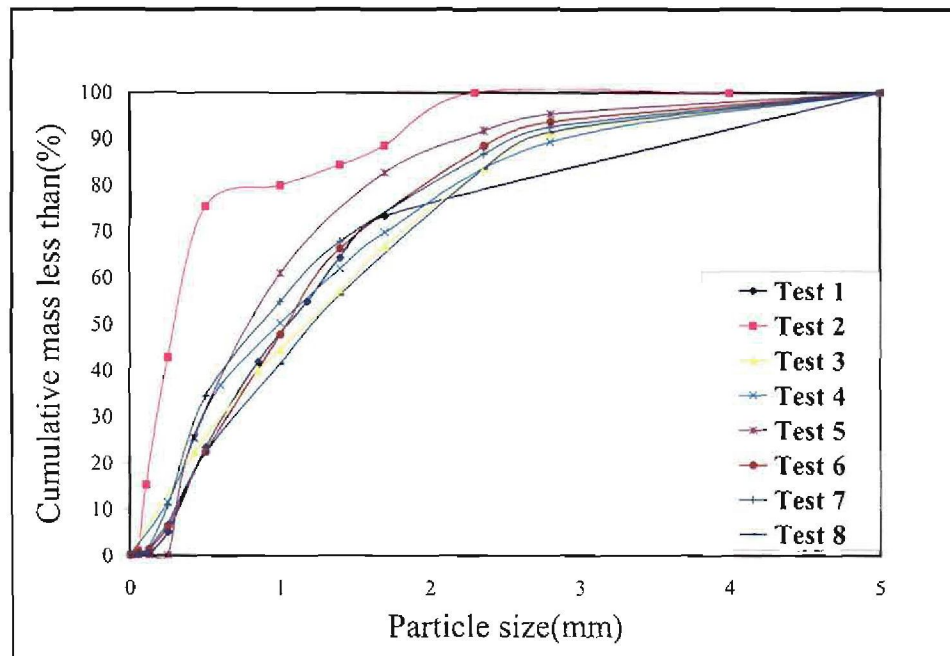


Figure B.8b: Particle size distribution of bed char

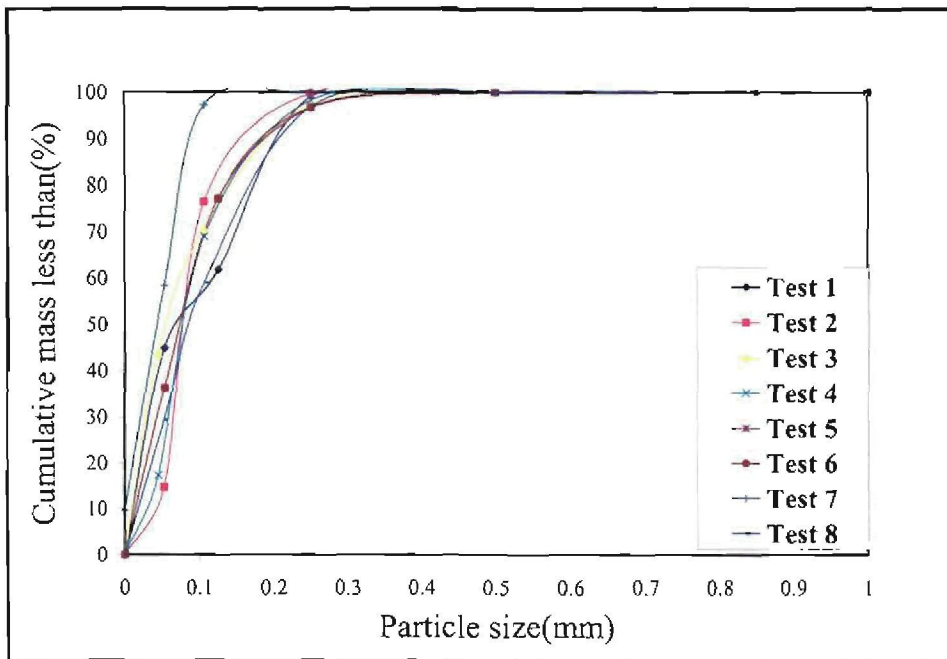


Figure B.8c: Particle size distribution of cyclone char

Appendix B.9: Coal, bed char and cyclone char

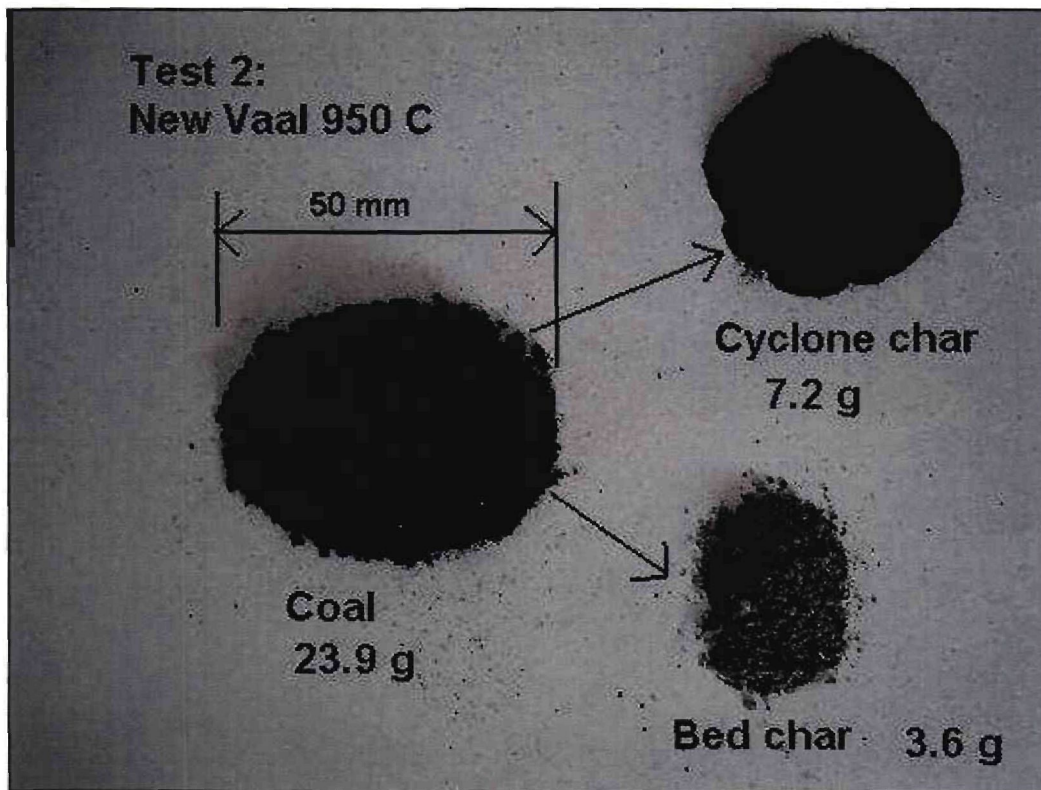


Figure B.9: Appearance and relative amounts of coal and char

Appendix B.10: Char particles removed from the gasifier



Figure B.10a: New Vaal bed char particle (2 mm)



Figure B.10b: Duvha bed char particle (2 mm)

Appendix B.11: Distributor of the fluidised bed gasifier (FBG)

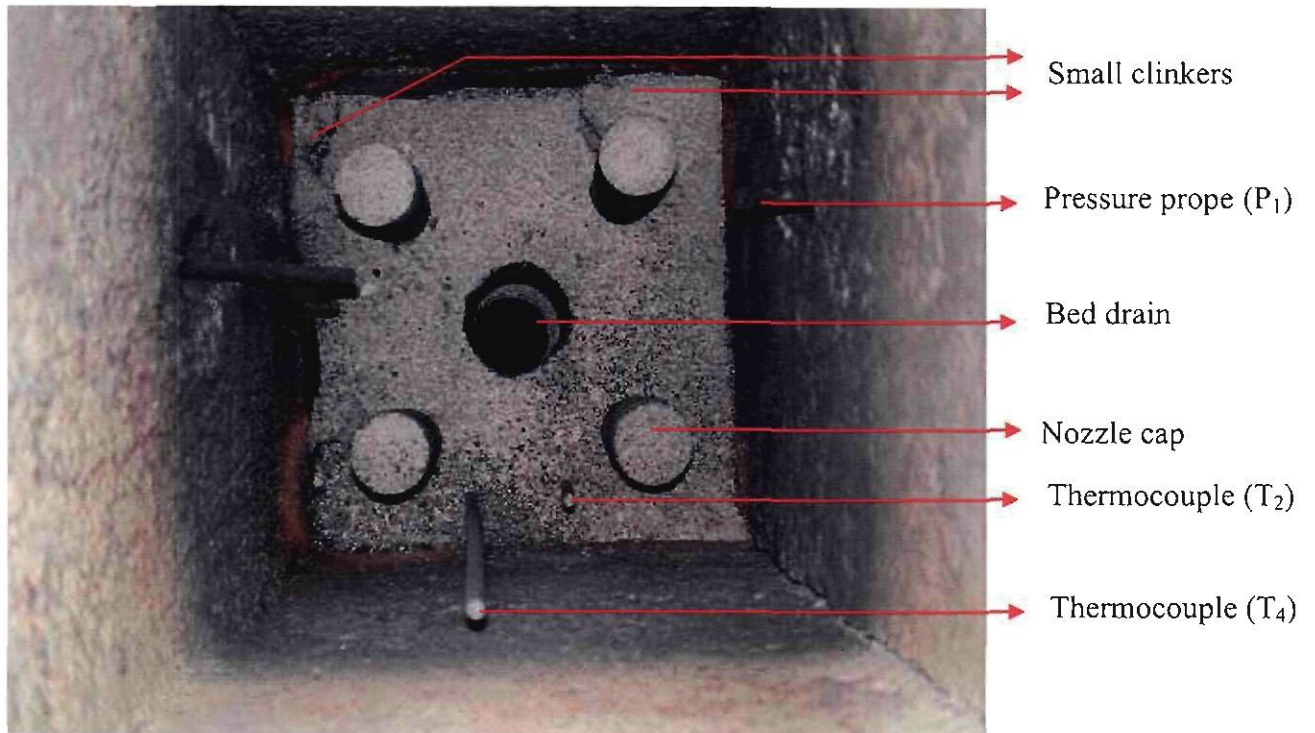


Figure B.11: Small clinkers in the corner of the FBG distributor